Simulating charge transport in organic semiconductors and devices: a review

2017 Rep. Prog. Phys. 80 026502

(http://iopscience.iop.org/0034-4885/80/2/026502)

IOP Publishing Reports on Progress in Physics
Rep. Prog. Phys. **80** (2017) 026502 (37pp) doi:10.1088/1361-6633/80/2/026502

Review

Simulating charge transport in organic semiconductors and devices: a review

C Groves

Durham University, School of Engineering and Computing Sciences, South Road, Durham, DH1 3LE, UK

E-mail: chris.groves@dur.ac.uk

Received 29 April 2016, revised 17 October 2016
Accepted for publication 8 November 2016
Published 19 December 2016

Corresponding Editor Professor Mark Geoghegan

Abstract

Charge transport simulation can be a valuable tool to better understand, optimise and design organic transistors (OTFTs), photovoltaics (OPVs), and light-emitting diodes (OLEDs). This review presents an overview of common charge transport and device models; namely drift-diffusion, master equation, mesoscale kinetic Monte Carlo and quantum chemical Monte Carlo, and a discussion of the relative merits of each. This is followed by a review of the application of these models as applied to charge transport in organic semiconductors and devices, highlighting in particular the insights made possible by modelling. The review concludes with an outlook for charge transport modelling in organic electronics.

Keywords: charge transport, organic electronics, semiconductor devices, Monte Carlo, drift diffusion, master equation

(Some figures may appear in colour only in the online journal)

Contents

1. Introduction

1.1. The need for simulation in organic electronics

Organic electronic devices are beginning to challenge their more established inorganic counterparts in a variety of applications. This is driven by the possibility of chemically tuning both the optical [1] and electronic properties [2, 3] of the organic semiconductor (OSC) over wide ranges, as well as their compatibility with scalable manufacture such as solution printing [4] and evaporation [5]. This makes OSCs particularly attractive for large-area, cheap electronic and optoelectronic device applications [6–8]. Indeed, the idiosyncratic properties of OSCs have made novel electronic devices possible, or at least feasible, in fields as diverse as medicine [9, 10],

chemical sensing [11, 12], 'rollable' displays [13, 14] and a host of other wearable [15] or flexible [16] applications. At time of writing, organic light-emitting diodes (OLEDs) are a billion dollar industry, primarily focussed on small, rigid displays such as cellphones and televisions, and is projected to grow to the tens of billions in the coming decade [17]. Organic thin film transistors (OTFTs) are similarly growing in utilisation, again particularly in display applications [8]. And while still largely in the phase of research and development, there are a range of photovoltaic technologies using OSCs which promise cheap, plentiful renewable energy. Such photovoltaics either use OSCs exclusively, as in organic photovoltaics (OPVs) [18], or in hybrid combination with other materials, as in solid-state dye-sensitised [19], singlet-fission [20, 21] and perovskite solar cells [22].

The capabilities of organic electronics ultimately rely on the properties of the OSC in the context of device operation. In many cases it is charge transport which limits the performance and applicability of organic electronic devices [8], hence better understanding and optimisation of charge transport is often key to improving the technology. However, modelling charge transport in organic and inorganic semiconductor devices are very different prospects. The regular crystal structure of inorganic semiconductors makes it possible to accurately calculate with the electronic bandstructure and phonon modes which underpin electronic transport. By contrast, the electronic coupling in OSCs tends to be weak, and proceed by hops from one molecule to the next rather than band transport. Furthermore, the structure of OSCs spans a range from amorphous tangles of polymers, to polycrystalline films of small molecules bisected by grain boundaries that snake randomly through the film. It is therefore a testament to the community of chemists, engineers, materials scientists and physicists, that progress from the first organic semiconductor [23] to the mass commercial exploitation of some organic electronic devices has been achieved.

Much of this progress has been made possible due to careful experiments, insight, and laborious trial-and-error optimisation of materials synthesis and device fabrication [24, 25]. However, given the importance of charge transport in the operation of many organic electronic devices, it is perhaps surprising that charge transport models have not had a larger role in the development of the technology. More mature, inorganic semiconductor technology has demonstrated that modelling can play an important role in research by allowing more meaningful experiments to be designed, as well as testing underpinning assumptions about how devices may operate [26]. While models are not a replacement for experiment, simulation and experiment can have a valuable symbiotic relationship which, arguably, is not currently realised for organic electronic devices. However, the pace at which charge transport models are being developed and used has increased markedly in the last decade. With these powerful tools, researchers have been able to better understand the processes which underpin device performance, and are on the verge of predictive models that will allow rational design [27]. The aim of this review is to provide objective background of the various models available and discuss their respective benefits (section 2); before reviewing how these models have been applied to understand charge transport (section 3) and device performance (section 4).

1.2. Charge hopping in OSCs

Before embarking on a discussion of the various modelling techniques we first introduce the basic physics of charge transport in OSCs. As one might expect, a full discussion of charge transport in OSCs would occupy more column inches than is available in a review of modelling techniques and their application. Hence we will largely restrict our discussion to hopping, which is the process of electron transfer between molecules (or segments of molecules) when electronic coupling is weak. Charge transport in most OSCs is limited by hopping, and as such, hopping models are commonly used to describe device behaviour [28–33]. Interested readers wishing a broader discussion of charge transport physics in OSCs are directed elsewhere [33–36].

OSC molecules are held together by relatively weak Van der Waal interactions, dipole–dipole interactions, or hydrogen bonding. In turn this allows individual OSC molecules many degrees of conformational freedom, while collections of OSC molecules can adopt a variety of relative orientations. This structural disorder, together with chemical impurities and electrostatic interactions, gives rise to static disorder which acts to localise charges. Another cause of charge localisation in OSCs are molecular vibrations, which interact with charges to distort the host molecule and form a polaron. The molecular distortion allows the charge to adopt a state which is both lower in energy and more localised than the highest occupied molecular orbital (HOMO) or lowest unoccupied molecular orbital (LUMO) level of the OSC molecule. Polarons form in many OSCs and can be observed directly in experiment [37]. Whatever the cause of localisation, charge transport is usually considered to proceed by a series of electron-transfer reactions (hops) between localised states rather than by band transport, as in inorganic semiconductors [33, 34]. Whether charge transport in a particular OSC is limited by static disorder or polaronic effects will influence how charge transport is simulated, hence it is important to determine which effects are important for the OSC in question. It is usually the case that charge transport in amorphous and semi-crystalline polymer OSCs are dominated by the effects of static disorder [38–41]. However, even amorphous polymer OSCs can approach a 'disorder-free' charge-transport regime (i.e. charges can be better described as polarons), if the polymer backbone is largely free from torsional disorder in a manner which is independent of molecular packing [42]. It may therefore be necessary to determine which mode of localisation is most important for the OSC in question prior to writing a simulation, this however is not trivial [43].

Electron transfer from one state, i to another state, j, is quantified by the hopping rate, W_{ij}. Two hopping rate expressions are often used in charge transport simulations, namely

those derived by Miller and Abrahams [44] and by Marcus [45]. The Miller–Abrahams rate assumes exchange of a single phonon during electron transfer between weakly coupled sites. It is usually quoted in simplified form below, which is valid in the range $|E_j - E_i| \gg 2kT$ [46]. In many OSCs this assumption would be expected to be valid since static energetic disorder, σ is often of the order of 100 meV. The simplified Miller–Abrahams expression is written as:

$$W_{ij} = \nu_0 \exp\left[-2\alpha r_{ij}\right] f(E_i, E_j), \tag{1}$$

where $f(E_i, E_j) = \exp\left[-(E_j - E_i)/kT\right]$ when $E_j \geqslant E_i$ and $f(E_i, E_j) = 1$ when $E_j < E_i$. Here, r_{ij} is the separation between the sites i and j, α is the inverse localization length of the charge wavefunction, k is Boltzmann's constant and T is the temperature. E_i and E_j are the site energies which include local variations in energy levels (i.e. energetic disorder), Coulomb interactions between charges and image charges, and the electric field. The pre-factor ν_0 is an empirical 'attempt to hop' frequency that is usually fitted to experimental data. Hops upward in energy are therefore modified by a Boltzmann term, whereas hops downward in energy proceed at the same rate. This implies that it is always possible to dissipate the energy lost in electron transfer. The Miller–Abrahams expression also permits hopping at a rate which decays exponentially with increasing hop length, i.e. variable range hopping (VRH). In many cases it is anticipated or assumed that the wavefunction is sufficiently localised that it is only necessary to calculate hopping rates to neighbouring sites (so-called nearest-neighbour hopping).

The semiclassical Marcus rate permits exchange of multiple phonons during electron transfer, and is written as [45]:

$$W_{ij} = \frac{|J_{ij}|^2}{\hbar}\sqrt{\frac{\pi}{\lambda kT}}\exp\left[-\frac{(E_j - E_i + \lambda)^2}{4\lambda kT}\right]. \tag{2}$$

Here J_{ij} is the electronic transfer integral and λ is the reorganisation energy associated with electron transfer. Hence the Marcus rate explicitly considers the energetic cost associated with the moving molecular distortion associated with a charge. For a polaron this reorganisation energy is $\lambda = E_p/2$, where E_p is the polaron binding energy. A consequence of molecular reorganisation during charge transfer is the so-called inverted regime, whereby the rate increases and then decreases with increasing driving energy, which has been observed experimentally in OSCs when the driving energy for electron transfer is large (>0.5 eV) [47]. The inverted regime is absent from the Miller–Abrahams expression. The Marcus rate can be evaluated either by directly calculating the electronic transfer integrals and reorganisation energies using quantum chemical approaches [28, 34], or empirically by fitting to experimental data [32]. The latter is common in KMC models and is practically implemented by replacing the prefactor of equation (2) with an 'attempt-to-hop' frequency that is fitted to give reasonable charge mobilities [48].

The two rate equations are therefore physically distinct and so one must decide which is appropriate for the circumstance at hand. Generally speaking, the Miller–Abrahams expression is valid in the case when the temperature is small or electron–phonon coupling is weak, while the Marcus expression is valid in the case when temperature is high or electron–phonon coupling is strong [34]. Furthermore, the Marcus expression considers the energy cost of moving the molecular distortion associated with a polaron. It has been argued that polaronic effects are observable when the reorganisation energy is comparable to the typical activation energy for hops within the static disorder [41]. However, notwithstanding these differences in underpinning physics, the predictions of device behaviour made by both rate equations are qualitatively similar under normal operating conditions [49].

Charge injection from the electrode to the OSC, and charge extraction in the opposite direction, can significantly affect the performance of OTFTs [50], OPVs [51] and OLEDs [52]. Hence the characterisation [53] and engineering [54] of metal-organic interfaces is often crucial to obtaining devices which are not injection-limited [55, 56]. The cited reviews describe these various issues in detail, so here we consider how charge injection and extraction can be simulated in charge transport models. While there are a variety of analytical models which describe charge injection into disordered materials [57], in lattice-based models of charge transport, such as master equation (ME) and kinetic Monte Carlo (KMC), the process can be modelled directly. In this case, the hop energy of the above expressions (i.e. $E_j - E_i$) is set to the difference in energy between the electrode workfunction and the energy of the site in question. The electrode workfunction is taken from experiment [51] while the site energies can are generated in accordance with the OSC in question. In some circumstances, however, the electrode is heterogeneous and this should be reflected in the injection model in order to accurately capture the behaviour of the device in question [58].

While it is anticipated that hopping between localised states determines the charge transport behaviour of many OSCs under normal conditions, there are of course exceptions. Highly ordered, ultra-pure OSC films have been shown to have mobilities, μ in excess of $\mu > 100\,\mathrm{cm^2\,V^{-1}\,s^{-1}}$ at low temperatures that are suggestive of band-like transport [59]. There have also been reports of band-like charge transport, or at least something which appears similar, in crystalline and polycrystalline OSC films at room temperature [60–65]. Whether or not a particular OSC film will give 'band-like' charge transport appears to depend strongly on the organisation of molecules within the crystal [65]. A discussion as to whether charge transport is due to delocalised bands is outside the scope of this review, however, it presently appears [63, 64, 66–68] that the data may instead be explained dynamic intermolecular thermal fluctuations which act to localise the charges [69]. Hence, the recent demonstration that such thermal fluctuations can be observed by experiment, raises the possibility that materials can be screened to select those which have weak fluctuations and, perhaps, high mobility [70]. From a theoretical point of view, analysis suggests that hopping has a 'speed limit' of sorts [71] which can be used as a starting point to quantify whether a hopping model or alternative [36] is more appropriate.

2. Charge transport and device models

It is important to note that there is no 'one size fits all' charge transport model. Even with ever increasing computer power, the complex structure of organic electronic devices spanning from the nano-scale to the macro-scale will likely evade complete description for years to come. As such, the choice of a model to solve a particular problem will remain a challenge for the foreseeable future. Fortunately there are many types of models which differ in the way they describe charge transport as well as the computational and practical difficulty in their implementation. Selecting a model appropriate to a particular task therefore requires a good knowledge of their relative merits and arguably some pragmatism, as inevitably there will be compromises inherent in the model chosen. A good general rule is to select a model that is sufficiently detailed and accurate to capture the physics of interest, but not more.

2.1. Drift diffusion (DD)

The DD model results from a simplification of the Boltzmann transport equation in which carrier motion is described by two components: drift, which describes the motion of carriers under an applied field; and diffusion, which describes the random walk of carriers driven by thermal energy [26]. DD models have been used extensively to understand and predict the behaviour of inorganic electronic devices, and have latterly been applied to their organic counterparts [72–76]. The principal advantage of DD models is the comparative ease with which one can solve for the current flowing through a device, and that this computational effort is largely independent of charge carrier density. This makes DD attractive for simulations which involve either large device dimensions or high charge carrier densities, such as OLEDs or OTFTs, which can be challenging for MC methods [31, 32, 77]. The computational efficiency of DD models is due to the efficient numerical algorithms [26, 78, 79] used to solve the equations for current continuity and electric field [26]. An example numerical scheme used to solve the DD equations by Koster *et al* [74] is shown in figure 1. Some aspects of the classical DD model have to be modified to make them more appropriate for OSCs, in particular the Einstein relationship between drift and diffusion (discussed in section 3, [80–85]). One should also consider using empirical expressions for the charge density-dependent and field-dependent mobility (discussed in section 3.2, [46, 86, 87]), and analytical models to describe the charge generation and recombination (section 4, [88–91]). Of course this means one must be confident that the assumptions underpinning the DD, and that the recombination models are appropriate in context. This is discussed further below, however, DD models have achieved quantitative agreement with experimental data for space charge limited diodes (SCLDs) [92], OLEDs [93], OPVs [94] and OTFTs [95].

The standard equations and method of solution for DD models are described in detail by Selberherr [26], and is implemented in many commercial finite-element simulation packages. Such commercial packages are particularly useful to examine complex 2D device geometries such as OTFTs

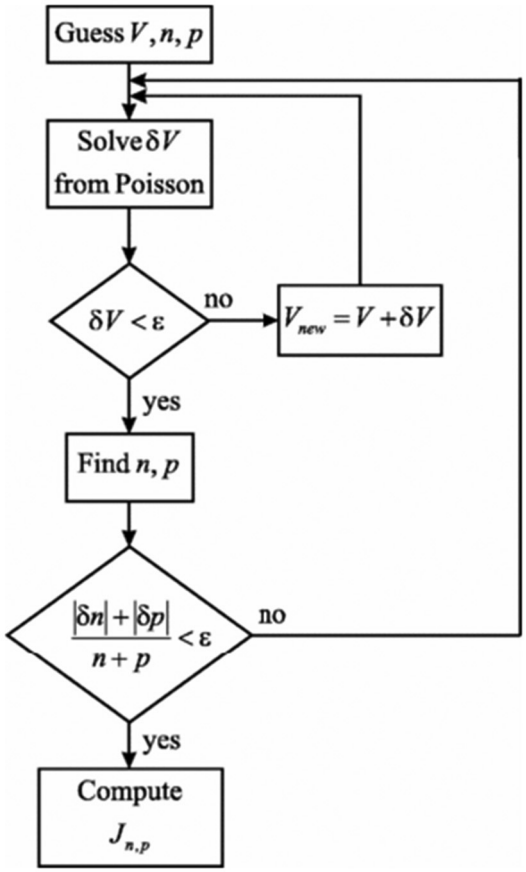

Figure 1. Numerical simulation scheme used by Koster *et al* [74] to solve the DD equations. Here an initial guess to the voltage (V), electron and hole densities (n and p respectively) are made. A correction to the initial guess at the voltage is made using the Poisson equation until convergence is reached (i.e. change in voltage drops below a threshold ε). The charge carrier densities are then updated and the process repeated until a self-consistent solution is reached, and the current densities calculated. Reprinted figure with permission from Koster *et al* [74]. Copyright 2005 by the American Physical Society.

[96–99], however, careful consideration and tuning is required to describe charge transport in OSCs rather than inorganic semiconductors [100]. Here we focus on three major considerations when using DD models for OSCs, namely charge generation and recombination, charge transport across a heterojunction, and heterogeneous current flow.

The analytical models of charge generation and recombination are a vital part of the DD models which describe organic electronic devices that absorb or emit of light (OPVs, OLEDs and light-emitting OTFTs) [73, 74]. Because hopping implies a small mean free path, it might be expected that recombination of charges injected from the contacts or different excitons, so-called non-geminate recombination (NGR), would be limited by diffusion and thus described by a Langevin rate [90]. However, as described in sections 4.2 and 4.3, the NGR rate has been shown to deviate significantly from the Langevin rate due to disorder, charge density, anisotropy of charge transport, morphology, presence of a heterojunction and electric field [101–104]. It is perhaps unsurprising that the Langevin expression is not always valid in OSCs since it

was not derived for use in that context, but nonetheless, this poses difficulties for DD modelling as it is not always *a priori* clear as to whether the Langevin expression or a reduced Langevin rate should be used. It should be noted however that sometimes the rate is simply treated as a fit parameter, and this approach has been used to demonstrate that NGR proceeds with a reduced Langevin rate in OPVs [105]. More recently, Shockley–Read–Hall (SRH) recombination [91] has been proposed as an additional mode of NGR in OSC materials since they are known to suffer from charge trapping in a distributed density of states (DoS) [40]. Consideration of both SRH recombination has been shown to improve the agreement between predictions of DD models and experimental data for OLEDs [93, 106] and OPVs [107, 108]. Modelling the rate of geminate recombination (GR), i.e. recombination of charges from the same exciton, in OPVs is somewhat more problematic. Part of the issue is that it is unclear whether field-dependent GR occurs at all in OPVs, and if so, in which materials and to what extent. However, this ongoing debate is discussed in section 4.2, so for now, we will discuss how one might include GR in a DD model if it were important to the OPV in question. If recombination is limited by diffusion, we might expect the proportion of charges which will undergo GR to be described by the Onsager expression [88]. However, experiment suggests that the recombination rate of adjacent charges in OSCs is not infinite, as assumed by Onsager, and so instead a modified version with a finite recombination rate of adjacent charges was proposed by Braun [89]. However, it has latterly been argued that the Braun expression incorrectly assumes that separation and recombination follow exponential kinetics [109]. However, from a pragmatic point of view, it is difficult to be critical of the Braun model as analytical expressions which more correctly account for transport environment in OSCs [110–112] still do not encompass all of the potentially relevant physics [113, 114]. Given that the GR model will (almost) inevitably not include physics relevant to the OPV in question, it is perhaps safest to consider the recombination rate in such models as a fitting parameter that is indicative of how good or bad GR is, but having no further quantitative meaning [73]. Modelling charge generation can be considered using the method described by Barker *et al* [73], in which the rate of exciton generation and dissociation is solved in in parallel with the charge continuity equations. The relative positions where excitons are created within the film can be calculated for the material and device geometry in question can be calculated directly using the transfer matrix method [115], as by Gao *et al* for example [116], or the rate of exciton generation can be assumed to be constant throughout the volume [74].

Many organic electronic devices are either spatially heterogeneous [117, 118] or multi-layered [119] and so it is important to consider how this might be included in a DD model. Transport of charges across a heterojunction is particularly important for OLED operation, as discussed further in section 4.3. Arkhipov *et al* [120] showed using a KMC model that one cannot simply model the process as thermionic emission over a potential barrier due to a 'backflow' of charges which depends on electric field and potential barrier. Houlli *et al* [121] demonstrated that that a 1D continuum approach significantly overestimates the effect of Coulomb interactions on current passing a heterojunction due to the effect of energetic disorder. This is inconvenient from a modelling perspective since DD models are computationally efficient, particularly at the large charge densities found in OLEDs. Cottaar *et al* [119] examined this problem in further detail using a KMC model, in particular focussing on what boundary conditions were necessary at hetero-interfaces when using a DD model, to ensure that the implied charge behaviour matched that of the more rigorous model. The resultant modifications demonstrated much improved agreement between KMC and DD, therefore demonstrating the benefits of using models in tandem to address physics-based inadequacies in models which are otherwise convenient.

DD rests on the assumption that the charge transport properties of the material can be described by homogeneous, layer-averaged quantities under operating conditions. This may not be the case in OSCs which display energetic [122, 123] or morphological [123, 124] disorder which have been shown to lead to filamentary (i.e. heterogeneous) transport. The impact of disorder and morphology on charge transport will be discussed further in section 3. However, from a modelling point of view it is important to consider whether the assumption of homogeneous charge transport is appropriate to the context examined, and by extension, whether DD might be expected to be accurate. Considering first energetic disorder, the important question is whether the lengthscale over which conductance fluctuations occur is larger than the lengthscale of the device. Massé *et al* [122] derived empirical expressions for the lengthscale of conductance fluctuations in OSCs using a KMC model assuming correlated and uncorrelated Gaussian disorder. Interestingly, it was shown that the lengthscale of conductance fluctuations for small molecule OSCs typically used in OLEDs can be of a similar order to the device thickness, suggesting that DD may be inappropriate if used in this context. Moving on to consider morphology, Koster [124] used an ME approach similar to that of Pasveer *et al* [86], to predict the mobility in bulk heterojunction (BHJ) morphologies. It was found that the field and charge density dependence of mobility in blends was significantly altered compared to 'neat' material. Most strikingly, it was shown in some circumstances that mobility has a positive field dependence in neat material, but a negative field dependence in a blend, even when all other transport parameters were the same. Practically this means that the parameterisation of mobility used in a DD model ought to be appropriate for the morphology in question.

2.2. Master equation (ME)

Here we use the term ME to describe a class of charge transport models based upon the Pauli master equation [125]. The distinguishing feature of this approach is that the charge distribution is described in terms of time-averaged site occupation probabilities, as compared to layer-average charge densities in DD and explicit charges in MC. The movement of charge in either one [86], two [126] or three [124] dimensions is described by hopping rates. In turn, this means that ME can

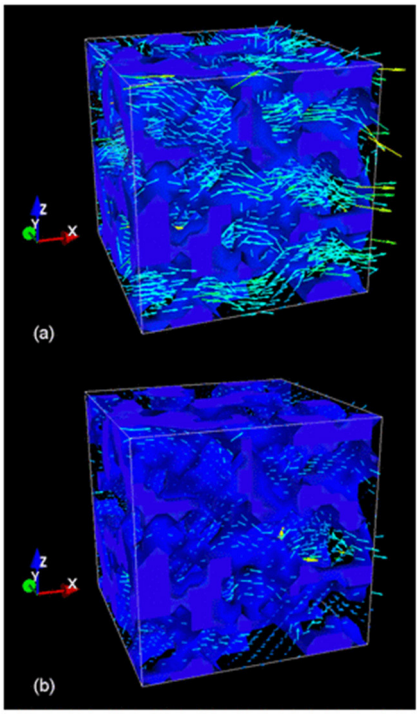

Figure 2. Spatially resolved current flow (arrows) predicted by ME in a binary blend where one component is conducting (transparent) and the other is non-conducting (opaque). Two fields are considered (a) 10^6 V m^{-1} and (b) 10^8 V m^{-1}. The length of the arrows is proportional to the current, but the vectors in (a) and (b) are not drawn to the same scale. It can be seen that the current at high electric field is more heterogeneous. Reprinted figure with permission from Koster [124]. Copyright 2010 by the American Physical Society.

be used to simulate charge transport in three dimensions, as shown for example in figure 2. ME is therefore more 'granular' than DD since it describes more explicitly the underlying charge transport mechanisms, as well as having the capability to describe quantities that vary on the nanoscale, such as energetic disorder and morphology. From the other side, ME is more numerically efficient than MC, particularly at high charge densities, which can lead to ME device models being an order of magnitude faster than their KMC counterparts [127]. However, the numerical efficiency of ME is due to the description of charges in terms of time-averaged probabilities. This has the consequence that charge is essentially treated as a continuous rather than discrete quantity, making Coulomb interactions between individual charges challenging to include. This is important when considering high charge density (i.e. approaching 1 charge per 100 sites) [128] and charge transport across a heterojunction [121] where short-range Coulomb interactions [129] have been shown to be important. Casalegno *et al* [127] describe a method which allows partial consideration of Coulomb interactions in ME, although this poses additional numerical challenges to implement self-consistently.

A broader point is that lattice models, such as ME and KMC, assume the molecular geometry of the OSC can be represented by a regular lattice of sites. This process of assigning electronic disorder and morphology to sites is discussed further in section 2.3.1. Although each site in the lattice notionally represents a molecule or segment which can host a charge, the exact relationship to the OSC molecule is lost. This loss of detail is significant, since in real OSCs, the active layer will comprise polymer chains of varying lengths, conformations and packings which will influence local charge transport [34]. In particular, the electronic transfer integral between states and/or molecules can be highly anisotropic [130–132]. However, since the link between individual molecules and sites which facilitate charge transport is lost, ME and KMC models instead assume isotropic electronic coupling. This has led to some justifiable criticism of lattice methods since ignoring the relationship between chain conformation and charge transport may not appropriate for the problem at hand [133].

Returning to discuss ME methods in particular, the steady-state Pauli master equation is given as:

$$\sum_j [W_{ij} n_i (1 - n_j) - W_{ji} n_j (1 - n_i)] = 0. \tag{3}$$

Where W_{ij} is the hopping rate from the origin site, i to destination sites, j, as described in section 1.2, and n is the occupation probability at that site. The first term describes flux out from site i, with the term $(1 - n_j)$ representing the probability of there being an empty site j to move to, thereby approximating a prohibition on double site occupancy due to Coulomb interactions. The second term describes flux of charges from sites j into the origin site i. This equation can be cast in 3D or 1D form, although in the latter case, careful tuning is required to ensure that artefacts are not introduced because of reduced dimensionality [134]. The Master equation is solved numerically, as described by Yu *et al* [125] for example. From the known values of n_i it is possible to calculate the steady-state mobility and/or current flowing through a device. ME methods have been instrumental in better understanding mobility in disordered [86] and blended [124] materials; predicting the device characteristics of OLED [135, 136] and OPV [127, 137] devices; and even modeling OPV photocurrent collection during a photoconductive atomic force microscopy measurement [138].

2.3. Monte Carlo (MC)

MC models use random numbers to simulate the behaviour of a system in accordance with statistical rules [77]. Because MC is seeded by random numbers, each individual MC simulation may result in a different outcome, and multiple simulations are required to build up a picture of how a system operates. The solutions provided by MC are therefore never exact, and also lack the 'neatness' of analytical treatments, but are nonetheless correct in their implementation of the underlying statistics. A great advantage of the MC framework is that it can be used to model the behaviour of systems of arbitrary complexity provided one knows the rules governing its behaviour. The principle challenges of realising a MC model are therefore to obtain accurate descriptions of the system and processes of interest, and to implement these in a simulation which has feasible run-time with the computing power available. The ever-increasing capabilities of computers, as well

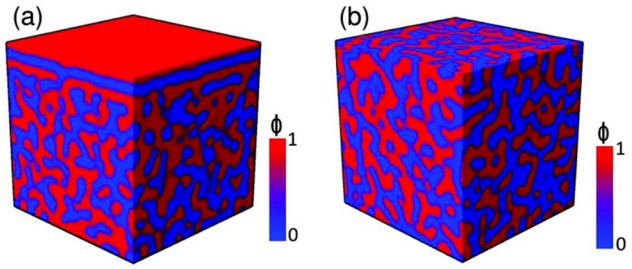

Figure 3. Cahn–Hilliard simulation of a binary blend morphology (a) considering the influence of surface energy interactions, and (b) ignoring the effects of surface energy interactions. Reprinted (adapted) with permission from Lyons *et al* [123]. Copyright 2011 American Chemical Society.

as an array of techniques to increase the speed of programs (section 2.3.3), are bringing increasingly complex problems within reach of MC simulation.

Charge transport in OSCs and devices is one such problem that is amenable to MC analysis. Here the 'behaviours of the system' are the various electronic processes, such as hops or recombination, and the statistics are the rates at which these processes occur. Here, MC models for charge transport in OSCs into two groups based on the way in which these rates are calculated. The first, which will be referred to as kinetic MC (KMC), is characterised by simplifying assumptions in molecular geometry and the resultant electronic coupling. The second, which will be referred to as quantum chemical MC (QCMC), generally includes a more explicit description of molecular geometries and electronic coupling which is calculated directly from this structure. Since KMC is less precise in its description of charge transport it is more capable of simulating large systems, such as devices under operating conditions [32, 139]. Conversely, although increased rigour of QCMC limits the scale of the systems that can be considered, it allows greater accuracy which may be vital in cases where the charge transport environment has a rich structure [132, 133]. The choice of using a KMC or QCMC model will therefore rest on whether examining charge transport in context, or explicit consideration of the impact of molecular geometry on charge transport, is more important to the question being posed.

2.3.1. Kinetic MC (KMC). The general MC method is to describe the initial conditions of the system, predict its subsequent behaviour in accordance with statistical rules, and repeat in order to build up a detailed picture of the system behaviour. Hence the first task in developing a KMC model is therefore to describe the OSC. The OSC is represented by a simulation volume which is divided into an array of sites in either 2 or 3 dimensions, usually assuming a Cartesian geometry. This simulation volume may then need to be further divided into regions corresponding to different OSCs. BHJ morphologies are usually generated using either a simulated annealing [140] or Cahn–Hilliard [123] model, as shown for example in figure 3. Various methods of generating morphologies are discussed further in section 4.4. Each hole- or electron-transporting site is assigned an energy which corresponds to the local HOMO or LUMO respectively. This energy is picked at random from a Gaussian or exponential DoS which corresponds to the OSC in question, hence while the link between the local energy levels and conformation of a particular OSC is lost, the bulk DoS is retained. Typically site energies are chosen to be uncorrelated with position within the simulation volume, however, for materials which have a strong dipole moment, site energies can be chosen such that they are spatially correlated [141].

The behaviour of charges within the OSC are then determined as follows. First, the processes which a charge might participate in, such as hops to different locations or recombination events, are listed. The rate for each process, W, is calculated and a corresponding wait time is generated as follows:

$$\tau = -\frac{\ln(X)}{W}. \tag{4}$$

Here X is a random number which is evenly distributed between 0 and 1. The process with the shortest wait time is selected as the behaviour for that charge. The simulation is therefore organised in terms of discrete events, which are the behaviours of the charges, separated by waiting times calculated using the above equation. The simulation progresses by advancing time to the next event, executing that event (e.g. a hop from point a to point b), before calculating the onward behaviour for the charge in its new state (provided the charge has not been removed from the simulation by, e.g. recombination) and repeating the process.

Like the ME technique, the hopping rates are calculated using the Miller–Abrahams or Marcus type hopping expressions. However, KMC models explicitly calculate Coulomb interactions. If charge transport is being modelled in the context of a device, one must ensure that the voltage boundary conditions at the electrodes are maintained by including additional 'image charges,' which are the reflection of charges in the OSC in the plane of the electrodes. Indeed, image charges of image charges (and so on) are required to strictly enforce voltage boundary conditions [129, 142], although these are sometimes ignored with no apparent impact on predictive capability [143]. The computational burden of calculating Coulomb interactions is significant, hence a number of authors have developed techniques to balance accuracy with run time as discussed further in section 2.3.3.

To calculate the current–voltage characteristics of a device it is necessary to allow charges to hop to the electrode from the semiconductor (extraction) and vice versa (injection). Extraction of charges from the semiconductor is a hopping process with the charge in energy set equal to the difference in energy between the site (including electrostatic interactions) and the Fermi level of the electrode. Injection, by contrast, is included by considering an array of charges stationed outside the device which can hop into the adjacent semiconductor [48, 129, 144]. In some cases the injection hops are restricted to the first layer of OSC sites within the device [48], consistent with nearest-neighbour hopping, or successive OSC layers into the device with an exponentially decreasing rate [144], consistent with variable-range hopping. Section 2.3.3 discusses in more detail how injection in KMC models can be modelled efficiently.

To model the process of charge generation in OPV devices, one must additionally consider the photogeneration, transport, relaxation and dissociation of excitons [145, 146]. In keeping with the ethos of KMC modelling, this is usually achieved by considering rate equations which are believed to be appropriate for OPV materials and fitting the model to experimental data [147, 148], although quantum chemical calculations can be integrated to examine exciton transport in more detail [146]. Photogenerated excitons are created at random sites within the simulation volume at a rate which is proportional to the incident light intensity and absorption length of the materials in question. Photogenerated excitons then hop with a modified Miller–Abrahams rate [145]:

$$W_{ij} = \nu_0 \left(\frac{R_0}{r_{ij}} \right)^6 f(E_i, E_j). \quad (5)$$

Where the terms have the same definition as in equation (1), and R_0 is the exciton localization radius. Exciton hopping competes with exciton relaxation characterised by a lifetime, τ_{ex}, which is chosen to match experimentally observed lifetimes. The remaining fitting parameters are chosen to give exciton diffusion length of the order of 5–10 nm seen in experiment [149]. Excitons which diffuse to a donor–acceptor interface are usually considered to immediately dissociate into a charge transfer (CT) state or electron–hole pair. This is in agreement with spectroscopy which shows fast exciton formation following photoexcitation. Those excitons which decay prior to dissociation are lost from the simulation.

We now move on consider charge recombination, which occurs in a wide range of bipolar electronic devices, such as OPVs [150], OLEDs [7], and ambipolar OTFTs [151]. In the case of OLEDs and ambipolar OTFTs the recombination of electrons and holes to form excitons does not (usually) involve significant energetic barriers or spatial separation of charges, and as such is usually assumed to be instantaneous for adjacent charges (i.e. the recombination rate, $W_{rec} \rightarrow \infty$) [139, 152]. The circumstances for OPVs are more complex as the CT state, which spans the donor and acceptor molecules, must be considered. The CT state is intermediate between free charges and excitons, and so is significant in both charge generation (i.e. the process whereby charges are generated by excitons) and charge recombination (i.e. the process whereby charges recombine to form an exciton of some description). The nature of CT states is discussed further in section 4.2 and elsewhere [153], and so here we will only highlight a few points relevant to the implementation of KMC models. First, experiments have shown that a manifold of CT states can be excited by a dissociating exciton, while charges recombining non-geminately are likely to be relaxed. Hence the recombination dynamics of GR and NGR may be different [154–156]. Second, calculations have shown the lifetime of the excited CT state to depends sensitively on the molecular arrangement of the donor and acceptor molecules in the region of the heterojunction [157, 158]. This poses particular challenges for solution processed devices which are inevitably disordered to some degree [159, 160], consequently leading to the possibility of a distribution of recombination rates. Small-molecule devices fabricated by evaporation may also be subject to this complication, as different molecular packing can lead to different OPV performance [161].

Now that we have discussed the various processes that may occur in a KMC model, we turn to consider the organisation of the program itself. MC models are naturally organised into a series of events (e.g. hops, recombination events) separated by waiting times, and as such, KMC simulations proceed by executing the successive events in the 'queue.' Inserting new events into the queue as the simulation evolves can be achieved efficiently using so-called heap algorithms [162]. It is important to note that the calculated behaviour for a particle is only valid provided the rates of the various possible behaviours do not change during the waiting period. Adding, moving or removing a charge within a device will change the electrostatic environment, meaning that to be strictly accurate the behaviour of all other charges should be recalculated. This recalculation implies a significant computational effort, and while some KMC models operate on this basis [141, 143], many instead use a simplification known as the first reaction method (FRM) [48, 147]. The FRM involves calculating the behaviour for a particle (a charge in this case) once only when it is first moved to its new position and not recalculating the behaviour thereafter [163]. Studies have found the impact of the FRM assumption on geminate charge pair dynamics to be minimal [164].

2.3.2. Quantum chemical MC (QCMC). Like the KMC model, the first step in performing a QCMC simulation is to define the system within which charge transport will occur. In a QCMC model this involves the calculation of a realistic morphology and the electronic properties derived from it. Such models therefore require significant human and computational effort but retain the explicit link between nano-scale form and function that is absent from their KMC counterparts. This section will outline the organisation of QCMC models as well as some of the considerations peculiar to the technique, however, this will necessarily be brief since QCMC modelling is both a broad and detailed subject. Interested readers are directed to recent reviews [36, 165–171] and papers with comprehensive descriptions of the techniques used [172] should more detail be required

The morphology in QCMC models requires atomic resolution to enable calculation of electronic properties. In the case of OSCs which are well-described by a crystal structure, one only needs to define the unit cell, which in turn can be determined by experiments such as wide-angle x-ray scattering and solid-state nuclear magnetic resonance [173, 174]. The morphology of disordered OSCs is usually determined by a molecular dynamics (MD) simulation, in which atoms or sections of molecules are considered as points which interact via force-fields. MD simulations may resolve atomic detail [175, 176], or be coarse-grained, in which case the molecular structure is simplified into structural units [177, 178]. In both cases the force-field must be calibrated for the OSC in question [179]. However, it should be noted that developing and calibrating force-fields is a detailed process for OSCs [177, 180–182]. An aim in the generation of the morphology is to

ensure that the simulation volume is sufficiently large that the bulk behaviour of the OSC is being sampled. When considering this issue, it is helpful to define the typical lengthscale over which conductance fluctuations occur, L_0 [122]. If the simulation volume is larger than L_0, it is likely that bulk behaviour is being measured, while if the simulation volume is smaller, it is likely that region-specific behaviour is being measured. A hallmark of measuring region-specific behaviour is that charge transport properties depend on simulation volume size [183, 184]. Course-grained models have an advantage when generating morphologies for disordered materials with small L_0, since larger volumes can be considered. However, while coarse-grained models have some advantages over their atomistic counterparts, one must be able to work backwards from the coarse-grained morphology to atom-level detail to allow calculations of electronic properties [172, 185].

Once the morphology has been produced, the next task is to divide it into conjugated segments where charges may reside. Here one considers whether structural flexibility in the OSC molecule may be sufficient to break the π-conjugation and form distinct conjugated segments. For example, in a polymer OSC, the π-conjugation along the polymer backbone may be broken by torsion or bending [186]. A morphology containing many OSC molecules will therefore be further sub-divided into conjugated sections between which a charge may hop. The hopping rate between segments requires calculation of the electronic transfer integral, J_{ij}, site energies, E, and reorganization energy, λ as shown in equation (2). Zerner's independent neglect of differential overlap (ZINDO) is a popular approximate technique to compute J_{ij} [187] which has been used successfully in disordered [188] and crystalline OSCs [189]. Where greater precision is required density functional theory (DFT) can be used instead [190, 191], albeit at significantly increased computational cost. Site energies can be calculated by summing electrostatic interactions from neighbouring atoms [192], while the reorganisation energy can be related to the energies of the neutral and cation species involved in the reaction [193]. With this information the hopping rates between segments can be calculated and the charge transport simulation can proceed in the same manner as for KMC described above.

2.3.3. Computational efficiency. Generally speaking, KMC models simplify some aspects of molecular geometry and its consequent impact on electronic coupling to describe 'large' problems containing many charges or even an entire device. QCMC models, by contrast, explicitly calculate the impact of molecular geometry on hopping rates in typically 'small' systems containing relatively few molecules and/or charges. In essence, MC models have a certain 'computational budget' that is either expended by greater precision in calculation of hopping rates (QCMC), or larger systems (KMC). As a result, molecularly precise, 'large-scale' MC charge transport models of an organic electronic device are not generally possible, even despite an abundance of computing resources. However, it is worth noting that MC models have been treated largely as tools to examine specific physics-based problems, rather than subjects of study in themselves. As a result, relatively little work has been published concerning how MC models for charge transport in OSCs can be made more efficient. This makes achieving greater computational efficiency in MC models a promising research area since any improvements in MC efficiency can be expended by examining problems in greater depth and realism. Indeed, there is a wealth of literature concerning interacting particle simulations from other research fields showing the significant improvements in performance can be achieved [194–200]. This section will present an overview of the literature which discusses the efficiency of MC charge transport models, as well as the measures that have been shown to improve it.

A significant task within the KMC model is to calculate the electrostatic interactions which determine hopping rates [142, 143], and as a consequence, there have been a number of papers considering how to calculate electrostatic interactions efficiently. In early KMC models, electrostatic interactions between charges and image charges were only calculated within a cut-off radius, r_c which was set to the Debye length [147, 201] or Coulomb capture radius [48]. While this is effective at reducing the computational demand, it has also been shown to reduce the accuracy of simulations for small values of r_c close to flat-band conditions [142]. An alternative approach is to calculate the electrostatic potential only at the origin and potential destination sites a charge may hop to [143]. This method reduces the computational burden in devices with low charge densities (e.g. OPVs) sufficiently that all charge and image charge interactions can be included. Furthermore, it is possible to also exploit the fact that calculations are performed on a lattice and hence can be precalculated before a simulation begins, in addition to exploiting the inherent symmetries in the potential function [142]. Using this latter approach Casalegno *et al* [142] were able to speed up OPV simulations by a factor of more than 7. An alternative approach is to in calculate Coulomb interactions explicitly for particle separations smaller than r_c, and as layer-averaged quantities for particle separations $>r_c$ [129, 202]. Although one has to be careful to ensure that charges are not double-counted [129], this approach allows one to trade-off speed and the accuracy of long-range Coulomb interactions through choice of r_c. An advantage of this approach is that it is possible to maintain the full accuracy of short range Coulomb interactions, which have been shown to assist detrapping of charge [129] and hence have a significant effect on predicted current [121]. Still further gains in efficiency are possible by borrowing ideas from interacting particle simulations. One such example is of a Barnes–Hutt tree code [199], which is an algorithm developed for efficiently calculating long-range force interactions in arbitrarily complicated 3D systems (e.g. galaxy formation). More specifically, it involves dividing the simulation region into cells, and representing the particles within that cell as a single pseudo-particle used for calculations. The structured way in which this is achieved allows significant increases in speed for parallel architectures whilst simultaneously allowing control over errors.

A computationally intensive task such as a MC model naturally lends itself to solution on a multi-core computer system such as a graphics processing unit (GPU) or a supercomputing

cluster. However, while offering greater computational resource, such systems require decisions to be made as to how those cores are used. One approach, termed 'embarrassingly parallel,' involves assigning an individual simulation (e.g. finding the current flowing through an OLED at 1 V) to an individual core. This approach minimises the slow process of copying data from one core to another, but also imposes a limit on how fast the simulation can complete since only one core is used per simulation. This can be mitigated by taking a distributed approach in which a single simulation is shared across many cores, typically meaning that each core represents a different area of the device in question [121]. When taking this approach one must be careful to ensure that the gains in speed obtained are not balanced out by the implied greater use of slow network communications. Furthermore, one must ensure that the simulation 'clock' on each node is synchronised. van der Kaap and Koster [203] developed an algorithm to address these issues for charge transport simulations using a GPU. Their work shows that the simulation parameters (e.g. charge density, strength of Coulomb interactions, size of simulation volume) and hardware (speed of communication network over the GPU) together determine the efficiency of the algorithm, with maximal performance in this case being achieved at charge densities of 1 charge per 100 sites. While this report suggests that optimising algorithms for distributed computing might be an empirical process, it nevertheless shows that distributed computing can be a significant benefit in high charge density simulations with which MC models have traditionally struggled.

A final challenge is to efficiently calculate charge injection at the contacts. In KMC, charge injection is modelled as a thermally assisted hop from the metal Fermi level to each of the sites adjacent to the electrode [48, 129, 141, 143]. The injection hop rate will vary across the contact due to local variations in site potential and electrostatic interactions, and so the waiting time for injection must be calculated for each interfacial site. In turn this means the number of calculations relating to injection scales as the electrode area. Furthermore, it is often likely that the injected charge will be to hop back into the electrode rather than into the bulk of the device [137]. Hence the charges at the interface are in a state of dynamic equilibrium, maintained by computationally expensive hops to and from the electrode. The computational expense becomes more significant as the energy barrier for injection reduces. In some cases this means that KMC (as currently implemented) are abandoned in favour of other approaches [137], or use multiscale methods [119]. However, such problems have been encountered in KMC models in other areas of research. For example, partitioned based searching of rates (e.g. for selection of the next event) [204], reduction of the rate for fast-repeating events (e.g. hopping to and from a contact) [198], or coarsening the simulation in regions where events are repeated (e.g. a *cul de sac* within a morphology) [205], have been demonstrated to speed the calculation of system behaviour when rates span many orders of magnitude. It is noted that KMC models of charge transport have shown similar computationally expensive and physically uninteresting 'back-and-forth' hops between energetically similar sites [205–207]. Consequently, standard charge transport simulations may also benefit from such techniques.

3. Application to charge transport

3.1. Mobility in OSCs

In this section we review the findings of simulations which examine mobility, μ in OSCs. This covers a wide range of issues that span from the meso-scale, such as the impact of energetic disorder, to the nano-scale, such as the impact of molecular morphology. However, before we discuss these studies, we will briefly summarise what is meant by mobility and the issues this presents for organic electronic materials and devices.

Charge transport is ultimately only interesting because it leads to electron or hole current in devices. The current densities for electrons (J_n) and holes (J_p) can be written most generally as:

$$\overrightarrow{J_n} = en\overrightarrow{v_n} \tag{6}$$

$$\overrightarrow{J_p} = ep\overrightarrow{v_p} \tag{7}$$

Where n and p are the electron and hole carrier densities respectively, and $\vec{v}$ is the ensemble average velocity for the given charge type. While these equations are simple, they are not useful in most circumstances since they require knowledge about the electron and hole velocity distributions. However, they can be re-cast as the Boltzmann transport equation and further simplified to yield the drift-diffusion equations [26]. As one might expect, the drift-diffusion model describes the velocity distribution of charges by two idealised contributions, drift and diffusion. Drift models the movement of charge due to the local electric field, as quantified by the drift velocity, $v_d = \mu E$. It is here where the concept of mobility arises. Whether drift and diffusion, and hence mobility, is a good approximation of the velocity distribution therefore depends on how appropriate the assumptions underpinning drift-diffusion [26] are for the material in question. Experiments have shown that energetically disordered materials can display behaviour which is anomalous in the context of the classical drift-diffusion model, most notably dispersive transport [208, 209] as well as charge density- and temperature-dependent mobility [210–212]. A variety of methods are used to measure mobility is measured in OSCs, including fitting to steady-state current–voltage curves (e.g. as for OTFTs [213] and SCLDs [214, 215]) or to the transient response resulting from changing voltage or light intensity (e.g. as in CELIV [216, 217] or time-of-flight [218] measurements). The non-classical behaviour of charge transport in OSCs can lead to different measurements giving different mobilities for the same material [219, 220].

The interesting questions these findings raise are discussed further below, but it is often the case that the assumptions underpinning mobility do not marry well with the charge transport physics in OSCs. As such, some of the original meaning of mobility in OSCs may be lost. This has been

discussed in more detail by Tessler and co-workers [29, 221]. Notwithstanding this, however, mobility is a convenient metric of how 'good' charge transport is in a particular material. Furthermore, the idea of mobility can be used in DD models to predict and interpret organic electronic device performance, although as described below, some corrections are required to describe the energetically disordered transport environment [29]. So, with health warnings concerning mobility duly noted, we move on to consider studies that examine mobility and its relationship to two common properties of OSCs: energetic disorder, and molecular (dis)order.

3.2. How mobility is affected by energetic disorder

Perhaps one of the most significant aspects that determine mobility in OSCs is the presence of energetic disorder. Energetic disorder is the local variation in the HOMO and LUMO of OSCs, which is largely a consequence of variations in local molecular order [34], and collectively leads to a distributed DoS function. The DoS can be determined by fitting to experiment [222] or calculated directly [223, 224]. Bässler and co-workers were amongst the first to use of KMC models to understand charge transport in OSCs [225]. A significant outcome of this work was the development of the so-called Gaussian disorder model (GDM), in which KMC was used to model the behaviour of charges in the low charge-density limit assuming a Gaussian distributed DoS of standard deviation σ, and site energies that were not spatially correlated. The GDM has been used to fit experimental time-of-flight data for a number of materials [225, 226]. However, experiments suggested Poole–Frenkel type mobility, i.e. $\mu \propto \sqrt{F}$ (where F is field) over a wide field range, while the GDM only shows such behaviour at high electric fields. It was argued that this apparent discrepancy was due to correlations in site energies not considered in the GDM [227, 228], for example, as may arise from charge-dipole interactions [227] or molecular geometry fluctuations [229]. A revised correlated disorder model (CDM), based on KMC modelling similar to the GDM, was demonstrated to show Poole–Frenkel behaviour over a wider field range [227]. However, it was later shown in both experiment [219] and simulation [230] that mobility is additionally charge-density dependent, which was not considered in either the GDM or CDM, since the simulations for both models were performed in the Boltzmann (i.e. low charge-density) limit. As charge density is increased from this Boltzmann regime, charges begin to interact, and so the ensemble is better described by Fermi–Dirac statistics [231]. In the Boltzmann regime, mobility is mostly charge independent, while in the Fermi–Dirac regime, mobility increases with charge density. The increase in mobility with charge-density is largely due to trap-filling within the DoS, since additional charges are less likely to be trapped than those that came before, and so on average, are likely to be more mobile [128]. Subsequent KMC simulations have shown that Coulomb interactions between charges also contribute to the charge-density dependence mobility [128, 129], since increased charge-density can 'declot' charges that may be stuck in deep traps [129].

Motivated by the charge-density dependence of mobility shown in experiment, Pasveer *et al* [86] developed a ME model which permitted variable charge density and assumed uncorrelated, Gaussian distributed energetic disorder. This included a prohibition on double occupancy of charges at a site, but did not include the impact of short-range Coulomb interactions. The resulting data were parameterised by an expression, commonly referred to as the extended Gaussian disorder model (EGDM), which is dependent on temperature (T), charge-density (p), electric field (F) and disorder (σ). The parameterised EGDM has subsequently been used in DD models to successfully fit a variety of rich experimental data, e.g. [92, 232, 233]. In particular, the EGDM revealed that the mobilities calculated by fitting the Mott–Gurney relationship (which assumes a constant mobility and drift-only transport [214]) for SCLDs to experimental data that showed anomalous thickness [135] and temperature dependence [233], could be explained by taking into account the charge-density dependence of mobility. However, while the EGDM has addressed important issues that were not considered in the GDM and CDM, it is noted that there are other models which include the effects of charge-density (not discussed here) but differ slightly in their assumptions [46, 87, 210]. When these alternative models and the EGDM are fitted to the same experimental data, differing values of σ are obtained [87, 92, 231]. While one can judge the appropriateness of the underlying assumptions of the model by its quality of fit to experimental data, one might need to be careful in the interpretation of σ given that multiple models lead to similar fits to data. However, while there are variations in the fitted σ between different materials and simulation methodologies, it is generally the case that σ is of the order of 0.1 eV in both solution-processed [92, 226, 234] and evaporated small molecule [235–237] OSCs.

It is anticipated that the assumption of a Gaussian DoS is a reasonable description of the real DoS in OSCs [225, 227]. Direct measurement of the DoS has shown this to be largely the case, but also that small deviations from this ideal can occur [222]. This can however be significant, since a complex DoS can impact mobility as per the arguments above [40], and further, the presence of trap states can lead to SRH recombination [106, 238, 239]. Hence it is useful in some circumstances to determine the DoS without assuming a functional form [240]. MacKenzie and co-workers [107, 108], for example, achieved this by fitting a DD model to transient photocurrent measurements in poly(3-hexylthiophene) (P3HT): Phenyl-C61butyric acid methyl ester ($PC_{61}BM$) OPVs. They showed the DoS to be a superposition of Gaussians, each of which may represent the DoS associated with different packing geometries [107]. This approach allows electrical investigation of the DoS under operating conditions which could be used, for example, to examine the presence or formation or traps, or to correlate features in the DoS brought with features in the morphology. However, it has been shown that one has to be careful about how experimental data is collected and interpreted to ensure unambiguous determination of the DoS [108]. A further approach which is useful when

the relationship between the DoS and molecular conformation or chemical impurities is of interest is to calculate the DoS directly. For example, Nicolai *et al* [40] used density functional theory to suggest that hydrated-oxygen complexes may introduce deep electron traps in a range of common polymer OSCs.

However, irrespective of the form of the DoS, energetic disorder is generally present in OSCs. Furthermore, the width of the DoS is generally significant with respect to the available thermal energy. This has a number of effects on charge transport that extend beyond charge-density dependent mobility. The next we will consider is diffusion. In the classical case of band transport in a non-degenerate semiconductor, the relationship between mobility and diffusivity when the field is small is given by the Einstein relation [241]:

$$\frac{D}{\mu} = \frac{kT}{q}, \tag{8}$$

where D is the diffusion coefficient. Charge transport in OSCs is however via thermally activated hopping through a broadened DoS, and so as one may expect, the relationship between mobility and diffusion coefficient may deviate from this relationship [82]. In particular, experiments on OSCs have shown larger than expected diffusion coefficients [242] and that charge transport that is more dispersive than expected [243]. Motivated by this deficiency, the generalised form of the Einstein relation has been solved to give analytical expressions for diffusion coefficient in the case of exponential- [85] and Gaussian-distributed [84] DoS. Later MC simulations in an OSC with a Gaussian DoS showed that deep traps enhance the apparent diffusion coefficient along the field direction to an extent that depends on field, as trapped carriers lag behind the 'diffusion front' of untrapped charges [244]. As such, the degree to which charge transport agrees with the classical Einstein relation depends upon the trap density [83], and indeed, diodes in which traps are discharged via recombination can be well-described by the classical Einstein expression [80]. This is an example of observable quantities depending on both material properties and the context in which charge transport occurs. Indeed, one could argue that charge transport in OSCs is sufficiently complex that alternative models are more helpful than the classical metrics of drift and diffusion, even when corrections are applied [245].

Energetic disorder also naturally leads to preferred charge transport routes through the OSC. Hence, one should expect some current heterogeneity in even 'neat' OSC films, since local current will depend to some extent on local energetic disorder. This was demonstrated by Yu *et al* [125] using an ME model to simulate the current paths through an energetically disordered Cartesian lattice as shown in figure 4. It can be seen that charge transport is heterogeneous at low electric field, and more homogeneous at higher electric field. More generally, the degree to which charge transport in OSCs is heterogeneous depends on the electric field, temperature and disorder [122, 126, 183, 246]. The heterogeneous nature of current flow in OSCs is, to some extent, shown in (photo) conductive AFM measurements [247], although it is important to note that the resolution of an AFM measurement is

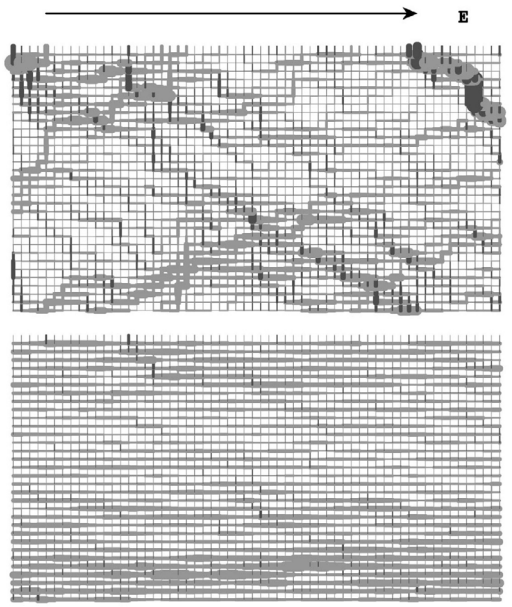

Figure 4. Carrier pathways for applied electric fields of 5×10^4 (upper panel) and 2×10^6 V cm^{-1} (lower panel). The widths of the lines represent the current flowing through the bond. Reprinted figure with permission from Yu *et al* [125]. Copyright 2001 by the American Physical Society.

determined by the tip geometry (~10 s of nm) and the shape of the electric field profile between the tip and plane electrodes [248]. Further experimental evidence is provided by the dispersive nature of time-of-flight characteristics [218]. Here the distribution in carrier transit times can be viewed as being (at least partly) due to a multitude of parallel paths through the film, each of which having different charge transport properties arising from local disorder [246].

The question of what behaviour charge transport obtains due to its heterogeneous nature is one that is very similar to those appearing in percolation theory [249, 250]. In this framework, hopping transport can be represented by a network of resistors with random values that relate to the hopping rate between sites. The resistor network can then be divided up into clusters of resistors with conductance above a critical value, which do contribute to conduction, and those which do not. Perhaps unsurprisingly, since charge transport in OSCs is not as 'binary' as that described by such models, the predictions of classical percolation theories differ to numerically exact approaches such as ME [231]. Nonetheless, the ideas of percolation theory, and variants of percolation theory [49], can be useful to describe charge transport in OSCs. For example, some have used percolation ideas to explain the temperature dependence of mobility associated with VRH [251] and how it depends on the DoS [81, 210, 252]. However, here we will focus attention on the consequences heterogeneous charge transport has for devices.

Massé *et al* [122] used an ME model to predict the length-scale over which significant conductance fluctuations occur in OSC devices due to disorder, L_0 (significant here being defined as when the mean square conductance fluctuation is at least as large as the mean conductance). It was found that a typical polymeric OSC with uncorrelated disorder has

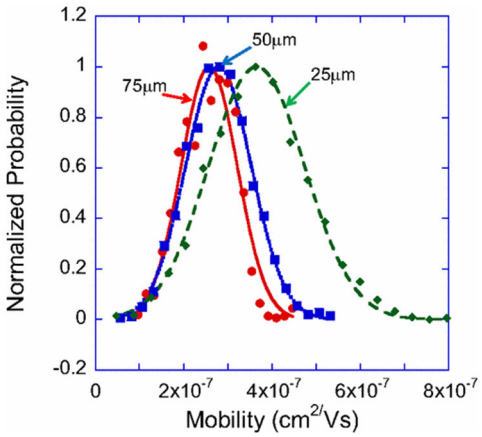

Figure 5. The distribution of mobilities assuming $\sigma = 3kT$ and an electric field of 5×10^4 V cm^{-1}. Three device thicknesses are shown, $d = 25$ μm, 50 μm, and 75 μm. Reprinted figure with permission from Rappaport *et al* [246]. Copyright 2007 by the American Physical Society.

$L_0 \sim 10$ nm. While this length is smaller than the thickness of most devices, it could be similar to the lengthscale over which significant charge density gradients occur. The small molecule tris(8-hydroxyquinoine) (Alq_3), having a large dipole moment that leads to correlated disorder, was predicted to have $L_0 \sim 100$ nm, which is similar or larger than the device thickness of most OLEDs. These data show that considering heterogeneity will be important in both model development and analysis of data for fairly typical organic electronic devices. This was further demonstrated in the context of a SCLD by van der Holst *et al* [253]. They showed that a 1D DD model underestimated current when the SCLD thickness was small and disorder large (i.e. when L_0 was big compared to the device thickness), notwithstanding the fact that the parameterisations of mobility used included the impact of energetic disorder and heterogeneous current. Simulations have also shown that spatial heterogeneity affects the transient behaviour of charge transport in addition to steady-state behaviour. Rappaport *et al* [246], for example, used an ME model to examine the impact of different configurations of energetic disorder on transit time through devices of varying thickness. Figure 5 shows the distribution of mobilities measured for different configurations of disorder, each of which corresponding to different routes through the film. The mobility distribution is shown to narrow as the device gets thicker, and more specifically that 'fast' routes through the film gradually disappear. Hence, it is again shown that both the OSC properties and the context in which charge transport occurs determine device behaviour.

So far we have largely ignored the role of the carrier energy distribution in charge transport. In the low-field, vanishing charge density limit, the carrier energy distribution is described by Boltzmann statistics, which in the case of hopping through a Gaussian DoS, leads to an equilibration energy σ^2/kT below the band centre [225]. Increasing (i.e. finite) charge density is instead described by Fermi–Dirac statistics. In the case of amorphous semiconductors, applying an electric field heats the carrier energy distribution with respect to that described by these classical models [254, 255]. Indeed, Preezant and Tessler showed that field-induced heating of the carrier energy distribution is equivalent to an increase in lattice temperature of up to 100 °C in some cases [255]. While the carrier energy distribution may be affected by the application of a DC [254, 255] or AC field [256], carriers may also be introduced into the device with a 'hot' energy distribution with respect to equilibrium, for example by photoinjection [154, 257–259] or injection from the contacts [144, 260]. Absent of any additional external source of energy, thermally activated hopping will naturally push such 'hot' carriers toward dynamic equilibrium [261]. Given that 'hot' charges are more mobile on average [225], non-equilibrium energy distributions will naturally lead to transiently enhanced mobility. A current open question is whether transiently enhanced mobility plays a significant role in the operation of organic electronic devices. For example, it has been argued that enhanced mobility following exciton dissociation in OPVs (NB—not invoking hot charge transfer states) leads to efficient charge generation [257, 258], although other reports disagree on this point [259, 260]. An area where there does appear to be agreement is that equilibration of the carrier energy distribution (and therefore mobility) can occur over surprisingly long timescales, reaching 10 s of nanoseconds in some cases [257, 258, 260]. However, the timescale over which equilibration occurs has been shown to depend sensitively on charge concentration and the degree of disorder [256], emphasising the importance of performing simulations relevant to the material at hand.

3.3. How mobility is affected by morphological order and disorder

The morphology of OSCs can have structure at multiple lengthscales [25, 262], and which of these morphologies is formed can have a significant impact on measured mobility [263–265]. However, unravelling the morphology-mobility relationship by experiment alone can be challenging. In this section we discuss some of the recent insights made possible by charge transport models focussed on the morphology-mobility relationship in OSCs. We begin with the impact of blend morphology, before moving on to consider molecular morphology in pristine OSC films.

Groves *et al* [117] and Koster [124] used KMC and ME methods respectively to examine the impact of donor–acceptor morphology in BHJ OPV blends. The morphologies were generated using a simulated annealing approach [140] which ignores molecular detail but nonetheless results in an isotropic, phase-separated structure. As may be expected, increasing the volume fraction of the non-conducting component reduces mobility, but it is shown that the drop in mobility is precipitous when the non-conducting component increases above 70%, and to an extent which depends on energetic disorder and domain size [117]. It was also shown that blend morphologies can lead to negative electric field dependence of mobility, as observed in experiment [266], since charges have to 'back-track' around morphological obstacles in the field direction [124]. KMC models have also been used to examine how morphology influences the dispersive nature of transport. Frost *et al* [267] modelled a 2-component blend morphology

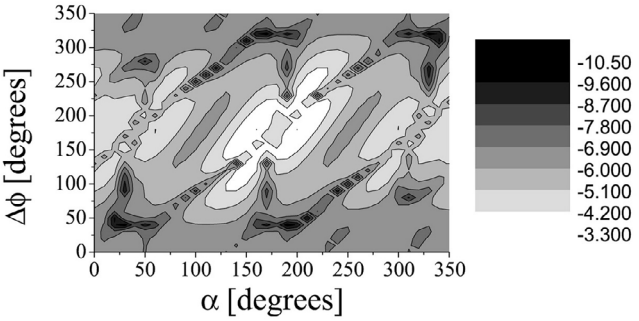

Figure 6. Electronic coupling (J^2) as a function of chain packing angle (α) and relative orientation ($\Delta\phi$) for aligned chains of PFO. Reprinted (adapted) with permission from Athanasopolous *et al* [132]. Copyright 2007 American Chemical Society.

in which polymer chains had either homophilic or heterophilic interactions, leading in turn to aggregated and dispersed morphologies respectively. They showed that aggregated morphologies have more dispersive transport than the dispersed morphologies, even when the hopping rates were the same. Like Koster [124], this was because the charges were increasingly likely to become morphologically trapped in the aggregated film as the field increased. Hence while these studies do not consider the molecular interactions between specific molecules, they nonetheless show the significant impact blend morphology can have upon measured mobility.

We now move on to consider the effect of molecular morphology on mobility in single OSC films. While KMC and ME models may be appropriate to examine the mobility in amorphous polymer OSCs [165], they unlikely to be suitable when considering materials with strong anisotropy in electronic coupling or morphological order. In such cases, QCMC models are instead used [165–168, 268, 269]. The importance of taking such an approach is demonstrated, for example, by Athanasopolous *et al* [132]. Figure 6 shows the predicted variation in electronic coupling as a function of packing and orientation for neighbouring straight chains of poly-(9,9′-dioctlyfluorene) (PFO), a high-mobility OSC used in OLEDs. The electronic coupling between PFO molecules can be seen to vary substantially with only minor changes in relative positon and orientation. The authors went on to show that different packing geometries of PFO can have mobilities which differ by more than 2 orders of magnitude. Such variations in electronic coupling with minor variations in relative position are not unique to polymers, for example, Brédas *et al* [270] showed that mere Ångröm-scale shifts in relative displacement of sexithienyl molecules can flip the assembly from favouring hole to electron transport and vice versa.

Anisotropy in electronic coupling and morphological (dis) order can lead to some routes through an OSC being more efficient at conducting charge than others in a similar way to energetic disorder. In some circumstances this can lead to the bulk OSC charge transport properties being dominated by a small number of relatively high conductivity 'filaments' that thread through the film. How these filaments are distributed through the film, i.e. the form of the percolation network, often determines the bulk mobility of the OSC [133]. An example of this is given by Kwiakowski *et al* [184] who simulated charge transport in ordered and disordered films of Alq_3. The distribution of hopping rates for the disordered film is shown to vary over 5 orders of magnitude whereas the crystalline film varies by a factor of ~2. Charges traversing through the disordered film therefore sample a much broader range of hopping rates, and as such, have widely different transit times through the film. However, they went on to show that such data cannot simply be explained by a distribution of isolated trap states with varying release times, since removing the deepest trap states made little difference to the simulated behaviour. Instead it was shown that carriers can be trapped in a *cul de sac* of interconnected molecules from which a carrier cannot easily escape to be collected by the contacts. This emphasises the importance of topology of the percolation network in addition to the properties of the individual molecules.

Examples such as this may give the impression that control or engineering of structural order is vital to enhancing mobility of OSCs, and indeed there are many examples of this [271–275]. However, the form of a percolation network is not only due to alignment (or not) or electronic transfer integrals between molecules, but also due to spatial variations in energetic disorder. These two networks may not overlap, leading to complex or unexpected behaviour. For example, Schrader *et al* [276] simulated charge transport in amorphous and smectic phases of a dicyanovinl-substituted oligothiophene, and found that the more ordered smectic phase had lower mobility despite also having lower energetic disorder. This puzzling result could be understood by considering the energetic disorder sampled by the charge, rather than the energetic disorder of the bulk film. In this case, the coupling resulting from smectic ordering encouraged charge to explore a 2D cross-section of the film, meaning that many values of energetic disorder were sampled. This compared to the amorphous film where more isotropic coupling enabled charges to explore a 3D route around energetic obstacles, thereby sampling a smaller subset of values of energetic disorder on the way to the contacts. As strong electronic coupling is often anisotropic, it may not always be the case that ordered films result in higher mobility, since charges would simultaneously become more prone to trapping or being unable to circumvent energetic obstacles. This sort of behaviour has been reported for a number of small-molecule OSCs [68, 130, 277, 278].

Examining the link between molecular morphology and mobility is challenging in polymer OSCs due to their high aspect ratio and many degrees of conformational freedom. However, simplified models of polymer OSCs can aid in developing intuitive models of how mobility and conformation are related. For example, Carbone and Troisi [279] developed coarse-grained models of archetypal polymer morphologies (namely rigid rods, Gaussian chains and worm-like chains) and examined what roles intra-chain and inter-chain hopping played in charge diffusion through them. Surprisingly, it was found that diffusion coefficient through rigid chains was limited by mostly by intra-chain hops, and by both intra-chain and inter-chain hops through 'floppier' chains to an extent that depends on the persistence length (i.e. the 'stiffness' of the chain). This is counter to the expectation that slower, inter-chain hops act as a rate-limiting step in

charge transport through an OSC film. Further studies have been published relating to specific, well-characterised OSC polymers such as P3HT [175, 176, 185, 186, 224, 280–282], poly(phenylenevinylene) (PPV) [283] and poly(2,5-bis(3-hexadecylthiophen-2-yl)thieno[3,2-b]thiophene) (PBTTT) [284, 285]. An important theme of this work is the impact of solubilizing side-chains on the DoS and electron transfer integrals through the film. P3HT is an example of a polymer OSC whose electronic properties are strongly influenced by the positional (dis)order imposed by side chains [186, 282]. Reducing the regioregularity of P3HT increases the bandgap and pushes quasi-band (high-mobility) states to less accessible energies [176]. Hence the degree of localization depends on energy, something that has been observed for other polymers [283], and is counter to the standard assumption in VRH models. For a relaxed P3HT chain, the lowest HOMO or LUMO level tends to be localised to a few thiophene units of the backbone [186]. The extent to which these low-lying states are localised and their energy largely depends on backbone torsion [224, 282], and to a lesser extent chain bending [186]. Such localization can have a significant impact on mobility, indeed, adding a small concentration of side-chain defects can reduce mobility by a factor of 10 [280].

P3HT and PBTTT, when processed appropriately, both form a lamellar structure [234, 286]. Simulations of such lamellar polymers have suggested that variations in the intermolecular spacing, or paracrystallinity, can limit the observed mobility [280, 284]. Experiments show that PBTTT shows a higher mobility that P3HT, which simulations suggest is due to the improved order in the former [287, 288]. However, while the mobility in lamellar structures may be limited by paracrystallinity, many solution cast films (including P3HT and PBTTT) are semi-crystalline with regions of amorphous polymer in-between [38]. Simulations show that complex structure can lead to complex charge transport behavior on multiple lengthscales, with short-range order determining transport within a crystal, but with crystallite connectivity also playing a role in long-range charge transport [185, 289]. The significant dependence of mobility on structure in these OSCs show that mobility can be engineered via processing and molecular design. Modelling charge transport in the new breed of high-performance OSCs [290–292] would seem to be an attractive area for ongoing research.

To summarize, these examples demonstrate the sometimes complex and counterintuitive charge transport behavior in OSCs. When one examines such materials in more detail, it is rarely the case that behavior is described by a single parameter or effect, and instead one needs to reconcile coincident processes to arrive at a balanced, quantitative understanding. Modelling has an advantage over experiment in such problems since it is possible to examine the behavior of individual charges, consider a range of OSCs and morphologies, and even turn various processes 'on' or 'off' to examine their relative influence. Charge transport models can therefore be an invaluable part of the 'toolkit' for providing quantitative understanding, as well as enabling rational design of molecules and processing conditions [2, 27, 273, 293].

4. Application to organic electronic devices

4.1. Organic thin-film transistors (OTFTs)

Organic thin-film transistors (OTFTs) have developed to a stage where their initial electrical performance now surpasses that of amorphous Silicon, with field-effect mobilities exceeding $1\,cm^2\,V^{-1}\,s^{-1}$ and on-off ratios of the order 10^6–10^8 [8, 41]. This has led OTFTs to become technologically important for a range of novel and low-cost electronic applications, such as rollable displays [13, 14], sensors [11, 12], radio frequency identification tags [294] and electronic circuits [295]. The viability of OTFTs is in large part due to development of OSC materials with high mobility [296–298] as well as better understanding of the physics underpinning bulk charge transport, as discussed in section 3 and elsewhere [41, 263]. The increased mobility of OSCs has increased the current-carrying capability of the OTFT channel, which in turn has placed increased demand on the interface between the electrode and OSC channel to supply this current [50]. A finite voltage is required to inject charges from the source into the channel, or extract charges from the channel into the drain. In an ideal device, this contact voltage will be small and vary linearly with current (i.e. the contact will be Ohmic), but it is often the case in OTFTs that the contact voltage will be significant and vary non-linearly with current (i.e. the contact will be non-Ohmic) [299]. High mobility OSCs will naturally lead to low channel resistances and hence it is more likely that an OTFT will be limited by the contact voltage rather than the intrinsic properties of the OSC [50, 300]. Shortening the OTFT channel to improve speed and reduce operating voltage [301, 302] also increases the relative importance of the contact voltage, which again may lead to an OTFT being contact-limited [50, 300]. Understanding and optimising charge injection from the electrode to the channel is therefore of significant, and growing importance to the operation of OTFTs.

The contact resistance, R_c is the resistance of the OTFT which does not scale with the length of the semiconductor channel, and can be quantified using the transmission-line method [300] or gated four-point-probe measurements [97]. Contact resistance is therefore an experimentally accessible measure of charge injection which quantifies the loss of channel voltage in an OTFT. Measurements have shown the contact resistance of OTFTs can be modified by doping [303], interlayers [304] and self-assembled monolayers [305] and more generally is influenced by film thickness [306], injection barrier [307] and electrode shape [308]. Such variations in contact resistance are predicted to have a substantial effect on the performance of OTFTs. Natali and Caironi [50] calculated the channel length that would result in the OTFT current being halved due to contact voltage, L_{MIN} as a function of mobility, μ and contact resistance, R_c, as shown in figure 7. It can be seen that $L_{MIN} < 10\ \mu m$ requires $R_c < 10^3\ \Omega\,cm$ if $\mu = 0.1\,cm^2\,V^{-1}\,s^{-1}$, which contrasts with the majority of experimental survey data (figure 7 symbols), which have R_c substantially larger than $10^3\ \Omega$ cm. This demonstrates that many high-performance OTFTs are contact limited to some extent, hence we will focus

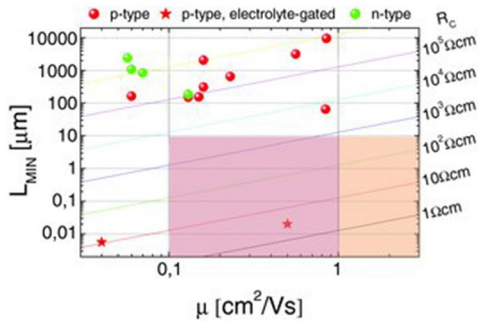

Figure 7. Predicted channel length for which current will be halved due to contact effects, L_{MIN} as a function of mobility, μ and contact resistance, R_c. Symbols denote experimental data for device types as per legend. Pink and orange regions represent required values for $L_{MIN} \leqslant 10$ μm and $\mu \geqslant 0.1$ and 1 $cm^2\,V^{-1}\,s^{-1}$ respectively. Natali and Caironi [50]. Copyright Wiley-VCH Verlag GmbH & Co. KGaA. Reproduced with permission.

our attention primarily on modelling studies which consider charge injection in OTFTs.

OTFTs are a multilayer structure in which the conductivity of an OSC channel is controlled by a gate contact that is separated from the channel by an insulating dielectric. If sufficient gate voltage is applied, charges can flow from the source electrode to the drain electrode through the OSC channel. Two geometries are commonly used: staggered, in which the source/drain electrodes and gate dielectric are on opposite sides of the OSC (commonly with the source/drain electrode on the top of the OSC); and coplanar, in which the source drain electrodes and gate dielectric are on the same side of the OSC (commonly underneath the OSC). Early studies using 2D DD models showed the importance of electrode workfunction and OTFT geometry [96, 309]. Tessler and Roichman [309] examined the electric field distribution in a staggered OTFT and showed that when the injection barrier was increased, the electric field around the electrodes was increased and that a greater proportion of the electrode was utilised. Charge injection in staggered OTFTs is therefore across a surface which is perpendicular to current flow, inevitably leading to some injected charges having to travel further to reach the semiconducting channel than others. How much of this surface is utilised is a balance between the resistance of the channel and that of the contact, further, it is shown that current density is higher at the edge of the contact (so-called current crowding) [97, 310, 311]. Modelling and experiment has shown that the effective size of the injection region increases with OSC conductivity [97, 311]. This can manifest itself as a reduction in the measured R_c with increasing gate voltage, which is due to an increase in OSC conductivity rather than a change in injection [97, 311]. Borndijk *et al* [312] argued that the gate voltage dependence of contact resistance is due to the gate voltage modulating the charge density at the source contact. Similar findings were also reported by Vinciguerra *et al* [313], who additionally noted that the precise variation of contact resistance with gate voltage depended on the form of trapping assumed. Gruber *et al* [314] performed detailed DD simulations on staggered OTFTs including the effects of thermionic emission and tunnelling on injection current. The utilised proportion of the electrode was shown to increase with injection barrier up to 0.6 eV, which coincided with the injection current being dominated by thermionic emission, while above 0.6 eV, the injection current was dominated by tunnelling and utilised area of the electrode was increasingly localised at the edge of the channel. These distinct regimes of injection leads to a non-linear relationship between injection barrier and contact resistance in staggered [314] and coplanar [315], OTFTs.

A comparison of OTFT geometries was performed by Hill [96] who used a DD model to calculate output characteristics for staggered and coplanar OTFT, and then calculated contact resistance in a similar manner to experiment. It was found that the mobility calculated from the simulated OTFT output was much lower than the simulation input for coplanar devices with channel lengths <100 μm. By contrast, the agreement between the apparent mobility and simulation input for staggered OTFTs was much better. It was predicted that contact resistance in staggered devices was both an order of magnitude less, and more dependent on gate voltage, than the coplanar counterpart. Both of these predictions agree well with later experiments performed on pentacene OTFTs [300]. Gundalch *et al* [300] also showed that showed that staggered OTFTs had lower contact resistance than coplanar OTFTs, although the performance was similar for smaller injection barriers. However, Gruber *et al* [315] instead suggests that coplanar devices can in fact perform slightly better than staggered devices when injection barriers are small. This is additionally counter to the results of Hill [96], and it is proposed that this difference may be due to the use of the transmission line method to extract contact resistance (in a similar way to some experiments), while Gruber *et al* [315] calculated contact resistance directly. Of course, there are other possible explanations of the observed difference between coplanar and staggered OTFTs. From an experimental point of view, it has been proposed that evaporation of metals to form source/drain electrodes in staggered OTFTs leads to penetration of the metal into the OSC films, in turn leading to lower contact resistance [316], which cannot be ruled out. Gupta *et al* [98] used a DD model to examine the impact of morphology on OTFTs assuming no injection barrier. It was shown that lower performance in coplanar devices could be alternatively be explained by low-mobility grain boundaries adjacent to the source/drain electrodes. Staggered devices, by contrast, were predicted to be more resilient to the effects of low mobility in the region of the electrodes.

Now we consider charge injection from the electrode into the OSC explicitly. A charge injected into the OSC experiences a potential landscape which is the superposition of the local energy levels, internal electric field, and image potential. If we disregard the possibility of energetic disorder for a moment, the image potential and electric field leads to the formation of a potential maximum a few nanometres away from the source contact. Charge transport in the immediate vicinity of the electrode is therefore critical to determining the eventual injection of charges, as has been demonstrated in experiment [55]. When charges have a low mobility, as is the case in OSCs, charge injection can be thought of as a competition between Langevin-type NGR with an image

charge, which leads to a reverse flow of current, and diffusion over a potential barrier, which leads to current in the bulk [317]. However, KMC simulations by Wolf and Bässler [144] showed that this picture needs to be modified in the presence of energetic disorder. One significant factor is that charges are injected with non-equilibrium energies, and that equilibration can give a sub-linear temperature dependence of injection yield when plotted on an Arrhenius plot, in a similar manner to geminate pair separation [318]. Equilibration within the DoS can therefore have a positive effect on charge injection, however, it can additionally reduce mobility, as described in section 3.2. The balance of these competing effects was examined [144], and it is found that increasing disorder enhances injection for large barriers (here 0.7 eV), but reduces injection for low barriers (<0.4 eV). van der Kaap and Koster [260] performed additional KMC simulations of an SCLD diode, i.e. at a higher charge density than for Wolf and Bässler [144], and showed that the current flowing through an SCLD was largely unaffected by the initial energy of the injected charge. This was further demonstrated by the carrier energy distribution, which was shown to have relaxed to the Fermi–Dirac distribution only ~6 nm from the contact. Hence while disorder may influence the injection probability of an individual charge, the behaviour of the charge ensemble in the context of a device appears to be more complex and, at present, not completely understood.

Injection of charges into a disordered semiconductor is therefore non-trivial, and presents a challenge as to which model to include in DD simulations of OTFT devices. For example, Hamandi and Natelson [319] used a 1D current injection model which assumed hopping in a Gaussian DoS to model the behaviour of coplanar P3HT OTFTs, suggesting that the temperature dependence of drain current could not be described using a simple thermionic emission model. However, Koehler *et al* [95] argued that such models do not reproduce experimentally observed potential drops near the contacts, and that coplanar P3HT OTFTs can be better modelled by instead assuming a combination of thermionic and diffusion-limited injection at the contact and space-charge limited current in the region surrounding it. Other authors also take the approach that injection current comprises a superposition of thermionic emission and tunnelling components [314, 315]. Given the challenge of selecting a model appropriate to the interface in question, one could argue that KMC methods, which do not require analytical injection models, could be used instead. However, KMC OTFT models are at present restricted to channel lengths of ~1 μm [320, 321], although as discussed in section 2.3.3, this may improve as computational efficiency increases further.

DD simulations show that the charge density and local electric field within both staggered and coplanar OTFTs vary significantly throughout the device which in turn may lead to local variations in mobility (as discussed in section 3.2). For example, analysis of experimental data by Tanase *et al* [322] suggested that the mobility of charges drops by more than a factor of 2 when moving only 2 nm from the gate dielectric in P3HT and poly(thienylene-vinylene) OTFTs. The influence of the charge- and field-dependence of mobility on the injection process has been examined, for example, by Schienert and Paasch [323, 324] who employed a 2D DD model using the EGDM [86]. They found that the field-dependence of mobility leads to non-linearity of the OTFT output characteristic with Schottky contacts at low drain–source bias voltages [323]. This was argued to be due to the competing effects of the depletion zone and electric field adjacent to the source electrode. Furthermore, using the EGDM resulted in a significant increase in saturation current when compared to a constant mobility. More generally, the results of simulations including and excluding the charge density dependence of mobility are not comparable, with the former showing curvature of the linear region of the transfer characteristic and an apparent change in the threshold voltage [324]. Given the successes of parameterisations of mobility for describing hopping transport through disordered OSCs in OLEDs and SCLDs [231], it would seem that further studies of OTFTs considering these effects would further improve understanding.

Before closing this section, we will consider briefly some modelling studies of ambipolar OTFTs [151] which are of interest for a range of applications including organic CMOS, light-emitting OTFTs, and electrically-pumped lasers [325]. Ambipolar OTFTs have drain and source electrodes with different workfunctions which allow both electrons and holes to be injected. Hence in order to model such devices one must allow for the possibility of recombination within the channel. Studies on light-emitting OTFTs are a useful benchmark of the recombination process in ambipolar devices since the rate of NGR can be determined by optical inspection of the light-emitting recombination zone [152, 326, 327]. Smith and Ruden [326] developed a model which assumed drift-dominated current and charge-density dependent mobility, and with it, were able to explain the rapid movement of the recombination zone across the channel as the gate voltage was varied. A similar approach was employed by Kemerink *et al* [327] to examine instead the width of the recombination zone. It was found that assuming a Langevin NGR rate generally underestimated the width of the recombination zone, i.e. Langevin over-estimated the rate of recombination. A possible explanation for the observed reduction in recombination rate may be explained by KMC simulations which show the NGR rate for a 2D sheet (i.e. as in an accumulation layer) is lower than that for 3-dimensions [102]. However, DD simulations by Zaumseil *et al* [152] show that charges are not well-confined to an accumulation layer in the recombination zone of a light-emitting OTFT. Hence, as is the case for both OPVs and OLEDs, modelling recombination appears to be one of the more significant challenges in simulation of organic electronic devices.

4.2. Organic photovoltaic diodes (OPVs)

Organic photovoltaic diodes (OPVs) have been the subject of much research due to their compatibility with scalable manufacture processes [4, 328, 329], the high optical absorption coefficients of OSCs matched to solar wavelengths [1], and the

mounting need for alternative energy sources [330]. However, the poor dielectric screening ($2 \leqslant \varepsilon \leqslant 4$) in OSCs means that photoabsorption leads to formation of an exciton with a binding energy larger than kT [331] rather than free carriers. Efficient charge generation therefore requires a heterojunction between two materials, the donor and acceptor, whose energy levels form a type-II heterojunction. Under these circumstances, charge transfer of the electron to acceptor (or hole to the donor) can be energetically favoured [332]. The nature of the charge transfer state following exciton dissociation is an active area of research [153, 333]. Some material combinations favour the formation of transiently 'hot' delocalised charge transfer state (HCT) [154–156], although whether the HCT is a necessary precursor to efficient free charge generation is currently unclear [334, 335]. However, leaving aside the detail of the charge transfer state for the time being, excitons may recombine before they have opportunity to dissociate. The diffusion length of a photogenerated exciton is of the order of ~10 nm in disordered OSCs [149], meaning that type-II heterojunctions need to be distributed through the active layer on a similar lengthscale to allow efficient dissociation. This so-called BHJ architecture can be achieved in solution-processed devices by dissolving the donor and acceptor in a common solvent prior to casting [336, 337], or in the case of evaporated OPVs by co-evaporation [338] or annealing [140]. While it is reasonably straightforward to control the BHJ morphology in a qualitative fashion, e.g. by annealing [339], choice of solvent [340] or solvent annealing [341], exerting precise control is challenging. Matters are further complicated by OPVs displaying structure on multiple lengthscales [247], the possibility of crystallisation or aggregation [38, 342], and the occasional presence of molecularly mixed phases [343, 344]. However, while the BHJ may have a complex form, it is an effective method of converting photogenerated excitons into charge transfer states of some description [345, 346]. However, in addition dissociating excitons, the resultant charges must avoid GR of the charge transfer state and NGR of free charges *en route* to the contacts if the absorbed photon is to result in useful current. Experiment has shown that which mode of charge recombination dominates depends on materials and morphology [347–351]. The efficiency with which absorbed photons are converted into extracted charges, the internal quantum efficiency (IQE), reaches 100% for some systems [352]. Why some OPVs show high IQE despite their apparent disadvantages is an ongoing matter of debate that will be discussed further below.

While the IQE quantifies the processes from photon absorption to charge collection, the amount of power an OPV harvests is of prime interest. The power conversion efficiency (PCE) of a photovoltaic device is given as:

$$\mathrm{PCE} = \frac{V_{\mathrm{oc}} J_{\mathrm{sc}} \mathrm{FF}}{P} \tag{9}$$

Here V_{oc} is the open-circuit voltage, J_{sc} is the short-circuit current density, FF is the fill factor and P is the incident AM 1.5 solar power density [353]. The processes that determine these circuit-level OPVs metrics are inter-related to some extent and so one cannot always optimise them individually [354–356]. That said, J_{sc} often has a strong dependence on morphology [342, 357–360] and, similar to IQE, is a measure of how effective an OPV is converting incident photons into collected charge [361–363]. V_{oc}, by contrast, is largely determined by the energy levels of the constituent OSCs [364–366] and contacts [367, 368]. Recent meta-analyses of OPVs have shown that PCE is strongly correlated with J_{sc}, but only has a weak relationship to FF and V_{oc} [369, 370]. This suggests that while tuning the energy levels of OSCs can certainly benefit to OPV performance [364], there are perhaps greater gains to be made in optimising morphological control through processing [370]. Hence, we focus particularly on studies of OPVs which consider morphology and factors which relate to IQE and J_{sc}.

The most significant differences between OPVs and the simple Onsager–Braun model [88, 89] are the presence of a donor–acceptor heterojunction and energetic disorder in the former, and the assumption of a homogenous iso-energetic material in the latter. Since electrons and holes are confined to the acceptor and donor phases respectively, it follows that the site of GR in OPVs is confined to, or near, the heterojunction. KMC simulations by Peumans and Forrest [371] predicted that GR in in the presence of a heterojunction is substantially lower than for the bulk case, as indeed is shown in experiment [332]. Later KMC simulations on bilayer devices by Groves *et al* [113] and Offermans *et al* [372] show that geminate charges which have yet to recombine or separate nonetheless do not stray far from the heterojunction due to mutual Coulomb attraction. Hence although a donor–acceptor heterojunction appear to only separate geminate charges slightly on average, this is apparently sufficient to markedly reduce the chances of GR. Groves *et al* [113] additionally examined the influence of heterojunction orientation on GR, and found that orientation had little effect unless a component of the electric field forces the geminate electron hole pair into the heterojunction, in which case increasing field increased GR. This behaviour was later observed in a P3HT:PC_{61}BM BHJ OPV at low temperatures by Athanasopolous *et al* [373]. Further KMC modelling by them showed that for such behaviour to be observed, low temperatures, energetic disorder and some degree of ultrafast charge-separation was necessary. However, even though this counter-intuitive behaviour is not often observed, this nonetheless shows the importance of considering nano-scale morphology when trying to understand GR. Albrecht and Bässler [318] were amongst the first to examine the impact of energetic disorder on GR in a single material (i.e. no heterojunction was considered), and found that GR was reduced significantly compared to the Onsager prediction [88]. This was due to charges being created with non-equilibrium energies within the DoS which gave them a transient opportunity to avoid GR. This equilibration of charges also reduced the temperature and electric field dependence of GR with respect to the Onsager prediction, in a manner which agreed with experimental data [374]. van Eersel *et al* [375] later used a similar model with parameters from experiment to show how this effect alone be used to explain low GR in poly[2-methoxy-5-(3′,7′-dimethyloctyloxy)-1,4-phenylenevinylene] (MDMO-PPV): PC_{61}BM OPVs. It is therefore reasonably well-established that equilibration of the geminate pair in an

energetically disordered DoS can suppress GR. A broad DoS also allows for the possibility of charge trapping in addition to equilibration. Groves *et al* [141] and van Eersel *et al* [375] both showed that trapping one charge adjacent to the interface had a surprisingly small effect on GR, and only trapping of both charges at the interface showed the expected reduction in GR. In a similar vein, OSCs with correlated energetic disorder have been shown to have lower GR than an OSC with uncorrelated energetic disorder due to a lower probability of charge trapping in the former [141]. Hence the most basic assumptions of charge transport physics relevant to OSCs and OPVs, namely the presence of energetic disorder and a donor–acceptor heterojunction, both have the effect of reducing GR with respect to the Onsager–Braun model [88, 89].

Bilayer OPVs are the simplest donor–acceptor morphology, and although they outperform OPVs comprising only one OSC [376], their exciton dissociation efficiency is too low for practical applications. Hence for OPVs which rely on conventional exciton dissociation, nano-structured morphologies are required, and device models have been used extensively to understand which forms of morphology are most favourable. As well as bilayers [73, 143, 377], morphologies examined include interdigitated pillars [48, 201, 378–380], gyroids [381], idealised BHJs [48, 147, 201, 380] and non-ideal BHJs [114, 123, 382, 383]. It is shown that interdigitated pillars have highest performance, since the electric field is either parallel or perpendicular to the plane of the heterojunction, while perhaps unexpectedly, gyroid and idealised BHJ morphologies have very similar performance [381]. However, since interdigitated OPVs are laborious to fabricate [384], we focus our attention on the impact of non-ideal (i.e. more realistic) BHJ morphologies on GR. The traditional picture of an ideal BHJ morphology includes sharp interfaces between the donor and acceptor, and domains which are both pure and of a size which balances the competing needs of exciton dissociation and charge transport [147, 385]. Lyons *et al* [114] used a KMC model to examine the relative impact of these morphological factors on OPV performance. Surprisingly, it was found that sharp interfaces between the donor and acceptor had a greater effect on GR than domain size. It was argued that this was because the Coulomb potential decays rapidly away from the heterojunction, and hence the driving force of entropy in the region around the heterojunction [386, 387] has a significant impact on GR. Later experiments and modelling by Yan *et al* [377] on non-annealed and annealed bilayer OPVs, such that the former had a sharper interface than the latter, supported the notion that interface morphology was important in determination of GR. Both Lyons *et al* [114] and Gagorik *et al* [382] showed that impure domains, where they lead to disconnected islands of donor material in the acceptor phase and vice versa, can act as charge recombination centres. This suggests that molecularly mixed phases reported in some in high performance OPVs [343, 344] support ambipolar charge transport [388], since if complete charge transport networks for both electrons and holes were not present in the mixed phase, trapping and recombination would occur.

A common theme of the work discussed thus far is that morphology or energetic disorder in the region of the heterojunction has a greater impact on GR than meso-scale characteristics. Indeed, recent molecular dynamics simulations of a range of OSCs suggest that only short-range order may be necessary for high-performance OPVs [293]. Hence we now move our focus towards the heterojunction itself, and begin by considering HCTs. As discussed earlier, HCTs are high-energy, delocalised charge transfer states that are posited to reduce GR compared to strongly-bound charge transfer states due to reduced Coulomb attraction and temporary band-like transport. Experiments by Bakulin *et al* [154] and others [155, 156, 389] give strong evidence for formation of HCTs, while quantum chemical calculations suggest that HCTs [390], and that long-range exciton dissociation in general [391], may be common in OPVs. HCTs also appear to be associated with aggregation of fullerene-type acceptors [392, 393], something which tallies with experimental studies on polymer:fullerene OPVs [342]. However, this picture is somewhat complicated by further experiments which seem to suggest that the efficiency of free-charge generation is unaffected by whether HCT or strongly-localised charge transfer states are created [334, 394–396]. Jones *et al* [397] used a KMC model to investigate the extent to which initial delocalisation of the HCT state, r resulted in reduced GR for a polymer:fullerene-like morphology. It was found that that the degree of GR depended strongly on r, with low GR as seen in experiment only being observed for r in the region of 10 nm, which is longer than some experimental indications of delocalisation [389] but shorter than others [398]. Hence while HCT states appear to play a role in the suppression of GR in some OPVs, it appears they are not a necessary precursor to high-performance OPVs. We now move on to consider energy 'cascades', that is, a reduction in the energy of the HOMO or LUMO level, Δ as one moves away from the heterojunction into the bulk of the donor or acceptor respectively. Such cascade regions have been predicted to occur at P3HT:$PC_{61}BM$ heterojunctions due to structural disorder in the P3HT chains adjacent to the interface, electrostatic interactions and polarization [399, 400]. Energy cascades of this type are additionally predicted to lead to long-range exciton dissociation [399]. QCMC simulations of charge separation in the 5 nm around a P3HT:$PC_{61}BM$ heterojunction suggested that these factors alone could explain GR as low as 50% for strongly-bound charge transfer states, in agreement with experiment. Other device-scale KMC simulations have shown similar reductions in GR from cascade regions [401, 402]. It should also be noted that the energy levels of aggregated PCBM are lower than those in the polymer:$PC_{61}BM$ mixed phase [342], hence aggregated fullerene within the OPV morphology may encourage HCT states and cascade regions simultaneously. Therefore it is possible that the present, apparently contradictory, experimental evidence is because two mechanisms with a common morphological cause is the reason for low GR in OPVs. Before leaving the discussion on GR, we note that cascade heterojunctions can be realised by multi-layer structures as well as by self-organisation. KMC simulations suggest a thin ($<$3 nm) 'cascade' layer between donor and acceptor, and $\Delta = 150$ meV is sufficient to reduce GR from over 90% to levels reported in P3HT:$PC_{61}BM$ OPVs [402]. Izawa *et al* [403],

Heidel *et al* [404], and Tan *et al* [405] all report experiments in which a thin layer (<2 nm) of 'cascade' material with $\Delta = 120$ meV, 300 meV and 400 meV respectively was interposed between the donor and acceptor. In all cases, PCE was improved compared to the equivalent donor–acceptor bilayer. It was additionally shown that increasing cascade layer thickness beyond 3 nm had little impact [405], or indeed reduced the benefit on performance [404], again in agreement with KMC simulations [402].

The debate as to why GR is low in some OPV systems will likely continue, but it is certainly the case that some OPVs are more limited by NGR [347–349, 406]. We note that NGR is the mechanism which leads to light emission in OLEDs, hence we will restrict our discussion to only those papers with reference to OPVs here, and discuss NGR in OLEDs in the next section. Since charge transport in OSCs is limited by hopping, one may expect NGR to be described by a Langevin rate which is proportional to the sum of electron and hole mobilities [90]. While the Langevin rate appears to describe NGR in some small molecule OSCs [407, 408], the measured NGR rate in BHJ OPVs is generally lower than that predicted by Langevin [105, 217, 409–411] and apparently charge-density dependent [351, 412, 413]. Koster *et al* [105] were amongst the first to examine NGR in the context of a BHJ OPV and found that experimental data could only be fitted to a DD model if the NGR rate were instead proportional to the lowest of mobility (the Koster rate) rather than the sum (the Langevin rate). It was also shown that the Langevin rate underestimated the FF of P3HT:$PC_{61}BM$ OPVs, indeed, it is a common finding that FF is strongly dependent on the degree of NGR for the particular device [413]. Koster argued that the reduced NGR rate was due to the faster charge 'waiting' at the heterojunction for the slower charge to arrive. Later KMC simulations by Groves and Greenham [102] suggested this was indeed the case, although the precise NGR rate fell between the Langevin and Koster predictions to an extent which depended on domain size and energetic disorder. Heiber *et al* [414] performed further KMC simulations examining NGR in BHJ blends over a wide range of domain sizes, as shown in figure 8. For small domains, the Langevin rate was recovered since both charges are likely to be close to an interface and so the effect of 'waiting' is reduced, while for large domains, the Koster rate was recovered since recombination was limited by the slow transit of charge across a large domain. An empirical expression for NGR rate based on the geometric mean of mobilities and shown to work well for the range of domain sizes expected in BHJ OPVs. One would expect the degree of NGR to be proportional to the product of electron and hole density, i.e. have a reaction order of 2, while measured reaction orders of greater than 2 are commonly reported [351, 412, 413]. However, it appears that the a major cause of this reaction rate is due to the manner in which charge extraction experiments used to measure NGR rates are interpreted. The NGR rate in experiments is calculated on the basis of an average charge density, although the electron and hole density is expected to vary significantly through the OPV if the device is thin (<100 nm) or the charge injection barrier is small (<0.1 eV) [415, 416]. DD models have shown that ignoring large charge carrier density

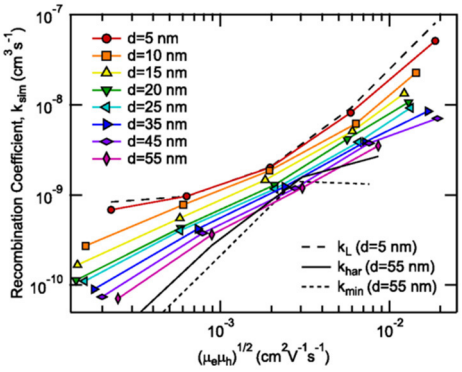

Figure 8. The effect of domain size, d and changing mobility upon measured NGR rate. k_L, k_{min} and k_{har} represent the NGR rate predicted by the Langevin, Koster and geometric mean of mobilities respectively. Reprinted figure with permission from Heiber *et al* [414]. Copyright 2015 by the American Physical Society.

gradients can lead apparent increases in reaction order at open circuit [417], as well as overestimation of the NGR rate [415]. The NGR reaction order greater than 2 can also be attributed to charge trapping [102, 351, 415] and trap-assisted recombination [418], both of which are a consequence of energetic disorder in the OSC. Trap-assisted recombination is described by the SRH model [91], which when included in DD models, can result in quantitative agreement with experimental data for a number of OPV systems [416, 418].

Simulations can also assist in the interpretation of experiments on OPVs. For example, spectroscopy is an invaluable technique to better understand the creation, evolution and decay of excited species. Data from such experiments are often interpreted using a kinetic model in which absorption or emission features are assigned to particular states (e.g. ground state, free charges and so on). Depending on the system in question, excitations can change from one state to another at a given rate. These rates can be determined by performing a global fit to experimental data, in turn, revealing information about the dynamic processes inside the OPV. Jones *et al* [419] used a KMC model as facsimile of a spectroscopy experiment of GR to examine how the rates derived by kinetic schemes related to the rates of underlying processes. Surprisingly it was found that while 'experimental' data created by the KMC could be well-fitted by kinetic schemes, the resulting rates had poor predictive capability when the recombination rate in the KMC model was changed. It was argued that the failure of the kinetic scheme was due to charge transport in OSCs being dispersive and hence not well-described by a single rate. This KMC study considered a single recombination rate and a variation in hopping rate due to disorder. More precise quantum chemical calculations have shown that the competing recombination and hopping rates are strongly dependent on molecular orientation for both polymer and small molecule donor–acceptor heterojunctions [157, 161, 420–422]. Furthermore, it has been shown that structural variability in the molecules can 'hide' slow decay channels [423]. Interpretation of spectroscopic data by first-order kinetics and a single recombination rate may therefore not always be appropriate.

4.3. Organic light-emitting diodes (OLEDs)

OLEDs are already widely used in display applications due to their capability to produce light across the visible spectrum [424] and tunability of the OSCs, optical and electrical properties through molecular design [425]. However, their compatibility with flexible substrates and cheap fabrication methods points to future applications in solid-state lighting and flexible displays [7, 426, 427]. The technological demands placed on such devices are significant, and for white OLEDs (WOLEDs) for solid-state lighting in particular, since lifetimes must be in excess of 10 000 h and power efficiencies in excess of 100 lumen W^{-1} to compete with fluorescent tubes [426], while precise control over the colour temperature is desirable [425]. It is often the case that white light is constructed from the electroluminescence from 2 or more OSCs. A WOLED can therefore be fabricated either by blending the light-emitting OSCs in solution or evaporating them in a multi-layer stack, although in either case, the relative emission from each OSC must be balanced to yield the desired colour temperature. Achieving this is a delicate process since one needs to control charge injection at both contacts, charge transport through (and between) energetically disordered OSCs, as well as where excitons are formed, diffuse and decay. Notwithstanding these challenges, there has been significant success in the predictive modelling of OLED [136, 428] and WOLED [139] device performance. In this section we will focus on the rate of NGR and device simulation in OLEDs, starting with single materials before moving onto multilayer OLEDs.

To recall, the NGR rate in a device is important for two reasons: first, an accurate rate allows modelling of OLED device performance using numerically efficient DD models; second, the NGR rate may reveal the physics of operation which may be used to optimise devices. Section 4.2 has already discussed the problems associated with applying the classical Langevin rate to describe NGR in OSCs with energetic disorder and BHJ morphology; here we extend this discussion to OLEDs. We should note at the outset that the Langevin expression has been used in DD models to successfully model OLED operation in single materials [429], however, we focus here on the exceptions which appear to be more numerous. In a single-material OLED, NGR happens in the context of energetic disorder but no further morphological impediment. KMC simulations by Albrecht and Bässler [430, 431] showed that NGR in such circumstances agreed with the Langevin rate when electric field and charge density is low. Increasing the field, however, was shown to increase the NGR rate with respect to the Langevin expression. Gartstein *et al* [432] argued that the enhanced rate was due to enhanced mobility along the field axis, which led to anisotropic charge transport. This tallies with other KMC simulations by Groves and Greenham [102], who examined the effect of anisotropy in the mobility tensor (e.g. as seen in some OSC crystals [433] and organised polymer OSCs [152]) on NGR. They also showed that anisotropy modified NGR rates, and more specifically, that the effective NGR rate could be modelled using a geometric average of the mobility along the high- and low-mobility axes. Further deviations from Langevin dynamics in single materials were reported by van der Holst *et al* [101], who showed that the NGR rate relative to the Langevin prediction dropped significantly above $\sigma = 75$ meV, reducing temperature, and increasing mismatch in electron and hole mobility. However, they showed that the Langevin rate could recover agreement with KMC predicted NGR rates if the bipolar mobility, in which the opposite charge increases effective disorder, was used. This effective change in energetic disorder may be accounted for in a simulation using the model of Arkhipov *et al* [434], although how one measures bipolar mobility in a device is not clear. It was argued [101] that the effective broadening of the DoS in the presence of the opposite charge carrier type would lead to narrower recombination zones than the unipolar Langevin prediction. This is because carriers penetrating further into the region of opposite charges progressively becoming slower, and more likely to recombine.

Langevin, however, is only one idealised model of recombination. Another model which has been successfully applied in DD models to fit experimental data [435] is trap-limited recombination, as described by SRH [91]. Charge transport in OSCs shares similarities with both the Langevin description of charge transport, i.e. small mean free path compared to the thermal capture radius (~20 nm in OSCs), and that of SRH, i.e. charges are trapped on occasion, so it is perhaps not surprising that either or both models may be applicable. Indeed, when the capture coefficient for one charge is much larger than the other in the SRH expression, an equation very similar to the Langevin expression is revealed [238]. More explicitly however, SRH recombination can lead an ideality factor of 2 [93], a faster 'turn on' of the OLED with increasing voltage [106], and an increased light-intensity dependence on open-circuit voltage [106, 238]. The latter experiment in particular can be used to determine the capture coefficients required in the SRH expression [238], showing that it is reasonably straightforward to determine parameters to describe NGR in a DD model of an OLED. Before moving on, we pause to note that NGR is a good demonstration of the imperfect nature of charge transport models and the inevitable compromises one has to make in order simulate devices. On the one hand, DD models can deal with large charge densities present in OLEDs, although they have to make use of a combination of NGR models, neither of which exactly corresponds to known behaviour. While on the other hand, KMC models can predict NGR rates largely without assumption, but require a great deal of effort to enable them to perform calculations in a reasonable length of time (see section 2.3.3). Notwithstanding these difficulties, both approaches have revealed insights that would have been challenging to achieve by experiment alone.

We now move on to consider the prediction of single-material OLED performance. Neumann *et al* [436] used a DD model to examine the effect of charge diffusion on the performance of a single-material OLED. They found that diffusion shifted the recombination zone into the centre of the device, in turn due to a redistribution of charge in the device. Coehoorn and van Mensfoort [134] extended this work by additionally considering the effect of energetic disorder using a 1D ME model. The rate of NGR used in the model was Langevin-like but was adjusted in such a way as to be in accordance

with the field-dependence of NGR as described by Albrecht and Bässler [430, 431]. They found that the electron and hole densities, and therefore mobilities, dropped very quickly once charges have moved beyond the recombination zone, which in turn led to swift recombination. Like diffusion, the charge density dependence of mobility also had the effect of pushing the recombination zone closer to the centre of the OLED. Van Mensfoort *et al* [136] later demonstrated that this 1D ME model, when fitted to the transport characteristics of electrons and holes, was capable of predicting the performance of single-material OLEDs. In particular, they were able to show the movement of the recombination zone through the device with voltage, and in doing so, predict and explain the peak current efficiency of the OLED. The additionally showed that relatively minor changes in the NGR rate (e.g. a factor of 2) can lead to noticeable differences in predicted OLED performance, re-affirming the importance of correct parameterisations of NGR rate.

Multilayer structures give greater flexibility to optimise the performance of OLEDs since each layer can be tuned to give the desired characteristics, such as efficient electron transport or emissive wavelength. Heterojunctions may also lead to accumulation of electrons and holes in a narrow region, in turn leading to higher recombination efficiencies [437] and reduced leakage [72]. While the beneficial effect of heterojunctions on recombination efficiency has been demonstrated experimentally, it is of interest to predict the NGR at a heterojunction to more precisely optimise the OLED geometry. We leave aside the discussion of charge transport across a heterojunction leading to recombination, since this is discussed in section 2.1, and instead focus on the effect of an impermeable heterojunction on NGR. Greenham and Bobbert [104] showed that under such circumstances the NGR rate becomes charge-density dependent, leading to greater than second-order kinetics even when disorder was absent. These data were then used in a DD model to show that efficient NGR can occur even at impermeable heterojunctions due to the 2D nature of charge transport at the interface, in turn explaining efficient operation of polyfluorene OLEDs [438]. Groves and Greenham [102] relaxed the assumption of charge transport occurring in a 2D plane, and instead assumed charges were confined to a 'slab' of thickness, l, which was infinite in extent for the other 2 Cartesian dimensions. In agreement with Greenham and Bobbert, they found that the rate of NGR in $l = 1$ nm planes was charge density dependent even in the absence of energetic disorder. They additionally derived an empirical expression which predicted that the Langevin rate in such 'slabs' would be modified by a factor $\gamma = 1.5n^{1/3}l$, where n is the charge density and the expression is valid when $\gamma < 1$. These studies demonstrate that NGR in the context of high-charge densities and confined charge transport, as often occurs at the heterojunction of multilayer OLEDs [72], should be expected to deviate from the predictions of the Langevin expression.

DD models have been used to predict the performance of multilayer OLEDs, and have indeed been shown to provide useful insight [30, 72], however, it is difficult in the confines of such models to accurately model NGR (as discussed above) and charge transport across a boundary (as discussed in section 2.2). Hence, we restrict discussion here to KMC models, since using this approach allows examination of the effect of heterojunctions on OLED performance without significant simplification. For example, Bailey *et al* [439] used a KMC model to determine the cause of experimentally observed increase in efficiency in polyfluorene OLEDs when an interlayer is used. Simulations showed that the interlayers increased OLED luminance primarily because of the blocking of excitons through the interlayer, and in doing so, reducing exciton quenching at the anode. As discussed at the outset of this section, WOLED devices rely on a precise balance of emission from separate OSC materials to construct the 'correct' white-light output. Mesta *et al* [139] performed KMC simulations on a multi-layer WOLED which comprised layers for electron- and hole-transport; red, green and blue light emission; and an exciton blocking layer. By fitting the charge and exciton transport properties of each material it was possible to re-create the experimentally observed emission profile from each emissive layer, showing that quantitative predictions with multilayer WOLEDs is possible. Furthermore, they showed that light emission is strongly heterogeneous since recombination mostly occurs via trap states. The heterogeneity of recombination, together with the nanometre scale of some of the WOLED layers and concentration gradients, underlines the value of using a 3D KMC model in this context. The effect of current heterogeneity on the performance of multilayer OLEDs was also examined by Shen and Giebink [440]. They simulated a range of *N*, *N*′-bis(1-napthyl)-*N*, *N*′-diphenyl-1, 1′biphenyl-4, 4′-diamine (NPD)/4, 4′bis(*N*-carbazolyl)-1, 1′biphenyl (CBP)/Alq_3 and NPD/Alq_3 OLEDs under operating conditions. The current in the NPD/Alq_3 OLED was shown to be heterogeneous, similar to that seen in unipolar devices [253], but that additionally the current filaments 'miss' one another. This in leads to a substantial leakage current and loss in luminance efficiency. Of course there is no particular reason why one might expect current filaments in electron- and hole-transporting material to 'match up', but this nonetheless quantifies the deleterious effect of filamentary transport in OLEDs. An effect of this is that a small number of molecules are responsible for a large proportion of light emission. The localisation of excitons and polarons this implies may lead to exciton-polaron annihilation, which has been identified as a degradation mechanism in OLED materials [441]. This was examined further for an NPD/CBP/Alq_3 OLED as shown in figure 9. Here the degree of heterogeneity is quantified by 'discrepancy,' with larger discrepancy meaning more heterogeneous current. Figure 9(c) shows that the OLED lifetime decreases with increasing current and increasing disorder, and more explicitly, that increasing heterogeneity leads to reduced lifetime. This is underscored in figure 9(d), which shows the overlap between degraded molecules (white circles) and local current densities. They also show the more experimentally-accessible luminance versus lifetime relationship, showing that lifetime reduces with increasing current (figure 9(a)) and disorder (figure 9(b)). Coehoorn *et al* [442] have also used a KMC model to examine degradation in OLEDs, and found that exciton-polaron quenching was the major cause of both IQE roll-off and degradation. This in turn allowed development of

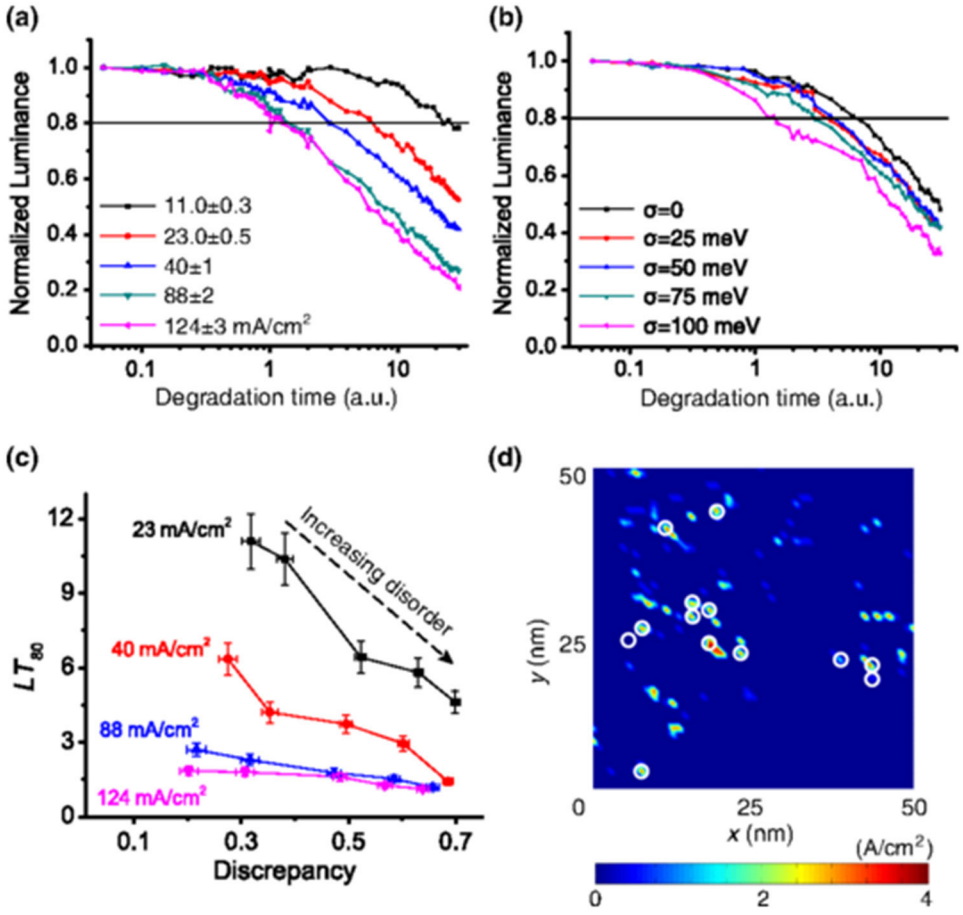

Figure 9. Normalised luminance as a function of time for both current (a) and energetic disorder (b). (c) Predicted OLED lifetime (LT_{80}) as a function of heterogeneity (discrepancy) for various current densities and assumed disorders ($\sigma = 0$, 25, 5, 75, 100 meV). (d) Positions of degraded molecules (marked by white circles) overlaid with current density distribution. Reprinted figure with permission from Shen and Geibink [440]. Copyright 2015 by the American Physical Society.

an analytical expression that relates the lifetime to parameters available in steady-state measurements. It is interesting to note that Shen and Geibink [440] observed that IQE and lifetime more explicitly depend on current density flowing through the filaments, rather than current density, for a range of σ. This dependence of device performance on utilised device area may account for the ability of simple models which ignore heterogeneity to fit experimental data, notwithstanding the clear effects of heterogeneity as revealed in KMC simulations.

4.4. Different ways of defining morphology

Previous sections have discussed the various ways in which the routes taken by charges through an OSC can affect measurable quantities. These routes may be imposed due to energetic disorder or blended morphology, but the end result is the same, namely that charge transport obtains characteristics due to the percolation network. This section discusses allied areas of research which allow different ways of defining the morphology of the network and interpret the resulting behaviour.

As discussed previously, there are a variety of atomistic and course-grained models which can generate morphologies to be used in QCMC, in turn allowing analysis of charge transport on the nano-scale. This has been shown to be critical in understanding how some devices operate, as for example in section 4.2, where charge transport in the vicinity of the donor–acceptor heterojunction of an OPV had a more substantial effect on GR than did the meso-scale morphology. However, some features on the meso-scale are of interest, such as the presence of wetting layers [443] which accumulate at the electrodes OPVs [444–448], or the degree of mixing of the matrix and dye in an OLED [449]. Furthermore, although research has generally centred on what optical and electronic properties using a blend of OSCs can endow a device (e.g. as in BHJ OPVs), it is notable that blending can also improve mechanical, thermal or chemical stability [450–452]. It is therefore of interest to know the meso-scale morphology that results from casting a mixture of OSCs or inert polymers, and determine the charge transport properties of the resultant blend. Meso-scale BHJ morphologies are often generated using a simulated annealing approach [140] which results in morphologies which are qualitatively similar those seen in experiment. However, the thermodynamics and kinetics of phase separation that occurs during solution processing, more specifically liquid–liquid demixing, can be better described by Cahn–Hilliard theory [453–456]. Liquid–liquid demixing has been shown to dominate phase-separation behaviour in at least some OSC-polymer blends [457–459]. Using the

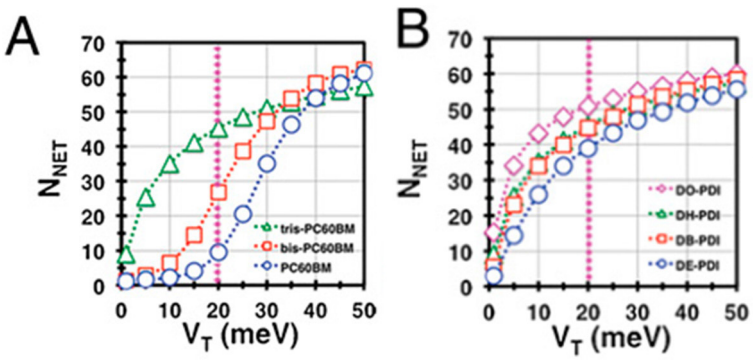

Figure 10. Predicted number of networks N_{NET} as a function of electronic coupling threshold, V_T for molecules based on (a) a PCBM functional unit and (b) a PDI functional unit. Reproduced (modified) from Savoie *et al* [133].

Cahn–Hilliard approach allows explicit links to be made between the physical parameters, such as molecular weights, surface energies and the solvent, and the resultant morphology. For example, Lyons *et al* [123] used Cahn–Hilliard to predict BHJ morphologies that result from asymmetric surface interactions, i.e. those leading to surface wetting layers, and used these as an input into a KMC model. It was shown that both the 'correct' and 'wrong' material at the electrode can affect photocurrent collection due to the presence of a blocking layer of largely 'wrong' material at the sub-surface or surface respectively, both of which have been observed in experiment [444]. However, the proportion of 'wrong' material in the blocking layer which could be tolerated without adversely affecting photocurrent was surprisingly large (up 85% by volume) since the layer was thin (~3 nm). Michels and Moons [455] went further by using Cahn–Hilliard to examine phase separation of a specific polyfluorene/$PC_{61}BM$ blend. They showed that phase separation was triggered by surface-solution interactions, which led to an oscillating composition profile moving from the surface into the bulk. There are of course challenges in the use of Cahn–Hilliard, such as how one models solvent evaporation [455, 456] or measures physical parameters [458, 460], however, these studies show it allows one to make links between processing conditions and polymer properties and resultant morphologies.

A novel approach to describing the morphology is to ignore the physics of phase separation entirely and instead focus on the stochastic properties of the network. Stenzel *et al* [461] used this method to first determine the statistical properties of a P3HT-zinc oxide (ZnO) blend from transmission electron microscope images and then use this information to generate equivalent morphologies. The equivalence of experimental and generated morphologies was then tested by simulating exciton dissociation efficiencies [461], as well as connectivity and mobility of the P3HT and ZnO phases [462], and good agreement was observed in all cases. Westhoff *et al* [463] demonstrated that parameterising the statistical properties of a range of polymer-fullerene blend with respect to a process variable (spin speed in this case) could accurately predict the morphology of a blend which was not used to train the stochastic model. The same techniques can be applied to charge transport modelling more directly. Baumeier *et al* [464] determined the statistical properties of an Alq_3 morphology (produced by an atomistic molecular dynamics simulation) as well as the dependent site energies and electronic couplings. This information was then used in a computationally simpler, but nonetheless statistically equivalent, KMC model. The agreement between the 'full' QCMC charge transport model using atomistic morphology and the trained KMC model was shown to be good. As discussed in section 2.3.3, the complexity of QCMC models limits their application to examining charge transport in relatively small simulation volumes and therefore high charge densities. Stochastic models can be used to partially circumvent this problem. Kordt *et al* [465] trained a KMC model to replicate the statistics of morphology and charge transport of a small molecule OSC, and then used it alongside a QCMC model to examine the predictions of mobility. It was found that the trained KMC model predicted mobilities which were significantly lower than the QCMC model due to the small simulation volume of the latter. The idea of examining charge transport as a network can be applied in different ways. Savoie *et al* [133] considered the OSC molecules and the connections between them as a graph. Morphologies of fullerene ($PC_{60}BM$) or perylene-diimide (PDI) molecules were generated and the electronic coupling between them was calculated. These morphologies were then sub-divided in networks, with a pair of molecules being considered as part of the same network if the electronic coupling between them was above a threshold, V_T. They then varied V_T, and counted the number of distinct networks N_{NET} for each morphology, as shown in figure 10. It can be seen that N_{NET} increases with V_T, i.e. the collection of molecules 'fragments' into separate clusters within which there is electronic coupling better than V_T. It can be seen that the PDI molecules fragment rapidly into clusters more rapidly with increasing threshold (figure 10(b)) when compared $PC_{60}BM$ (figure 10(a)). This indicates that $PC_{60}BM$ is more robust to fluctuations in electronic coupling than PDI. Furthermore, changing the fullerene adduct leads to significant variations in the relationship between V_T and N_{NET}, for instance tris-$PC_{60}BM$ is shown to produce less robust networks than $PC_{60}BM$. Examining the network in this way clarifies the relationship between structural disorder and charge transport. If changing V_T by a small amount dramatically increases N_{NET}, one would expect charge transport to be dominated by a small-number of pathways with good electronic coupling, and consequently bulk charge transport may be expected to suffer.

5. Summary and outlook

Organic semiconductors offer the opportunity to enable cheap, scalable manufacture of large-area electronic devices such as photovoltaics and solid-state lighting, as well as novel concepts such as rollable displays. Often the performance of such devices is determined by charge transport; hence their future development is reliant upon better understanding of charge transport and its subsequent control through molecular structure, processing or device design. This review has discussed the application of various charge transport models to organic semiconductors both in the context of mobility, and in the operation devices; namely OTFTs, photovoltaics and light-emitting diodes. In all cases it has been shown that the energetic and morphological disorder inherent in most organic semiconductors gives rise to behaviour that may be unexpected in their inorganic counterparts. The properties and organisation of organic semiconductors at the nano-scale in particular have been shown to determine macro-scale observable quantities such as mobility or degree of recombination. Furthermore, it has been shown that the context in which charge transport or recombination occurs is also vitally important in understanding device operation. This emphasises the need for accurate models of charge transport and morphology of organic semiconductors on the nano-scale, as well as computationally efficient models which can consider devices on the macro-scale. While this is challenging to achieve, it has been demonstrated that such models can reveal information that would be difficult, or even impossible, by experiment alone. The last decade has seen numerous reports of charge transport models that are capable of quantitative prediction of device characteristics. Looking forward it seems likely that charge transport models will continue to develop and play a larger role in the optimisation and design of organic semiconductors and devices.

References

[1] Li Y 2012 Molecular design of photovoltaic materials for polymer solar cells: toward suitable electronic energy levels and broad absorption *Acc. Chem. Res.* **45** 723–33

[2] May F, Al-Helwi M, Baumeier B, Kowalsky W, Fuchs E, Lennartz C and Andrienko D 2012 Design rules for charge-transport efficient host materials for phosphorescent organic light-emitting diodes *J. Am. Chem. Soc.* **134** 13818–22

[3] Mei J G, Diao Y, Appleton A L, Fang L and Bao Z N 2013 Integrated materials design of organic semiconductors for field-effect transistors *J. Am. Chem. Soc.* **135** 6724–46

[4] Arias A C, MacKenzie J D, McCulloch I, Rivnay J and Salleo A 2010 Materials and applications for large area electronics: solution-based approaches *Chem. Rev.* **110** 3–24

[5] Forrest S R 2004 The path to ubiquitous and low-cost organic electronic appliances on plastic *Nature* **428** 911–8

[6] Brabec C J 2004 Organic photovoltaics: technology and market *Sol. Energy Mater. Sol. Cells* **83** 273–92

[7] Gather M C, Kohnen A and Meerholz K 2011 White organic light-emitting diodes *Adv. Mater.* **23** 233–48

[8] Sirringhaus H 2014 25th anniversary article: organic field-effect transistors: the path beyond amorphous silicon *Adv. Mater.* **26** 1319–35

[9] Lochner C M, Khan Y, Pierre A and Arias A C 2014 All-organic optoelectronic sensor for pulse oximetry *Nat. Commun.* **5** 5754

[10] Simon D T, Kurup S, Larsson K C, Hori R, Tybrandt K, Goiny M, Jager E W H, Berggren M, Canlon B and Richter-Dahlfors A 2009 Organic electronics for precise delivery of neurotransmitters to modulate mammalian sensory function *Nat. Mater.* **8** 742–6

[11] Janata J and Josowicz M 2003 Conducting polymers in electronic chemical sensors *Nat. Mater.* **2** 19–24

[12] Bai H and Shi G 2007 Gas sensors based on conducting polymers *Sensors* **7** 267

[13] Sekitani T, Nakajima H, Maeda H, Fukushima T, Aida T, Hata K and Someya T 2009 Stretchable active-matrix organic light-emitting diode display using printable elastic conductors *Nat. Mater.* **8** 494–9

[14] Gelinck G, Heremans P, Nomoto K and Anthopoulos T D 2010 Organic transistors in optical displays and microelectronic applications *Adv. Mater.* **22** 3778–98

[15] Barbaro M, Caboni A, Cosseddu P, Mattana G and Bonfiglio A 2010 Active devices based on organic semiconductors for wearable applications *IEEE Trans. Inf. Technol. Biomed.* **14** 758–66

[16] Rogers J A, Someya T and Huang Y 2010 Materials and mechanics for stretchable electronics *Science* **327** 1603–7

[17] Chansin G, Ghaffarzadeh K and Zervos H 2015 OLED display forecasts 2015–2025: the rise of plastic and flexible displays *Technical Report* IDTechEx

[18] Kippelen B and Bredas J-L 2009 Organic photovoltaics *Energy Environ. Sci.* **2** 251–61

[19] Li B, Wang L, Kang B, Wang P and Qiu Y 2006 Review of recent progress in solid-state dye-sensitized solar cells *Sol. Energy Mater. Sol. Cells* **90** 549–73

[20] Yang L, Tabachnyk M, Bayliss S L, Böhm M L, Broch K, Greenham N C, Friend R H and Ehrler B 2015 Solution-processable singlet fission photovoltaic devices *Nano Lett.* **15** 354–8

[21] Ehrler B, Wilson M W B, Rao A, Friend R H and Greenham N C 2012 Singlet exciton fission-sensitized infrared quantum dot solar cells *Nano Lett.* **12** 1053–7

[22] Malinkiewicz O, Yella A, Lee Y H, Espallargas G M, Graetzel M, Nazeeruddin M K and Bolink H J 2014 Perovskite solar cells employing organic charge-transport layers *Nat. Photon.* **8** 128–32

[23] Chiang C K, Fincher C R, Park Y W, Heeger A J, Shirakawa H, Louis E J, Gau S C and MacDiarmid A G 1977 Electrical conductivity in doped polyacetylene *Phys. Rev. Lett.* **39** 1098–101

[24] DeLongchamp D M, Kline R J and Herzing A 2012 Nanoscale structure measurements for polymer-fullerene photovoltaics *Energy Environ. Sci.* **5** 5980–93

[25] Giridharagopal R and Ginger D S 2010 Characterizing morphology in bulk heterojunction organic photovoltaic systems *J. Phys. Chem. Lett.* **1** 1160–9

[26] Selberherr S 1984 *Analysis and Simulation of Semiconductor Devices* (New York: Springer)

[27] Baumeier B, May F, Lennartz C and Andrienko D 2012 Challenges for in silico design of organic semiconductors *J. Mater. Chem.* **22** 10971–6

[28] Nelson J, Kwiatkowski J J, Kirkpatrick J and Frost J M 2009 Modeling charge transport in organic photovoltaic materials *Acc. Chem. Res.* **42** 1768–78

[29] Tessler N, Preezant Y, Rappaport N and Roichman Y 2009 Charge transport in disordered organic materials and its relevance to thin-film devices: a tutorial review *Adv. Mater.* **21** 2741–61

[30] Coehoorn R and Bobbert P A 2012 Effects of Gaussian disorder on charge carrier transport and recombination in organic semiconductors *Phys. Status Solidi* a **209** 2354–77

[31] Walker A B 2009 Multiscale modeling of charge and energy transport in organic light-emitting diodes and photovoltaics *Proc. IEEE* **97** 1587–96

[32] Groves C 2013 Developing understanding of organic photovoltaic devices: kinetic Monte Carlo models of geminate and non-geminate recombination, charge transport and charge extraction *Energy Environ. Sci.* **6** 3202–17

[33] Brédas J-L, Beljonne D, Coropceanu V and Cornil J 2004 Charge-transfer and energy-transfer processes in π-conjugated oligomers and polymers: a molecular picture *Chem. Rev.* **104** 4971–5004

[34] Coropceanu V, Cornil J, da Silva D A, Olivier Y, Silbey R and Bredas J L 2007 Charge transport in organic semiconductors *Chem. Rev.* **107** 926–52

[35] Pope M and Swenburg C E 1982 *Electronic Processes in Organic Crystals* (Oxford: Oxford University Press)

[36] Troisi A 2011 Charge transport in high mobility molecular semiconductors: classical models and new theories *Chem. Soc. Rev.* **40** 2347–58

[37] Brown P J, Sirringhaus H, Harrison M, Shkunov M and Friend R H 2001 Optical spectroscopy of field-induced charge in self-organized high mobility poly(3-hexylthiophene) *Phys. Rev.* B **63** 125204

[38] Noriega R, Rivnay J, Vandewal K, Koch F P V, Stingelin N, Smith P, Toney M F and Salleo A 2013 A general relationship between disorder, aggregation and charge transport in conjugated polymers *Nat. Mater.* **12** 1038–44

[39] Rivnay J, Noriega R, Northrup J E, Kline R J, Toney M F and Salleo A 2011 Structural origin of gap states in semicrystalline polymers and the implications for charge transport *Phys. Rev.* B **83** 121306

[40] Nicolai H T, Kuik M, Wetzelaer G A H, de Boer B, Campbell C, Risko C, Brédas J L and Blom P W M 2012 Unification of trap-limited electron transport in semiconducting polymers *Nat. Mater.* **11** 882–7

[41] Sirringhaus H 2005 Device physics of solution-processed organic field-effect transistors *Adv. Mater.* **17** 2411–25

[42] Venkateshvaran D *et al* 2014 Approaching disorder-free transport in high-mobility conjugated polymers *Nature* **515** 384–8

[43] Chang J F, Sirringhaus H, Giles M, Heeney M and McCulloch I 2007 Relative importance of polaron activation and disorder on charge transport in high-mobility conjugated polymer field-effect transistors *Phys. Rev.* B **76** 12

[44] Miller A and Abrahams E 1960 Impurity conduction at low concentrations *Phys. Rev.* **120** 745–55

[45] Marcus R A 1993 Electron-transfer reactions in chemistry—theory and experiment (nobel lecture) *Angew. Chem., Int. Ed. Engl.* **32** 1111–21

[46] Fishchuk I I, Hertel D, BÃ¤ssler H and Kadashchuk A K 2002 Effective-medium theory of hopping charge-carrier transport in weakly disordered organic solids *Phys. Rev.* B **65** 125201

[47] Coffey D C, Larson B W, Hains A W, Whitaker J B, Kopidakis N, Boltalina O V, Strauss S H and Rumbles G 2012 An optimal driving force for converting excitons into free carriers in excitonic solar cells *J. Phys. Chem.* C **116** 8916–23

[48] Marsh R A, Groves C and Greenham N C 2007 A microscopic model for the behavior of nanostructured organic photovoltaic devices *J. Appl. Phys.* **101** 083509

[49] Cottaar J, Koster L J A, Coehoorn R and Bobbert P A 2011 Scaling theory for percolative charge transport in disordered molecular semiconductors *Phys. Rev. Lett.* **107** 4

[50] Natali D and Caironi M 2012 Charge injection in solution-processed organic field-effect transistors: physics, models and characterization methods *Adv. Mater.* **24** 1357–87

[51] Steim R, Kogler F R and Brabec C J 2010 Interface materials for organic solar cells *J. Mater. Chem.* **20** 2499–512

[52] Meyer J, Hamwi S, Kroger M, Kowalsky W, Riedl T and Kahn A 2012 Transition metal oxides for organic electronics: energetics, device physics and applications *Adv. Mater.* **24** 5408–27

[53] Hwang J, Wan A and Kahn A 2009 Energetics of metal–organic interfaces: new experiments and assessment of the field *Mater. Sci. Eng.* R **64** 1–31

[54] Ratcliff E L, Zacher B and Armstrong N R 2011 Selective interlayers and contacts in organic photovoltaic cells *J. Phys. Chem. Lett.* **2** 1337–50

[55] Baldo M A and Forrest S R 2001 Interface-limited injection in amorphous organic semiconductors *Phys. Rev.* B **64** 085201

[56] Arkhipov V I, von Seggern H and Emelianova E V 2003 Charge injection versus space-charge-limited current in organic light-emitting diodes *Appl. Phys. Lett.* **83** 5074–6

[57] Bässler H 1998 Injection, transport and recombination of charge carriers in organic light-emitting diodes *Polym. Adv. Technol.* **9** 402–18

[58] Zacher B and Armstrong N R 2011 Modeling the effects of molecular length scale electrode heterogeneity in organic solar cells *J. Phys. Chem.* C **115** 25496–507

[59] Karl N, Kraft K-H, Marktanner J, Münch M, Schatz F, Stehle R and Uhde H-M 1999 Fast electronic transport in organic molecular solids? *J. Vac. Sci. Technol.* A **17** 2318–28

[60] Pernstich K P, Rossner B and Batlogg B 2008 Field-effect-modulated Seebeck coefficient in organic semiconductors *Nat. Mater.* **7** 321–5

[61] Koller G, Berkebile S, Oehzelt M, Puschnig P, Ambrosch-Draxl C, Netzer F P and Ramsey M G 2007 Intra- and intermolecular band dispersion in an organic crystal *Science* **317** 351–5

[62] Ostroverkhova O, Cooke D G, Shcherbyna S, Egerton R F, Hegmann F A, Tykwinski R R and Anthony J E 2005 Bandlike transport in pentacene and functionalized pentacene thin films revealed by subpicosecond transient photoconductivity measurements *Phys. Rev.* B **71** 035204

[63] Fratini S and Ciuchi S 2009 Bandlike motion and mobility saturation in organic molecular semiconductors *Phys. Rev. Lett.* **103** 266601

[64] Sakanoue T and Sirringhaus H 2010 Band-like temperature dependence of mobility in a solution-processed organic semiconductor *Nat. Mater.* **9** 736–40

[65] Minder N A, Ono S, Chen Z H, Facchetti A and Morpurgo A F 2012 Band-Like electron transport in organic transistors and implication of the molecular structure for performance optimization *Adv. Mater.* **24** 503

[66] Troisi A 2011 Dynamic disorder in molecular semiconductors: charge transport in two dimensions *J. Chem. Phys.* **134** 10

[67] Chang J-F, Sakanoue T, Olivier Y, Uemura T, Dufourg-Madec M-B, Yeates S G, Cornil J, Takeya J, Troisi A and Sirringhaus H 2011 Hall-effect measurements probing the degree of charge-carrier delocalization in solution-processed crystalline molecular semiconductors *Phys. Rev. Lett.* **107** 066601

[68] Vehoff T, Baumeier B, Troisi A and Andrienko D 2010 Charge transport in organic crystals: role of disorder and topological connectivity *J. Am. Chem. Soc.* **132** 11702–8

[69] Troisi A and Orlandi G 2006 Charge-transport regime of crystalline organic semiconductors: diffusion limited by thermal off-diagonal electronic disorder *Phys. Rev. Lett.* **96** 086601

[70] Eggeman A S, Illig S, Troisi A, Sirringhaus H and Midgley P A 2013 Measurement of molecular motion

in organic semiconductors by thermal diffuse electron scattering *Nat. Mater.* **12** 1044–8
[71] Troisi A 2011 The speed limit for sequential charge hopping in molecular materials *Org. Electron.* **12** 1988–91
[72] Crone B K, Davids P S, Campbell I H and Smith D L 2000 Device model investigation of bilayer organic light emitting diodes *J. Appl. Phys.* **87** 1974–82
[73] Barker J A, Ramsdale C M and Greenham N C 2003 Modeling the current–voltage characteristics of bilayer polymer photovoltaic devices *Phys. Rev.* B **67** 9
[74] Koster L J A, Smits E C P, Mihailetchi V D and Blom P W M 2005 Device model for the operation of polymer/fullerene bulk heterojunction solar cells *Phys. Rev.* B **72** 085205
[75] Davids P S, Campbell I H and Smith D L 1997 Device model for single carrier organic diodes *J. Appl. Phys.* **82** 6319–25
[76] Gommans H H P, Kemerink M, Kramer J M and Janssen R A J 2005 Field and temperature dependence of the photocurrent in polymer/fullerene bulk heterojunction solar cells *Appl. Phys. Lett.* **87** 122104
[77] Jacoboni C and Lugli P 1989 *The Monte Carlo Method for Semiconductor Device Simulation* (New York: Springer)
[78] Gummel H K 1964 A self-consistent iterative scheme for one-dimensional steady state transistor calculations *IEEE Trans. Electron Devices* **11** 455–65
[79] Scharfetter D L and Gummel H K 1969 Large-signal analysis of a silicon Read diode oscillator *IEEE Trans. Electron Devices* **16** 64–77
[80] Wetzelaer G A H, Koster L J A and Blom P W M 2011 Validity of the Einstein Relation in Disordered Organic Semiconductors *Phys. Rev. Lett.* **107** 066605
[81] Nenashev A V, Jansson F, Oelerich J O, Huemmer D, Dvurechenskii A V, Gebhard F and Baranovskii S D 2013 Advanced percolation solution for hopping conductivity *Phys. Rev.* B **87** 235204
[82] Bisquert J 2008 Interpretation of electron diffusion coefficient in organic and inorganic semiconductors with broad distributions of states *Phys. Chem. Chem. Phys.* **10** 3175–94
[83] Li L, Lu N, Liu M and Bässler H 2014 General Einstein relation model in disordered organic semiconductors under quasiequilibrium *Phys. Rev.* B **90** 214107
[84] Roichman Y and Tessler N 2002 Generalised Einstein relation for disordered semiconductors - implicatiosn for device performance *Appl. Phys. Lett.* **80** 1948–50
[85] Baranovskii S D, Faber T, Hensel F, Thomas P and Adriaenssens G J 1996 Einstein's relationship for hopping electrons *J. Non-Cryst. Solids* **198–200** 214–7
[86] Pasveer W F, Cottaar J, Tanase C, Coehoorn R, Bobbert P A, Blom P W M, de Leeuw D M and Michels M A J 2005 Unified description of charge-carrier mobilities in disordered semiconducting polymers *Phys. Rev. Lett.* **94** 206601
[87] Bouhassoune M, Mensfoort S L M v, Bobbert P A and Coehoorn R 2009 Carrier-density and field-dependent charge-carrier mobility in organic semiconductors with correlated Gaussian disorder *Org. Electron.* **10** 437–45
[88] Onsager L 1938 *Phys. Rev.* **54** 554
[89] Braun C L 1984 Electric field assisted dissociation of charge transfer states as a mechanism of photocarrier production *J. Chem. Phys.* **80** 4157–61
[90] Langevin P 1903 *Ann. Chim. Phys.* **28** 433
[91] Shockley W and Read W T 1952 *Phys. Rev.* **87** 835
[92] Blakesley J C, Clubb H S and Greenham N C 2010 Temperature-dependent electron and hole transport in disordered semiconducting polymers: analysis of energetic disorder *Phys. Rev.* B **81** 045210
[93] Wetzelaer G A H, Kuik M, Nicolai H T and Blom P W M 2011 Trap-assisted and Langevin-type recombination in organic light-emitting diodes *Phys. Rev.* B **83** 165204
[94] Kniepert J, Lange I, Heidbrink J, Kurpiers J, Brenner T J K, Koster L J A and Neher D 2015 Effect of solvent additive on generation, recombination, and extraction in PTB7:PCBM solar cells: a conclusive experimental and numerical simulation study *J. Phys. Chem.* C **119** 8310–20
[95] Koehler M, Biaggio I and da Luz M G E 2008 Resolving the contact voltage dilemma in organic field effect transistors *Phys. Rev.* B **78** 153312
[96] Hill I G 2005 Numerical simulations of contact resistance in organic thin-film transistors *Appl. Phys. Lett.* **87** 163505
[97] Richards T J and Sirringhaus H 2007 Analysis of the contact resistance in staggered, top-gate organic field-effect transistors *J. Appl. Phys.* **102** 094510
[98] Gupta D, Katiyar M and Gupta D 2009 An analysis of the difference in behavior of top and bottom contact organic thin film transistors using device simulation *Org. Electron.* **10** 775–84
[99] Shim C H, Maruoka F and Hattori R 2010 Structural analysis on organic thin-film transistor with device simulation *IEEE Trans. Electron Devices* **57** 195–200
[100] Scheinert S and Paasch G 2004 Fabrication and analysis of polymer field-effect transistors *Phys. Status Solidi* a **201** 1263–301
[101] van der Holst J J M, van Oost F W A, Coehoorn R and Bobbert P A 2009 Electron–hole recombination in disordered organic semiconductors: validity of the Langevin formula *Phys. Rev.* B **80** 235202
[102] Groves C and Greenham N C 2008 Bimolecular recombination in polymer electronic devices *Phys. Rev.* B **78** 155205
[103] Jurić I, Batistić I and Tutiš E 2008 Recombination at heterojunctions in disordered organic media: modeling and numerical simulations *Phys. Rev.* B **77** 165304
[104] Greenham N C and Bobbert P A 2003 Two-dimensional electron–hole capture in a disordered hopping system *Phys. Rev.* B **68** 245301
[105] Koster L J A, Mihailetchi V D and Blom P W M 2006 Bimolecular recombination in polymer/fullerene bulk heterojunction solar cells *Appl. Phys. Lett.* **88** 052104
[106] Kuik M, Nicolai H T, Lenes M, Wetzelaer G-J A H, Lu M and Blom P W M 2011 Determination of the trap-assisted recombination strength in polymer light emitting diodes *Appl. Phys. Lett.* **98** 093301
[107] MacKenzie R C I, Shuttle C C, Chablinyc M L and Nelson J 2012 Extracting microscopic device parameters from transient photocurrent measurements of P3HT:PCBM solar cells *Adv. Energy Mater.* **2** 662–9
[108] MacKenzie R C I, Shuttle C G, Dibb G F, Treat N, von Hauff E, Robb M J, Hawker C J, Chabinyc M L and Nelson J 2013 Interpreting the density of states extracted from organic solar cells using transient photocurrent measurements *J. Phys. Chem.* C **117** 12407–14
[109] Wojcik M and Tachiya M 2009 Accuracies of the empirical theories of the escape probability based on Eigen model and Braun model compared with the exact extension of Onsager theory *J. Chem. Phys.* **130** 8
[110] Tachiya M and Seki K 2010 Theory of bulk electron–hole recombination in a medium with energetic disorder *Phys. Rev.* B **82** 085201
[111] Sano H and Tachiya M 1979 Partially diffusion-controlled recombination *J. Chem. Phys.* **71** 1276–82
[112] Rubel O, Baranovskii S D, Stolz W and Gebhard F 2008 Exact solution for hopping dissociation of geminate electron–hole pairs in a disordered chain *Phys. Rev. Lett.* **100** 196602
[113] Groves C, Marsh R A and Greenham N C 2008 Monte Carlo modeling of geminate recombination in polymer-polymer photovoltaic devices *J. Chem. Phys.* **129** 114903

[114] Lyons B P, Clarke N and Groves C 2012 The relative importance of domain size, domain purity and domain interfaces to the performance of bulk-heterojunction organic photovoltaics *Energy Environ. Sci.* **5** 7657–63
[115] Pettersson L A A, Roman L S and Inganäs O 1999 Modeling photocurrent action spectra of photovoltaic devices based on organic thin films *J. Appl. Phys.* **86** 487–96
[116] Gao F, Wang J, Blakesley J C, Hwang I, Li Z and Greenham N C 2012 Quantifying loss mechanisms in polymer: fullerene photovoltaic devices *Adv. Energy Mater.* **2** 956–61
[117] Groves C, Koster L J A and Greenham N C 2009 The effect of morphology upon mobility: Implications for bulk heterojunction solar cells with nonuniform blend morphology *J. Appl. Phys.* **105** 094510
[118] Haney P M 2011 Organic photovoltaic bulk heterojunctions with spatially varying composition *J. Appl. Phys.* **110** 024305
[119] Cottaar J, Coehoorn R and Bobbert P A 2012 Modeling of charge transport across disordered organic heterojunctions *Org. Electron.* **13** 667–72
[120] Arkhipov V I, Emelianova E V and Bassler H 2001 Charge carrier transport and recombination at the interface between disordered organic dielectrics *J. Appl. Phys.* **90** 2352–7
[121] Houlli H, Tutis E, Batistic I and Zuppiroli L 2006 Investigation of the charge transport through disordered organic molecular heterojunctions *Appl. Phys. Lett.* **100** 033702
[122] Massé A, Coehoorn R and Bobbert P A 2014 Universal size-dependent conductance fluctuations in disordered organic semiconductors *Phys. Rev. Lett.* **113** 116604
[123] Lyons B P, Clarke N and Groves C 2011 The quantitative effect of surface wetting layers on the performance of organic bulk heterojunction photovoltaic devices *J. Phys. Chem.* C **115** 22572–7
[124] Koster L J A 2010 Charge carrier mobility in disordered organic blends for photovoltaics *Phys. Rev.* B **81** 205318
[125] Yu Z G, Smith D L, Saxena A, Martin R L and Bishop A R 2001 Molecular geometry fluctuation model for the mobility of conjugated polymers *Phys. Rev.* B **63** 085202
[126] Pasveer W F, Bobbert P A, Huinink H P and Michels M A J 2005 Scaling of current distributions in variable-range hopping transport on two- and three-dimensional lattices *Phys. Rev.* B **72** 6
[127] Casalegno M, Bernardi A and Raos G 2013 Numerical simulation of photocurrent generation in bilayer organic solar cells: comparison of master equation and kinetic Monte Carlo approaches *J. Chem. Phys.* **139** 13
[128] Zhou J, Zhou Y C, Zhao J M, Wu C Q, Ding X M and Hou X Y 2007 Carrier density dependence of mobility in organic solids: a Monte Carlo simulation *Phys. Rev.* B **75** 153201
[129] van der Holst J J M, van Oost F W A, Coehoorn R and Bobbert P A 2011 Monte Carlo study of charge transport in organic sandwich-type single-carrier devices: effects of Coulomb interactions *Phys. Rev.* B **83** 085206
[130] Schrader M, Fitzner R, Hein M, Elschner C, Baumeier B, Leo K, Riede M, Bauerle P and Andrienko D 2012 Comparative study of microscopic charge dynamics in crystalline acceptor-substituted oligothiophenes *J. Am. Chem. Soc.* **134** 6052–6
[131] Cornil J *et al* 2013 Exploring the energy landscape of the charge transport levels in organic semiconductors at the molecular scale *Acc. Chem. Res.* **46** 434–43
[132] Athanasopoulos S, Kirkpatrick J, Martinez D, Frost J M, Foden C M, Walker A B and Nelson J 2007 Predictive study of charge transport in disordered semiconducting polymers *Nano Lett.* **7** 1785–8
[133] Savoie B M, Kohlstedt K L, Jackson N E, Chen L X, de la Cruz M O, Schatz G C, Marks T J and Ratner M A 2014 Mesoscale molecular network formation in amorphous organic materials *Proc. Natl Acad. Sci. USA* **111** 10055–60
[134] Coehoorn R and van Mensfoort S L M 2009 Effects of disorder on the current density and recombination profile in organic light-emitting diodes *Phys. Rev.* B **80** 11
[135] van Mensfoort S L M and Coehoorn R 2008 Effect of Gaussian disorder on the voltage dependence of the current density in sandwitch-type devices based on organic semiconductors *Phys. Rev.* B **78** 085207
[136] van Mensfoort S L M, Billen J, Carvelli M, Vulto S I E, Janssen R A J and Coehoorn R 2011 Predictive modeling of the current density and radiative recombination in blue polymer-based light-emitting diodes *J. Appl. Phys.* **109** 064502
[137] Casalegno M, Carbonera C, Luzzati S and Raos G 2012 Coarse-grained kinetic modelling of bilayer heterojunction organic solar cells *Org. Electron.* **13** 750–61
[138] Blakesley J C and Castro F A 2015 Simulating photoconductive atomic-force microscopy on disordered photovoltaic materials *Phys. Rev.* B **91** 144202
[139] Mesta M *et al* 2013 Molecular-scale simulation of electroluminescence in a multilayer white organic light-emitting diode *Nat. Mater.* **12** 652–8
[140] Peumans P, Uchida S and Forrest S R 2003 Efficient bulk heterojunction photovoltaic cells using small-molecular-weight organic thin films *Nature* **425** 158–62
[141] Groves C, Blakesley J C and Greenham N C 2010 Effect of charge trapping on geminate recombination and polymer solar cell performance *Nano Lett.* **10** 1063–9
[142] Casalegno M, Raos G and Po R 2010 Methodological assessment of kinetic Monte Carlo simulations of organic photovoltaic devices: the treatment of electrostatic interactions *J. Chem. Phys.* **132** 094705
[143] Kimber R G E, Wright E N, O'Kane S E J, Walker A B and Blakesley J C 2012 Mesoscopic kinetic Monte Carlo modeling of organic photovoltaic device characteristics *Phys. Rev.* B **86** 235206
[144] Wolf U, Arkhipov V I and Bassler H 1999 Current injection from a metal to a disordered hopping system. I. Monte Carlo simulation *Phys. Rev.* B **59** 7507–13
[145] Scheidler M, Lemmer U, Kersting R, Karg S, Riess W, Cleve B, Mahrt R F, Kurz H, Bassler H, Gobel E O and Thomas P 1996 Monte Carlo study of picosecond exciton relaxation and dissociation in poly(phenylenevinylene) *Phys. Rev.* B **54** 5536–44
[146] Athanasopoulos S, Emelianova E V, Walker A B and Beljonne D 2009 Exciton diffusion in energetically disordered organic materials *Phys. Rev.* B **80** 195209
[147] Watkins P K, Walker A B and Verschoor G L B 2005 Dynamical Monte Carlo modelling of organic solar cells: the dependence of internal quantum efficiency on morphology *Nano Lett.* **5** 1814–8
[148] Feron K, Zhou X, Belcher W J and Dastoor P C 2012 Exciton transport in organic semiconductors: Forster resonance energy transfer compared with a simple random walk *J. Appl. Phys.* **111** 044510
[149] Scully S R and McGehee M D 2006 Effects of optical interference and energy transfer on exciton diffusion length measurements in organic semiconductors *J. Appl. Phys.* **100** 034907
[150] Clarke T M and Durrant J R 2010 Charge photogeneration in organic solar cells *Chem. Rev.* **110** 6736–67
[151] Zaumseil J and Sirringhaus H 2007 Electron and ambipolar transport in organic field-effect transistors *Chem. Rev.* **107** 1296–323
[152] Zaumseil J, Groves C, Winfield J M, Greenham N C and Sirringhaus H 2008 Electron–hole recombination in

uniaxially aligned semiconducting polymers *Adv. Funct. Mater.* **18** 3630–7
[153] Deibel C, Strobel T and Dyakonov V 2010 Role of the charge transfer state in organic donor–acceptor solar cells *Adv. Mater.* **22** 4097–111
[154] Bakulin A A, Rao A, Pavelyev V G, van Loosdrecht P H M, Pshenichnikov M S, Niedzialek D, Cornil J, Beljonne D and Friend R H 2012 The role of driving energy and delocalized states for charge separation in organic semiconductors *Science* **335** 1340–4
[155] Grancini G, Maiuri M, Fazzi D, Petrozza A, Egelhaaf H J, Brida D, Cerullo G and Lanzani G 2013 Hot exciton dissociation in polymer solar cells *Nat. Mater.* **12** 29–33
[156] Jailaubekov A E *et al* 2013 Hot charge-transfer excitons set the time limit for charge separation at donor/acceptor interfaces in organic photovoltaics *Nat. Mater.* **12** 66–73
[157] Huang Y S, Westenhoff S, Avilov I, Sreearunothai P, Hodgkiss J M, Deleener C, Friend R H and Beljonne D 2008 Electronic structures of interfacial states formed at polymeric semiconductor heterojunctions *Nat. Mater.* **7** 483–9
[158] Tempelaar R, Koster L J A, Havenith R W A, Knoester J and Jansen T L C 2016 Charge recombination suppressed by destructive quantum interference in heterojunction materials *J. Phys. Chem. Lett.* **7** 198–203
[159] Brabec C J, Heeney M, McCulloch I and Nelson J 2011 Influence of blend microstructure on bulk heterojunction organic photovoltaic performance *Chem. Soc. Rev.* **40** 1185–99
[160] McNeill C R 2012 Morphology of all-polymer solar cells *Energy Environ. Sci.* **5** 5653–67
[161] Rand B P *et al* 2012 The impact of molecular orientation on the photovoltaic properties of a phthalocyanine/fullerene heterojunction *Adv. Funct. Mater.* **22** 2987–95
[162] Sedgewick R and Wayne K 2011 *Algorithms* (Reading, MA: Addison-Wesley)
[163] Lukkien J J, Segers J P L, Hilbers P A J, Gelten R J and Jansen A P J 1998 Efficient Monte Carlo methods for the simulation of catalytic surface reactions *Phys. Rev.* E **58** 2598–610
[164] Groves C, Kimber R G E and Walker A B 2010 Simulation of loss mechanisms in organic solar cells: a description of the mesoscopic Monte Carlo technique and an evaluation of the first reaction method *J. Chem. Phys.* **133** 144110
[165] Mladenović M and Vukmirović N 2015 Charge carrier localization and transport in organic semiconductors: insights from atomistic multiscale simulations *Adv. Funct. Mater.* **25** 1915–32
[166] Cheung D L and Troisi A 2008 Modelling charge transport in organic semiconductors: from quantum dynamics to soft matter *Phys. Chem. Chem. Phys.* **10** 5941–52
[167] Olivier Y, Niedzialek D, Lemaur V, Pisula W, Mullen K, Koldemir U, Reynolds J R, Lazzaroni R, Cornil J and Beljonne D 2014 25th anniversary article: high-mobility hole and electron transport conjugated polymers: how structure defines function *Adv. Mater.* **26** 2119–36
[168] Kordt P, van der Holst J J M, Al Helwi M, Kowalsky W, May F, Badinski A, Lennartz C and Andrienko D 2015 Modeling of organic light emitting diodes: from molecular to device properties *Adv. Funct. Mater.* **25** 1955–71
[169] Bredas J L, Norton J E, Cornil J and Coropceanu V 2009 Molecular understanding of organic solar cells: the challenges *Acc. Chem. Res.* **42** 1691–9
[170] Bernardi M and Grossman J C 2016 Computer calculations across time and length scales in photovoltaic solar cells *Energy Environ. Sci.* **9** 2197–218
[171] Do K, Ravva M K, Wang T and Brédas J-L 2016 Computational methodologies for developing structure-morphology-performance relationships in organic solar cells: a protocol review *Chem. Mater.* at press
[172] Ruhle V, Lukyanov A, May F, Schrader M, Vehoff T, Kirkpatrick J, Baumeier B and Andrienko D 2011 Microscopic simulations of charge transport in disordered organic semiconductors *J. Chem. Theory Comput.* **7** 3335–45
[173] Leenen M A M *et al* 2010 Electronic properties and supramolecular organization of terminal bis(alkylethynyl)-substituted benzodithiophenes *J. Phys. Chem.* B **114** 14614–20
[174] Beaujuge P M *et al* 2012 Synthetic principles directing charge transport in low-band-gap dithienosilole-benzothiadiazole copolymers *J. Am. Chem. Soc.* **134** 8944–57
[175] Vukmirović N and Wang L-W 2009 Charge carrier motion in disordered conjugated polymers: a multiscale *ab initio* study *Nano Lett.* **9** 3996–4000
[176] McMahon D P, Cheung D L, Goris L, Dacuna J, Salleo A and Troisi A 2011 Relation between microstructure and charge transport in polymers of different regioregularity *J. Phys. Chem.* C **115** 19386–93
[177] Schwarz K N, Kee T W and Huang D M 2013 Coarse-grained simulations of the solution-phase self-assembly of poly(3-hexylthiophene) nanostructures *Nanoscale* **5** 2017–27
[178] Ruhle V, Junghans C, Lukyanov A, Kremer K and Andrienko D 2009 Versatile object-oriented toolkit for coarse-graining applications *J. Chem. Theory Comput.* **5** 3211–23
[179] Kremer K and Müller-Plathe F 2002 Multiscale simulation in polymer science *Mol. Simul.* **28** 729–50
[180] DuBay K H, Hall M L, Hughes T F, Wu C, Reichman D R and Friesner R A 2012 Accurate force field development for modeling conjugated polymers *J. Chem. Theory Comput.* **8** 4556–69
[181] To T T and Adams S 2014 Modelling of P3HT:PCBM interface using coarse-grained forcefield derived from accurate atomistic forcefield *Phys. Chem. Chem. Phys.* **16** 4653–63
[182] Ruhle V, Kirkpatrick J, Kremer K and Andrienko D 2008 Coarse-grained modelling of polypyrrole morphologies *Phys. Status Solidi* b **245** 844–8
[183] Lukyanov A and Andrienko D 2010 Extracting nondispersive charge carrier mobilities of organic semiconductors from simulations of small systems *Phys. Rev.* B **82** 4
[184] Kwiatkowski J J, Nelson J, Li H, Bredas J L, Wenzel W and Lennartz C 2008 Simulating charge transport in tris(8-hydroxyquinoline) aluminium (Alq3) *Phys. Chem. Chem. Phys.* **10** 1852–8
[185] Jones M L, Huang D M, Chakrabarti B and Groves C 2016 Relating molecular morphology to charge mobility in semicrystalline conjugated polymers *J. Phys. Chem.* C **120** 4240–50
[186] Vukmirović N and Wang L-W 2009 Electronic structure of disordered conjugated polymers: polythiophenes *J. Phys. Chem.* B **113** 409–15
[187] Kirkpatrick J 2008 An approximate method for calculating transfer integrals based on the ZINDO Hamiltonian *Int. J. Quantum Chem.* **108** 51–6
[188] Ruhle V, Kirkpatrick J and Andrienko D 2010 A multiscale description of charge transport in conjugated oligomers *J. Chem. Phys.* **132** 9
[189] Vehoff T, Chung Y S, Johnston K, Troisi A, Yoon D Y and Andrienko D 2010 Charge transport in self-assembled semiconducting organic layers: role of dynamic and static disorder *J. Phys. Chem.* C **114** 10592–7
[190] Valeev E F, Coropceanu V, da Silva Filho D A, Salman S and Brédas J-L 2006 Effect of electronic polarization

on charge-transport parameters in molecular organic semiconductors *J. Am. Chem. Soc.* **128** 9882–6
[191] Risko C, Kushto G P, Kafati Z H and Brédas J L 2004 Electronic properties of silole-based organic semiconductors *J. Chem. Phys.* **121** 9031–8
[192] Kirkpatrick J, Marcon V, Kremer K, Nelson J and Andrienko D 2008 Columnar mesophases of hexabenzocoronene derivatives. II. Charge carrier mobility *J. Chem. Phys.* **129** 094506
[193] Hutchison G R, Ratner M A and Marks T J 2005 Hopping transport in conductive heterocyclic oligomers: reorganization energies and substituent effects *J. Am. Chem. Soc.* **127** 2339–50
[194] Springel V 2005 The cosmological simulation code GADGET-2 *Mon. Not. R. Astron. Soc.* **364** 1105–34
[195] Vahedi V and Surendra M 1995 A Monte-Carlo collision model for the particle-in-cell method—applications to argon and oxygen discharges *Comput. Phys. Commun.* **87** 179–98
[196] Greengard L and Rokhlin V 1987 A fast algorithm for particle simulations *J. Comput. Phys.* **73** 325–48
[197] Appel A W 1985 An efficient program for many-body simulation *SIAM J. Sci. Stat. Comput.* **6** 85–103
[198] Chatterjee A and Voter A F 2010 Accurate acceleration of kinetic Monte Carlo simulations through the modification of rate constants *J. Chem. Phys.* **132** 12
[199] Barnes J and Hut P 1986 A hierarchical O(*N* log *N*) force-calculation algorithm *Nature* **324** 446–9
[200] Chatterjee A and Vlachos D G 2007 An overview of spatial microscopic and accelerated kinetic Monte Carlo methods *J. Comput. Aided Mater. Des.* **14** 253–308
[201] Yang F and Forrest S R 2008 Photocurrent generation in nanostructured organic solar cells *ACS Nano* **2** 1022–32
[202] Meng L Y, Wang D, Li Q K, Yi Y P, Bredas J L and Shuai Z G 2011 An improved dynamic Monte Carlo model coupled with Poisson equation to simulate the performance of organic photovoltaic devices *J. Chem. Phys.* **134** 124102
[203] van der Kaap N J and Koster L J A 2016 Massively parallel kinetic Monte Carlo simulations of charge carrier transport in organic semiconductors *J. Comput. Phys.* **307** 321–32
[204] Schulze T P 2008 Efficient kinetic Monte Carlo simulation *J. Comput. Phys.* **227** 2455–62
[205] Brereton T, Stenzel O, Baumeier B, Andrienko D, Schmidt V and Kroese D 2014 Efficient simulation of markov chains using segmentation *Methodol. Comput. Appl. Probab.* **16** 465–84
[206] Mendels D and Tessler N 2013 The topology of hopping in the energy domain of systems with rapidly decaying density of states *J. Phys. Chem.* C **117** 24740–5
[207] Gonzalez-Vazquez J P, Anta J A and Bisquert J 2009 Random walk numerical simulation for hopping transport at finite carrier concentrations: diffusion coefficient and transport energy concept *Phys. Chem. Chem. Phys.* **11** 10359–67
[208] Scher H and Montroll E 1975 Anomalous transit time dispersion in amorphous solids *Phys. Rev.* B **12** 2455–77
[209] Borsenberger P M, Pautmeier L T and Bässler H 1992 Nondispersive-to-dispersive charge-transport transition in disordered molecular solids *Phys. Rev.* B **46** 12145–53
[210] Vissenberg M C J M and Matters M 1998 Theory of the field-effect mobility in amorphous organic transistors *Phys. Rev.* B **57** 12964–7
[211] Blom P W M, de Jong M J M and van Munster M G 1997 Electric-field and temperature dependence of the hole mobility in poly(p-phenylene vinylene) *Phys. Rev.* B **55** R656–9
[212] Brütting W, Berleb S and Mückl A G 2001 Space-charge limited conduction with a field and temperature dependent mobility in Alq light-emitting devices *Synth. Met.* **122** 99–104
[213] Bao Z, Dodabalapur A and Lovinger A J 1996 Soluble and processable regioregular poly(3-hexylthiophene) for thin film field-effect transistor applications with high mobility *Appl. Phys. Lett.* **69** 4108–10
[214] Mott N and Gurney R 1940 *Electronic Processes in Ionic Crystals* (Oxford: Oxford University Press)
[215] Murgatroyd P N 1970 Theory of space-charge-limited current enhanced by Frenkel effect *J. Phys. D: Appl. Phys.* **3** 151
[216] Juška G, Arlauskas K, Viliūnas M and Kočka J 2000 Extraction current transients: new method of study of charge transport in microcrystalline silicon *Phys. Rev. Lett.* **84** 4946–9
[217] Pivrikas A, Sariciftci N S, Juška G and Österbacka R 2007 A review of charge transport and recombination in polymer/fullerene organic solar cells *Prog. Photovolt., Res. Appl.* **15** 677–96
[218] Khan R U A, Poplavskyy D, Kreouzis T and Bradley D D C 2007 Hole mobility within arylamine-containing polyfluorene copolymers: a time-of-flight transient-photocurrent study *Phys. Rev.* B **75** 035215
[219] Tanase C, Meijer E J, Blom P W M and de Leeuw D M 2003 Unification of the hole transport in polymeric field-effect transistors and light-emitting diodes *Phys. Rev. Lett.* **91** 216601
[220] Li H, Duan L, Zhang D, Dong G, Qiao J, Wang L and Qiu Y 2014 Relationship between mobilities from time-of-flight and dark-injection space-charge-limited current measurements for organic semiconductors: a Monte Carlo study *J. Phys. Chem.* C **118** 6052–8
[221] Rappaport N, Bar Y, Solomeshch O and Tessler N 2006 Mobility spatial distribution function: comparative method for conjugated polymers/molecules *Appl. Phys. Lett.* **89** 3
[222] Hulea I N, Brom H B, Houtepen A J, Vanmaekelbergh D, Kelly J J and Meulenkamp E A 2004 Wide energy-window view on the density of states and hole mobility in poly(p-phenylene vinylene) *Phys. Rev. Lett.* **93** 166601
[223] Street R A, Song K W, Northrup J E and Cowan S 2011 Photoconductivity measurements of the electronic structure of organic solar cells *Phys. Rev.* B **83** 165207
[224] Frost J M, Kirkpatrick J, Kirchartz T and Nelson J 2014 Parameter free calculation of the subgap density of states in poly(3-hexylthiophene) *Faraday Discuss.* **174** 255–66
[225] Bassler H 1993 Charge transport in disordered organic photoconductors—a Monte-Carlo simulation study *Phys. Status Solidi* b **175** 15–56
[226] Martens H C F, Blom P W M and Schoo H F M 2000 Comparative study of hole transport in poly(p-phenylene vinylene) derivatives *Phys. Rev.* B **61** 7489–93
[227] Novikov S V, Dunlap D H, Kenkre V M, Parris P E and Vannikov A V 1998 Essential role of correlations in governing charge transport in disordered organic materials *Phys. Rev. Lett.* **81** 4472–5
[228] Gartstein Y N and Conwell E M 1995 High-field hopping mobility in molecular-systems with spatially correlated energetic disorder *Chem. Phys. Lett.* **245** 351–8
[229] Yu Z G, Smith D L, Saxena A, Martin R L and Bishop A R 2000 Molecular geometry fluctuation model for the mobility of conjugated polymers *Phys. Rev. Lett.* **84** 721–4
[230] Roichman Y and Tessler N 2003 Charge transport in conjugated polymers—the influence of charge concentration *Synth. Met.* **135–6** 443–4
[231] Coehoorn R, Pasveer W F, Bobbert P A and Michels M A J 2005 Charge-carrier concentration dependence of the hopping mobility in organic materials with Gaussian disorder *Phys. Rev.* B **72** 155206
[232] Katsouras I, Najafi A, Asadi K, Kronemeijer A J, Oostra A J, Koster L J A, de Leeuw D M and Blom P W M 2013

Charge transport in poly(p-phenylene vinylene) at low temperature and high electric field *Org. Electron.* **14** 1591–6
[233] van Mensfoort S L M, Vulto S I E, Janssen R A J and Coehoorn R 2008 Hole transport in polyfluorene-based sandwich-type devices: quantitative analysis of the role of energetic disorder *Phys. Rev.* B **78** 085208
[234] Sirringhaus H *et al* 1999 Two-dimensional charge transport in self-organized, high-mobility conjugated polymers *Nature* **401** 685–8
[235] Heun S and Borsenberger P M 1995 A comparative study of hole transport in vapor-deposited molecular glasses of *N*,*N*′,*N*″,*N*‴-tetrakis(4-methylphenyl)-(1,1′-biphenyl)-4,4′-diamine and *N*,*N*′-diphenyl-N,N′-bis(3-methylphenyl)-(1,1′-biphenyl)-4,4′-diamine *Chem. Phys.* **200** 245–55
[236] Rommens J, Van der Auweraer M, De Schryver F C, Terrell D and De Meutter S 1996 Electron transport in 1,3-Bis(dicyanomethylene)indans *J. Phys. Chem.* **100** 10673–80
[237] Tal O, Rosenwaks Y, Preezant Y, Tessler N, Chan C K and Kahn A 2005 Direct determination of the hole density of states in undoped and doped amorphous organic films with high lateral resolution *Phys. Rev. Lett.* **95** 256405
[238] Kuik M, Koster L J A, Wetzelaer G A H and Blom P W M 2011 Trap-assisted recombination in disordered organic semiconductors *Phys. Rev. Lett.* **107** 256805
[239] MacKenzie R C I, Kirchartz T, Dibb G F A and Nelson J 2011 Modeling nongeminate recombination in P3HT:PCBM solar cells *J. Phys. Chem.* C **115** 9806–13
[240] Nelson J 2003 Diffusion-limited recombination in polymer-fullerene blends and its influence on photocurrent collection *Phys. Rev.* B **67** 155209
[241] Einstein A 1905 The motion of elements suspended in static liquids as claimed in the molecular kinetic theory of heat *Ann. Phys.* **17** 549–60
[242] Pinner D J, Friend R H and Tessler N 1999 Transient electroluminescence of polymer light emitting diodes using electrical pulses *J. Appl. Phys.* **86** 5116–30
[243] Blom P W M and Vissenberg M C J M 1998 Dispersive hole transport in poly(p-phenylene vinylene) *Phys. Rev. Lett.* **80** 3819–22
[244] Nenashev A V, Jansson F, Baranovskii S D, Österbacka R, Dvurechenskii A V and Gebhard F 2010 Effect of electric field on diffusion in disordered materials. II. Two- and three-dimensional hopping transport *Phys. Rev.* B **81** 115204
[245] Mendels D and Tessler N 2013 Drift and diffusion in disordered organic semiconductors: the role of charge density and charge energy transport *J. Phys. Chem.* C **117** 3287–93
[246] Rappaport N, Preezant Y and Tessler N 2007 Spatially dispersive transport: a mesoscopic phenomenon in disordered organic semiconductors *Phys. Rev.* B **76** 235323
[247] Groves C, Reid O G and Ginger D S 2010 Heterogeneity in polymer solar cells: local morphology and performance in organic photovoltaics studied with scanning probe microscopy *Acc. Chem. Res.* **43** 612–20
[248] Reid O G, Munechika K and Ginger D S 2008 Space charge limited current measurements on conjugated polymer films using conductive atomic force microscopy *Nano Lett.* **8** 1602–9
[249] Essam J W 1980 Percolation theory *Rep. Prog. Phys.* **43** 833–912
[250] Schlovskii B and Efros A 1984 *Electronic Properties of Doped Semiconductors* vol 45 (Berlin: Springer)
[251] Mott N F 1969 Conduction in non-crystalline materials *Phil. Mag.* **19** 835–52
[252] Grünewald M and Thomas P 1979 A hopping model for activated charge transport in amorphous silicon *Phys. Status Solidi* b **94** 125–33
[253] van der Holst J J M, Uijttewaal M A, Balasubramanian R, Coehoorn R, Bobbert P A, de Wijs G A and de Groot R A 2009 Modeling and analysis of the three-dimensional current density in sandwich-type single-carrier devices of disordered organic semiconductors *Phys. Rev.* B **79** 085203
[254] Marianer S and Shklovskii B I 1992 Effective temperature of hopping electrons in a strong electric field *Phys. Rev.* B **46** 13100–3
[255] Preezant Y and Tessler N 2006 Carrier heating in disordered organic semiconductors *Phys. Rev.* B **74** 235202
[256] Germs W C, Van der Holst J J M, Van Mensfoort S L M, Bobbert P A and Coehoorn R 2011 Modeling of transient mobility in disordered organic semiconductors with a Gaussian density of states *Phys. Rev.* B **84** 165210
[257] Melianas A, Pranculis V, Devižis A, Gulbinas V, Inganäs O and Kemerink M 2014 Dispersion-dominated photocurrent in polymer: fullerene solar cells *Adv. Funct. Mater.* **24** 4507–14
[258] Howard I A, Etzold F, Laquai F and Kemerink M 2014 Nonequilibrium charge dynamics in organic solar cells *Adv. Energy Mater.* **4** 1301743
[259] Philippa B, Stolterfoht M, Burn P L, Juška G, Meredith P, White R D and Pivrikas A 2014 The impact of hot charge carrier mobility on photocurrent losses in polymer-based solar cells *Sci. Rep.* **4** 5695
[260] van der Kaap N J and Koster L J A 2016 Charge carrier thermalization in organic diodes *Sci. Rep.* **6** 19794
[261] Hoffmann S T, Athanasopoulos S, Beljonne D, Bassler H and Kohler A 2012 How do triplets and charges move in disordered organic semiconductors? A Monte Carlo study comprising the equilibrium and nonequilibrium regime *J. Phys. Chem.* C **116** 16371–83
[262] Salleo A, Kline R J, DeLongchamp D M and Chabinyc M L 2010 Microstructural characterization and charge transport in thin films of conjugated polymers *Adv. Mater.* **22** 3812–38
[263] Salleo A 2007 Charge transport in polymeric transistors *Mater. Today* **10** 38–45
[264] Facchetti A 2007 Semiconductors for organic transistors *Mater. Today* **10** 28–37
[265] Murphy A R and Fréchet J M J 2007 Organic semiconducting oligomers for use in thin film transistors *Chem. Rev.* **107** 1066–96
[266] McNeill C R and Greenham N C 2008 Charge transport dynamics of polymer solar cells under operating conditions: influence of trap filling *Appl. Phys. Lett.* **93** 203310
[267] Frost J M, Cheynis F, Tuladhar S M and Nelson J 2006 Influence of polymer-blend morphology on charge transport and photocurrent generation in donor-acceptor polymer blends *Nano Lett.* **6** 1674–81
[268] Ortmann F, Radke K S, Günther A, Kasemann D, Leo K and Cuniberti G 2015 Materials meets concepts in molecule-based electronics *Adv. Funct. Mater.* **25** 1933–54
[269] Wang L J, Prezhdo O V and Beljonne D 2015 Mixed quantum-classical dynamics for charge transport in organics *Phys. Chem. Chem. Phys.* **17** 12395–406
[270] Brédas J L, Calbert J P, da Silva Filho D A and Cornil J 2002 Organic semiconductors: a theoretical characterization of the basic parameters governing charge transport *Proc. Natl Acad. Sci.* **99** 5804–9
[271] Ide J, Fazzi D, Casalegno M, Meille S V and Raos G 2014 Electron transport in crystalline PCBM-like fullerene derivatives: a comparative computational study *J. Mater. Chem.* C **2** 7313–25

[272] Kwiatkowski J J, Frost J M and Nelson J 2009 The effect of morphology on electron field-effect mobility in disordered c60 thin films *Nano Lett.* **9** 1085–90

[273] Feng X L, Marcon V, Pisula W, Hansen M R, Kirkpatrick J, Grozema F, Andrienko D, Kremer K and Mullen K 2009 Towards high charge-carrier mobilities by rational design of the shape and periphery of discotics *Nat. Mater.* **8** 421–6

[274] Niedzialek D, Lemaur V, Dudenko D, Shu J, Hansen M R, Andreasen J W, Pisula W, Mullen K, Cornil J and Beljonne D 2013 Probing the relation between charge transport and supramolecular organization down to Angstrom resolution in a benzothiadiazole-cyclopentadithiophene copolymer *Adv. Mater.* **25** 1939–47

[275] May F, Marcon V, Hansen M R, Grozema F and Andrienko D 2011 Relationship between supramolecular assembly and charge-carrier mobility in perylenediimide derivatives: the impact of side chains *J. Mater. Chem.* **21** 9538–45

[276] Schrader M, Korner C, Elschner C and Andrienko D 2012 Charge transport in amorphous and smectic mesophases of dicyanovinyl-substituted oligothiophenes *J. Mater. Chem.* **22** 22258–64

[277] Elschner C, Schrader M, Fitzner R, Levin A A, Bauerle P, Andrienko D, Leo K and Riede M 2013 Molecular ordering and charge transport in a dicyanovinyl-substituted quaterthiophene thin film *RSC Adv.* **3** 12117–23

[278] Kirkpatrick J, Marcon V, Nelson J, Kremer K and Andrienko D 2007 Charge mobility of discotic mesophases: a multiscale quantum and classical study *Phys. Rev. Lett.* **98** 4

[279] Carbone P and Troisi A 2014 Charge diffusion in semiconducting polymers: analytical relation between polymer rigidity and time scales for intrachain and interchain hopping *J. Phys. Chem. Lett.* **5** 2637–41

[280] Poelking C and Andrienko D 2013 Effect of polymorphism, regioregularity and paracrystallinity on charge transport in poly(3-hexylthiophene) P3HT nanofibers *Macromolecules* **46** 8941–56

[281] Gemunden P, Poelking C, Kremer K, Andrienko D and Daoulas K C 2013 Nematic ordering, conjugation, and density of states of soluble polymeric semiconductors *Macromolecules* **46** 5762–74

[282] Cheung D L, McMahon D P and Troisi A 2009 Computational study of the structure and charge-transfer parameters in low-molecular-mass P3HT *J. Phys. Chem.* B **113** 9393–401

[283] Qin T and Troisi A 2013 Relation between structure and electronic properties of amorphous MEH-PPV polymers *J. Am. Chem. Soc.* **135** 11247–56

[284] Poelking C, Cho E, Malafeev A, Ivanov V, Kremer K, Risko C, Bredas J L and Andrienko D 2013 Characterization of charge-carrier transport in semicrystalline polymers: electronic couplings, site energies, and charge-carrier dynamics in poly(bithiophene-alt-thienothiophene) PBTTT *J. Phys. Chem.* C **117** 1633–40

[285] Liu T and Troisi A 2014 Understanding the microscopic origin of the very high charge mobility in PBTTT: tolerance of thermal disorder *Adv. Funct. Mater.* **24** 925–33

[286] Chabinyc M L, Toney M F, Kline R J, McCulloch I and Heeney M 2007 X-ray scattering study of thin films of poly(2,5-bis(3-alkylthiophen-2-yl)thieno[3,2-b]thiophene) *J. Am. Chem. Soc.* **129** 3226–37

[287] Do K, Huang D M, Faller R and Moule A J 2010 A comparative MD study of the local structure of polymer semiconductors P3HT and PBTTT *Phys. Chem. Chem. Phys.* **12** 14735–9

[288] Northrup J E 2007 Atomic and electronic structure of polymer organic semiconductors: P3HT, PQT, and PBTTT *Phys. Rev.* B **76** 245202

[289] Mollinger S A, Krajina B A, Noriega R, Salleo A and Spakowitz A J 2015 Percolation, tie-molecules, and the microstructural determinants of charge transport in semicrystalline conjugated polymers *ACS Macro Lett.* **4** 708–12

[290] Zhang F *et al* 2013 Critical role of alkyl chain branching of organic semiconductors in enabling solution-processed N-channel organic thin-film transistors with mobility of up to 3.50 $cm^2 V^{-1} s^{-1}$ *J. Am. Chem. Soc.* **135** 2338–49

[291] Kang I, Yun H-J, Chung D S, Kwon S-K and Kim Y-H 2013 Record high hole mobility in polymer semiconductors via side-chain engineering *J. Am. Chem. Soc.* **135** 14896–9

[292] Sun B, Hong W, Yan Z, Aziz H and Li Y 2014 Record high electron mobility of 6.3 $cm^2 V^{-1} s^{-1}$ achieved for polymer semiconductors using a new building block *Adv. Mater.* **26** 2636–42

[293] Jackson N E, Kohlstedt K L, Savoie B M, Olvera de la Cruz M, Schatz G C, Chen L X and Ratner M A 2015 Conformational order in aggregates of conjugated polymers *J. Am. Chem. Soc.* **137** 6254–62

[294] Rotzoll R, Mohapatra S, Olariu V, Wenz R, Grigas M, Dimmler K, Shchekin O and Dodabalapur A 2006 Radio frequency rectifiers based on organic thin-film transistors *Appl. Phys. Lett.* **88** 3

[295] Mandal S *et al* 2015 Fully-printed, all-polymer, bendable and highly transparent complementary logic circuits *Org. Electron.* **20** 132–41

[296] Newman C R, Frisbie C D, da Silva D A, Bredas J L, Ewbank P C and Mann K R 2004 Introduction to organic thin film transistors and design of n-channel organic semiconductors *Chem. Mater.* **16** 4436–51

[297] Facchetti A 2011 pi-conjugated polymers for organic electronics and photovoltaic cell applications *Chem. Mater.* **23** 733–58

[298] Klauk H 2010 Organic thin-film transistors *Chem. Soc. Rev.* **39** 2643–66

[299] Necliudov P V, Shur M S, Gundlach D J and Jackson T N 2000 Modeling of organic thin film transistors of different designs *J. Appl. Phys.* **88** 6594–7

[300] Gundlach D J, Zhou L, Nichols J A, Jackson T N, Necliudov P V and Shur M S 2006 An experimental study of contact effects in organic thin film transistors *J. Appl. Phys.* **100** 024509

[301] Noh Y Y, Zhao N, Caironi M and Sirringhaus H 2007 Downscaling of self-aligned, all-printed polymer thin-film transistors *Nat. Nanotechnol.* **2** 784–9

[302] Sekitani T, Noguchi Y, Zschieschang U, Klauk H and Someya T 2008 Organic transistors manufactured using inkjet technology with subfemtoliter accuracy *Proc. Natl Acad. Sci.* **105** 4976–80

[303] Minari T, Miyadera T, Tsukagoshi K, Aoyagi Y and Ito H 2007 Charge injection process in organic field-effect transistors *Appl. Phys. Lett.* **91** 3

[304] Zhou Y H *et al* 2012 A universal method to produce low-work function electrodes for organic electronics *Science* **336** 327–32

[305] Acton O *et al* 2011 Simultaneous modification of bottom-contact electrode and dielectric surfaces for organic thin-film transistors through single-component spin-cast monolayers *Adv. Funct. Mater.* **21** 1476–88

[306] Pesavento P V, Puntambekar K P, Frisbie C D, McKeen J C and Ruden P P 2006 Film and contact resistance in pentacene thin-film transistors: dependence on film thickness, electrode geometry, and correlation with hole mobility *J. Appl. Phys.* **99** 10

[307] Wang S D, Minari T, Miyadera T, Tsukagoshi K and Aoyagi Y 2007 Contact-metal dependent current injection in pentacene thin-film transistors *Appl. Phys. Lett.* **91** 3

[308] Street R A and Salleo A 2002 Contact effects in polymer transistors *Appl. Phys. Lett.* **81** 2887–9

[309] Tessler N and Roichman Y 2001 Two-dimensional simulation of polymer field-effect transistor *Appl. Phys. Lett.* **79** 2987–9

[310] Chun-sung C, Sandrine M, Jerzy K, Yasuhiro U, Teizo Y and Shu T 1998 Top-gate staggered amorphous silicon thin-film transistors: series resistance and nitride thickness effects *Japan. J. Appl. Phys.* **37** 5914

[311] Wang S D, Yan Y and Tsukagoshi K 2010 Understanding contact behavior in organic thin film transistors *Appl. Phys. Lett.* **97** 063307

[312] Brondijk J J, Torricelli F, Smits E C P, Blom P W M and de Leeuw D M 2012 Gate-bias assisted charge injection in organic field-effect transistors *Org. Electron.* **13** 1526–31

[313] Vinciguerra V, Rosa M L, Nicolosi D, Sicurella G and Occhipinti L 2009 Modeling the gate bias dependence of contact resistance in staggered polycrystalline organic thin film transistors *Org. Electron.* **10** 1074–81

[314] Gruber M, Schürrer F and Zojer K 2012 Relation between injection barrier and contact resistance in top-contact organic thin-film transistors *Org. Electron.* **13** 1887–99

[315] Gruber M, Zojer E, Schürrer F and Zojer K 2013 Impact of materials versus geometric parameters on the contact resistance in organic thin-film transistors *Adv. Funct. Mater.* **23** 2941–52

[316] Pesavento P V, Chesterfield R J, Newman C R and Frisbie C D 2004 Gated four-probe measurements on pentacene thin-film transistors: contact resistance as a function of gate voltage and temperature *J. Appl. Phys.* **96** 7312–24

[317] Scott J C and Malliaras G G 1999 Charge injection and recombination at the metal–organic interface *Chem. Phys. Lett.* **299** 115–9

[318] Albrecht U and Bassler H 1995 Yield of geminate pair dissociation in an energetically random hopping system *Chem. Phys. Lett.* **235** 389–93

[319] Hamadani B H and Natelson D 2005 Nonlinear charge injection in organic field-effect transistors *J. Appl. Phys.* **97** 064508

[320] Gagorik A G and Hutchison G R 2012 Simulating charge injection and dynamics in microscale organic field-effect transistors *J. Phys. Chem.* C **116** 21232–9

[321] Madison T A, Gagorik A G and Hutchison G R 2012 Charge transport in imperfect organic field effect transistors: effects of charge traps *J. Phys. Chem.* C **116** 11852–8

[322] Tanase C, Meijer E J, Blom P W M and de Leeuw D M 2003 Local charge carrier mobility in disordered organic field-effect transistors *Org. Electron.* **4** 33–7

[323] Scheinert S and Paasch G 2009 Interdependence of contact properties and field- and density-dependent mobility in organic field-effect transistors *J. Appl. Phys.* **105** 014509

[324] Scheinert S and Paasch G 2014 Influence of the carrier density in disordered organics with Gaussian density of states on organic field-effect transistors *J. Appl. Phys.* **115** 7

[325] Bisri S Z, Piliego C, Gao J and Loi M A 2014 Outlook and emerging semiconducting materials for ambipolar transistors *Adv. Mater.* **26** 1176–99

[326] Smith D L and Ruden P P 2007 Device modeling of light-emitting ambipolar organic semiconductor field-effect transistors *J. Appl. Phys.* **101** 6

[327] Kemerink M, Charrier D S H, Smits E C P, Mathijssen S G J, de Leeuw D M and Janssen R A J 2008 On the width of the recombination zone in ambipolar organic field effect transistors *Appl. Phys. Lett.* **93** 3

[328] Andersen T R *et al* 2014 Scalable, ambient atmosphere roll-to-roll manufacture of encapsulated large area, flexible organic tandem solar cell modules *Energy Environ. Sci.* **7** 2925–33

[329] Krebs F C, Tromholt T and Jorgensen M 2010 Upscaling of polymer solar cell fabrication using full roll-to-roll processing *Nanoscale* **2** 873–86

[330] MacKay J 2009 *Sustainable Energy—Without the Hot Air* (Cambridge: UIT Cambridge)

[331] Scholes G D and Rumbles G 2006 Excitons in nanoscale systems *Nat. Mater.* **5** 683–96

[332] Tang C W 1986 2-layer organic photovoltaic cell *Appl. Phys. Lett.* **48** 183–5

[333] Silva C 2013 Organic photovoltaics some like it hot *Nat. Mater.* **12** 5–6

[334] Albrecht S, Vandewal K, Tumbleston J R, Fischer F S U, Douglas J D, Fréchet J M J, Ludwigs S, Ade H, Salleo A and Neher D 2014 On the Efficiency of charge transfer state splitting in polymer: fullerene solar cells *Adv. Mater.* **26** 2533–9

[335] Koen V *et al* 2014 Efficient charge generation by relaxed charge-transfer states at organic interfaces *Nat. Mater.* **13** 63–8

[336] Yu G, Gao J, Hummelen J C, Wudl F and Heeger A J 1995 POLYMER photovoltaic cells—enhanced efficiencies via a network of internal donor-acceptor heterojunctions *Science* **270** 1789–91

[337] Halls J J M, Walsh C A, Greenham N C, Marseglia E A, Friend R H, Moratti S C and Holmes A B 1995 Efficient photodiodes from interpenetrating polymer networks *Nature* **376** 498–500

[338] Gebeyehu D, Maennig B, Drechsel J, Leo K and Pfeiffer M 2003 Bulk-heterojunction photovoltaic devices based on donor–acceptor organic small molecule blends *Sol. Energy Mater. Sol. Cells* **79** 81–92

[339] Padinger F, Rittberger R S and Sariciftci N S 2003 Effects of postproduction treatment on plastic solar cells *Adv. Funct. Mater.* **13** 85–8

[340] Arias A C, MacKenzie J D, Stevenson R, Halls J J M, Inbasekaran M, Woo E P, Richards D and Friend R H 2001 Photovoltaic performance and morphology of polyfluorene blends: a combined microscopic and photovoltaic investigation *Macromolecules* **34** 6005–13

[341] Li G, Yao Y, Yang H, Shrotriya V, Yang G and Yang Y 2007 'Solvent annealing' effect in polymer solar cells based on poly(3-hexylthiophene) and methanofullerenes *Adv. Funct. Mater.* **17** 1636–44

[342] Jamieson F C, Domingo E B, McCarthy-Ward T, Heeney M, Stingelin N and Durrant J R 2012 Fullerene crystallisation as a key driver of charge separation in polymer/fullerene bulk heterojunction solar cells *Chem. Sci.* **3** 485–92

[343] Ma W, Tumbleston J R, Wang M, Gann E, Huang F and Ade H 2013 Domain purity, miscibility, and molecular orientation at donor/acceptor interfaces in high performance organic solar cells: paths to further improvement *Adv. Energy Mater.* **3** 864–72

[344] Collins B A, Gann E, Guignard L, He X, McNeill C R and Ade H 2010 Molecular miscibility of polymer-fullerene blends *J. Phys. Chem. Lett.* **1** 3160–6

[345] Peet J, Heeger A J and Bazan G C 2009 'Plastic'Solar cells: self-assembly of bulk heterojunction nanomaterials by spontaneous phase separation *Acc. Chem. Res.* **42** 1700–8

[346] Deibel C and Dyakonov V 2010 Polymer-fullerene bulk heterojunction solar cells *Rep. Prog. Phys.* **73** 39

[347] Dibb G F A, Jamieson F C, Maurano A, Nelson J and Durrant J R 2013 Limits on the fill factor in organic photovoltaics: distinguishing nongeminate and geminate recombination mechanisms *J. Phys. Chem. Lett.* **4** 803–8

[348] Keivanidis P E, Clarke T M, Lilliu S, Agostinelli T, Macdonald J E, Durrant J R, Bradley D D C and Nelson J 2010 Dependence of charge separation efficiency on film microstructure in poly(3-hexylthiophene-2,5-diyl): [6,6]-phenyl-C-61 butyric acid methyl ester blend films *J. Phys. Chem. Lett.* **1** 734–8
[349] Koster L J A, Kemerink M, Wienk M M, Maturová K and Janssen R A J 2011 Quantifying bimolecular recombination losses in organic bulk heterojunction solar cells *Adv. Mater.* **23** 1670–4
[350] Hamilton R, Shuttle C G, O'Regan B, Hammant T C, Nelson J and Durrant J R 2010 Recombination in annealed and nonannealed polythiophene/fullerene solar cells: transient photovoltage studies versus numerical modeling *J. Phys. Chem. Lett.* **1** 1432–6
[351] Rauh D, Deibel C and Dyakonov V 2012 Charge density dependent nongeminate recombination in organic bulk heterojunction solar Cells *Adv. Funct. Mater.* **22** 3371–7
[352] Park S H, Roy A, Beaupre S, Cho S, Coates N, Moon J S, Moses D, Leclerc M, Lee K and Heeger A J 2009 Bulk heterojunction solar cells with internal quantum efficiency approaching 100% *Nat. Photon.* **3** 297–302
[353] Nelson J 2003 *The Physics of Solar Cells* (London: Imperial College Press)
[354] Rand B P, Burk D P and Forrest S R 2007 Offset energies at organic semiconductor heterojunctions and their influence on the open-circuit voltage of thin-film solar cells *Phys. Rev.* B **75** 115327
[355] Koster L J A, Mihailetchi V D and Blom P W M 2006 Ultimate efficiency of polymer/fullerene bulk heterojunction solar cells *Appl. Phys. Lett.* **88** 093511
[356] Servaites J D, Ratner M A and Marks T J 2009 Practical efficiency limits in organic photovoltaic cells: functional dependence of fill factor and external quantum efficiency *Appl. Phys. Lett.* **95** 163302
[357] Yan H, Collins B A, Gann E, Wang C, Ade H and McNeill C R 2012 Correlating the efficiency and nanomorphology of polymer blend solar cells utilizing resonant soft x-ray scattering *ACS Nano* **6** 677–88
[358] Yang X N, Loos J, Veenstra S C, Verhees W J H, Wienk M M, Kroon J M, Michels M A J and Janssen R A J 2005 Nanoscale morphology of high-performance polymer solar cells *Nano Lett.* **5** 579–83
[359] Ma W L, Yang C Y, Gong X, Lee K and Heeger A J 2005 Thermally stable, efficient polymer solar cells with nanoscale control of the interpenetrating network morphology *Adv. Funct. Mater.* **15** 1617–22
[360] Liang Y Y, Xu Z, Xia J B, Tsai S T, Wu Y, Li G, Ray C and Yu L P 2010 For the bright future-bulk heterojunction polymer solar cells with power conversion efficiency of 7.4% *Adv. Mater.* **22** E135–8
[361] Kotlarski J D, Blom P W M, Koster L J A, Lenes M and Slooff L H 2008 Combined optical and electrical modeling of polymer:fullerene bulk heterojunction solar cells *J. Appl. Phys.* **103** 084502
[362] Oosterhout S D, Wienk M M, van Bavel S S, Thiedmann R, Jan Anton Koster L, Gilot J, Loos J, Schmidt V and Janssen R A J 2009 The effect of three-dimensional morphology on the efficiency of hybrid polymer solar cells *Nat. Mater.* **8** 818–24
[363] Monestier F, Simon J-J, Torchio P, Escoubas L, Flory F, Bailly S, de Bettignies R, Guillerez S and Defranoux C 2007 Modeling the short-circuit current density of polymer solar cells based on P3HT:PCBM blend *Sol. Energy Mater. Sol. Cells* **91** 405–10
[364] Scharber M C, Mühlbacher D, Koppe M, Denk P, Waldauf C, Heeger A J and Brabec C J 2006 Design rules for donors in bulk-heterojunction solar cells—towards 10% energy-conversion efficiency *Adv. Mater.* **18** 789–94
[365] Veldman D, Meskers S C J and Janssen R A J 2009 The energy of charge-transfer states in electron donor–acceptor blends: insight into the energy losses in organic solar cells *Adv. Funct. Mater.* **19** 1939–48
[366] Brabec C J, Cravino A, Meissner D, Sariciftci N S, Fromherz T, Rispens M T, Sanchez L and Hummelen J C 2001 Origin of the open circuit voltage of plastic solar cells *Adv. Funct. Mater.* **11** 374–80
[367] Blakesley J C and Greenham N C 2009 Charge transfer at polymer-electrode interfaces: the effect of energetic disorder and thermal injection on band bending and open-circuit voltage *J. Appl. Phys.* **106** 034507
[368] Blakesley J C and Neher D 2011 Relationship between energetic disorder and open-circuit voltage in bulk heterojunction organic solar cells *Phys. Rev.* B **84** 075210
[369] Jorgensen M *et al* 2013 The state of organic solar cells-A meta analysis *Sol. Energy Mater. Sol. Cells* **119** 84–93
[370] Jackson N E, Savoie B M, Marks T J, Chen L X and Ratner M A 2015 The next breakthrough for organic photovoltaics? *J. Phys. Chem. Lett.* **6** 77–84
[371] Peumans P and Forrest S R 2004 Separation of geminate charge-pairs at donor–acceptor interfaces in disordered solids *Chem. Phys. Lett.* **398** 27–31
[372] Offermans T, Meskers S C J and Janssen R A J 2005 Monte-Carlo simulations of geminate electron–hole pair dissociation in a molecular heterojunction: a two-step dissociation mechanism *Chem. Phys.* **308** 125–33
[373] Athanasopoulos S, Greenham N C, Friend R H and Chepelianskii A D 2015 Field-enhanced recombination at low temperatures in an organic photovoltaic blend *Phys. Rev.* B **92** 10
[374] Barth S, Hertel D, Tak Y-H and Horhold H H 1997 Geminate pair dissociation in random organic systems *Chem. Phys. Lett.* **274** 165–70
[375] van Eersel H, Janssen R A J and Kemerink M 2012 Mechanism for efficient photoinduced charge separation at disordered organic heterointerfaces *Adv. Funct. Mater.* **22** 2700–8
[376] Chamberlain G A 1983 Organic solar-cells—a review *Sol. Cells* **8** 47–83
[377] Yan H, Swaraj S, Wang C, Hwang I, Greenham N C, Groves C, Ade H and McNeill C R 2010 Influence of annealing and interfacial roughness on the performance of bilayer donor/acceptor polymer photovoltaic devices *Adv. Funct. Mater.* **20** 4329–37
[378] Buxton G A and Clarke N 2006 Predicting structure and property relations in polymeric photovoltaic devices *Phys. Rev.* B **74** 085207
[379] Williams J and Walker A B 2008 Two-dimensional simulations of bulk heterojunction solar cell characteristics *Nanotechnology* **19** 424011
[380] Meng L Y, Shang Y, Li Q K, Li Y F, Zhan X W, Shuai Z G, Kimber R G E and Walker A B 2010 Dynamic Monte Carlo simulation for highly efficient polymer blend photovoltaics *J. Phys. Chem.* B **114** 36–41
[381] Kimber R G E, Walker A B, Schroder-Turk G E and Cleaver D J 2010 Bicontinuous minimal surface nanostructures for polymer blend solar cells *Phys. Chem. Chem. Phys.* **12** 844–51
[382] Gagorik A G, Mohin J W, Kowalewski T and Hutchison G R 2013 Monte Carlo simulations of charge transport in 2D organic photovoltaics *J. Phys. Chem. Lett.* **4** 36–42
[383] Bartesaghi D and Koster L J A 2015 The effect of large compositional inhomogeneities on the performance of organic solar cells: a numerical study *Adv. Funct. Mater.* **25** 2013–23
[384] He X M, Gao F, Tu G L, Hasko D, Huttner S, Steiner U, Greenham N C, Friend R H and Huck W T S 2010

Formation of nanopatterned polymer blends in photovoltaic devices *Nano Lett.* **10** 1302–7
[385] McNeill C R, Westenhoff S, Groves C, Friend R H and Greenham N C 2007 Influence of nanoscale phase separation on the charge generation dynamics and photovoltaic performance of conjugated polymer blends: balancing charge generation and separation *J. Phys. Chem.* C **111** 19153–60
[386] Gregg B A 2011 Entropy of charge separation in organic photovoltaic cells: the benefit of higher dimensionality *J. Phys. Chem. Lett.* **2** 3013–5
[387] Giazitzidis P, Argyrakis P, Bisquert J and Vikhrenko V S 2014 Charge separation in organic photovoltaic cells *Org. Electron.* **15** 1043–9
[388] Mayer A C, Toney M F, Scully S R, Rivnay J, Brabec C J, Scharber M, Koppe M, Heeney M, McCulloch I and McGehee M D 2009 Bimolecular crystals of fullerenes in conjugated polymers and the implications of molecular mixing for solar cells *Adv. Funct. Mater.* **19** 1173–9
[389] Gelinas S, Rao A, Kumar A, Smith S L, Chin A W, Clark J, van der Poll T S, Bazan G C and Friend R H 2014 Ultrafast long-range charge separation in organic semiconductor photovoltaic diodes *Science* **343** 512–6
[390] Vazquez H and Troisi A 2013 Calculation of rates of exciton dissociation into hot charge-transfer states in model organic photovoltaic interfaces *Phys. Rev.* B **88** 205304
[391] Caruso D and Troisi A 2012 Long-range exciton dissociation in organic solar cells *Proc. Natl Acad. Sci.* **109** 13498–502
[392] Savoie B M, Rao A, Bakulin A A, Gelinas S, Movaghar B, Friend R H, Marks T J and Ratner M A 2014 Unequal partnership: asymmetric roles of polymeric donor and fullerene acceptor in generating free charge *J. Am. Chem. Soc.* **136** 2876–84
[393] Nan G, Zhang X and Lu G 2015 Do 'Hot' charge-transfer excitons promote free carrier generation in organic photovoltaics? *J. Phys. Chem.* C **119** 15028–35
[394] van der Hofstad T G J, Di Nuzzo D, van den Berg M, Janssen R A J and Meskers S C J 2012 Influence of photon excess energy on charge carrier dynamics in a polymer-fullerene solar cell *Adv. Energy Mater.* **2** 1095–9
[395] Vandewal K *et al* 2014 Efficient charge generation by relaxed charge-transfer states at organic interfaces *Nat. Mater.* **13** 63–8
[396] Lee J, Vandewal K, Yost S R, Bahlke M E, Goris L, Baldo M A, Manca J V and Voorhis T V 2010 Charge transfer state versus hot exciton dissociation in polymer-fullerene blended solar cells *J. Am. Chem. Soc.* **132** 11878–80
[397] Jones M L, Dyer R, Clarke N and Groves C 2014 Are hot charge transfer states the primary cause of efficient free-charge generation in polymer:fullerene organic photovoltaic devices? A kinetic Monte Carlo study *Phys. Chem. Chem. Phys.* **16** 20310–20
[398] Hahn T, Geiger J, Blase X, Duchemin I, Niedzialek D, Tscheuschner S, Beljonne D, Bassler H and Kohler A 2015 Does excess energy assist photogeneration in an organic low-bandgap solar cell? *Adv. Funct. Mater.* **25** 1287–95
[399] McMahon D P, Cheung D L and Troisi A 2011 Why holes and electrons separate so well in polymer/fullerene photovoltaic cells *J. Phys. Chem. Lett.* **2** 2737–41
[400] D'Avino G, Muccioli L, Zannoni C, Beljonne D and Soos Z G 2014 Electronic polarization in organic crystals: a comparative study of induced dipoles and intramolecular charge redistribution schemes *J. Chem. Theory Comput.* **10** 4959–71
[401] Burke T M and McGehee M D 2014 How high local charge carrier mobility and an energy cascade in a three-phase bulk heterojunction enable >90% quantum efficiency *Adv Mater.* **26** 1923–8
[402] Groves C 2013 Suppression of geminate charge recombination in organic photovoltaic devices with a cascaded energy heterojunction *Energy Environ. Sci.* **6** 1546–51
[403] Izawa S, Nakano K, Suzuki K, Hashimoto K and Tajima K 2015 Dominant effects of first monolayer energetics at donor/acceptor interfaces on organic photovoltaics *Adv. Mater.* **27** 3025–31
[404] Heidel T D, Hochbaum D, Sussman J M, Singh V, Bahlke M E, Hiromi I, Lee J and Baldo M A 2011 Reducing recombination losses in planar organic photovoltaic cells using multiple step charge separation *J. Appl. Phys.* **109** 104502
[405] Tan Z-K, Johnson K, Vaynzof Y, Bakulin A A, Chua L-L, Ho P K H and Friend R H 2013 Suppressing recombination in polymer photovoltaic devices via energy-level cascades *Adv. Mater.* **25** 4131–8
[406] Street R A, Cowan S and Heeger A J 2010 Experimental test for geminate recombination applied to organic solar cells *Phys. Rev.* B **82** 121301
[407] Kepler R G and Coppage F N 1966 Generation and recombination of holes and electrons in anthracene *Phys. Rev.* **151** 610–4
[408] Silver M and Sharma R 1967 Carrier generation and recombination in anthracene *J. Chem. Phys.* **46** 692–6
[409] Juška G, Arlauskas K, Stuchlik J and Osterbaka R 2006 Non-Langevin bimolecular recombination in low-mobility materials *J. Non-Cryst. Solids* **352** 1167–71
[410] Sliaužys G, Juška G, Arlauskas K, Pivrikas A, Österbacka R, Scharber M, Mozer A and Sariciftci N S 2006 Recombination of photogenerated and injected charge carriers in π-conjugated polymer/fullerene blends *Thin Solid Films* **511–2** 224–7
[411] Shuttle C G, O'Regan B, Ballantyne A M, Nelson J, Bradley D D C and Durrant J R 2008 Bimolecular recombination losses in polythiophene: fullerene solar cells *Phys. Rev.* B **78** 113201
[412] Shuttle C G, O'Regan B, Ballantyne A M, Nelson J, Bradley D D C, de Mello J and Durrant J R 2008 Experimental determination of the rate law for charge carrier decay in a polythiophene: fullerene solar cell *Appl. Phys. Lett.* **92** 093311
[413] Shuttle C G, Hamilton R, O'Regan B C, Nelson J and Durrant J R 2010 Charge-density-based analysis of the current–voltage response of polythiophene/fullerene photovoltaic devices *Proc. Natl Acad. Sci. USA* **107** 16448–52
[414] Heiber M C, Baumbach C, Dyakonov V and Deibel C 2015 Encounter-limited charge-carrier recombination in phase-separated organic semiconductor blends *Phys. Rev. Lett.* **114** 136602
[415] Deibel C, Wagenpfahl A and Dyakonov V 2009 Origin of reduced polaron recombination in organic semiconductor devices *Phys. Rev.* B **80** 7
[416] Deledalle F, Shakya Tuladhar P, Nelson J, Durrant J R and Kirchartz T 2014 Understanding the apparent charge density dependence of mobility and lifetime in organic bulk heterojunction solar cells *J. Phys. Chem.* C **118** 8837–42
[417] Kirchartz T and Nelson J 2012 Meaning of reaction orders in polymer:fullerene solar cells *Phys. Rev.* B **86** 165201
[418] Kirchartz T, Pieters B E, Kirkpatrick J, Rau U and Nelson J 2011 Recombination via tail states in polythiophene: fullerene solar cells *Phys. Rev.* B **83** 13
[419] Jones M L, Chakrabarti B and Groves C 2014 Monte Carlo simulation of geminate pair recombination dynamics in organic photovoltaic devices: multi-exponential,

field-dependent kinetics and its interpretation *J. Phys. Chem.* C **118** 85–91
[420] Yi Y, Coropceanu V and Brédas J-L 2009 Exciton-Dissociation and charge-recombination processes in pentacene/C60 solar cells: theoretical insight into the impact of interface geometry *J. Am. Chem. Soc.* **131** 15777–83
[421] Idé J *et al* 2014 Charge dissociation at interfaces between discotic liquid crystals: the surprising role of column mismatch *J. Am. Chem. Soc.* **136** 2911–20
[422] Lemaur V, Steel M, Beljonne D, Bredas J L and Cornil J 2005 Photoinduced charge generation and recombination dynamics in model donor/acceptor pairs for organic solar cell applications: a full quantum-chemical treatment *J. Am. Chem. Soc.* **127** 6077–86
[423] Liu T, Cheung D L and Troisi A 2011 Structural variability and dynamics of the P3HT/PCBM interface and its effects on the electronic structure and the charge-transfer rates in solar cells *Phys. Chem. Chem. Phys.* **13** 21461–70
[424] Kido J, Hongawa K, Okuyama K and Nagai K 1994 White light-emitting organic electroluminescent devices using the poly(n-vinylcarbazole) emitter layer doped with 3 fluorescent dyes *Appl. Phys. Lett.* **64** 815–7
[425] Kamtekar K T, Monkman A P and Bryce M R 2010 Recent advances in white organic light-emitting materials and devices (WOLEDs) *Adv. Mater.* **22** 572–82
[426] So F, Kido J and Burrows P 2008 Organic light-emitting devices for solid-state lighting *MRS Bull.* **33** 663–9
[427] D'Andrade B W and Forrest S R 2004 White organic light-emitting devices for solid-state lighting *Adv. Mater.* **16** 1585–95
[428] Kuik M, Wetzelaer G, Nicolai H T, Craciun N I, De Leeuw D M and Blom P W M 2014 25th Anniversary article: charge transport and recombination in polymer light-emitting diodes *Adv. Mater.* **26** 512–31
[429] Garcia-Belmonte G, Montero J M, Barea E M, Bisquert J and Bolink H J 2007 Millisecond radiative recombination in poly(phenylene vinylene)-based light-emitting diodes from transient electroluminescence *J. Appl. Phys.* **101** 114506
[430] Albrecht U and Bassler H 1995 Efficiency of charge recombination in organic light-emitting-diodes *Chem. Phys.* **199** 207–14
[431] Albrecht U and Bassler H 1995 Langevin-type charge-carrier recombination in a disordered hopping system *Phys. Status Solidi* b **191** 455–9
[432] Gartstein Y N, Conwell E M and Rice M J 1996 Electron–hole collision cross-section in discrete hopping systems *Chem. Phys. Lett.* **249** 451–8
[433] Crossland E J W, Tremel K, Fischer F, Rahimi K, Reiter G, Steiner U and Ludwigs S 2012 Anisotropic charge transport in spherulitic poly(3-hexylthiophene) films *Adv. Mater.* **24** 839–44
[434] Arkhipov V I, Heremans P, Emelianova E V and Bässler H 2005 Effect of doping on the density-of-states distribution and carrier hopping in disordered organic semiconductors *Phys. Rev.* B **71** 045214
[435] Burrows P E, Shen Z, Bulovic V, McCarty D M, Forrest S R, Cronin J A and Thompson M E 1996 Relationship between electroluminescence and current transport in organic heterojunction light-emitting devices *J. Appl. Phys.* **79** 7991–8006
[436] Neumann F, Genenko Y A, Schmechel R and Seggern H V 2005 Role of diffusion on SCLC transport in double injection devices *Synth. Met.* **150** 291–6
[437] Greenham N C, Moratti S C, Bradley D D C, Friend R H and Holmes A B 1993 Efficient light-emitting diodes based on polymers with high electron affinities *Nature* **365** 628–30
[438] Morteani A C, Dhoot A S, Kim J S, Silva C, Greenham N C, Murphy C, Moons E, Ciná S, Burroughes J H and Friend R H 2003 Barrier-free electron–hole capture in polymer blend heterojunction light-emitting diodes *Adv. Mater.* **15** 1708–12
[439] Bailey J, Wright E N, Wang X H, Walker A B, Bradley D D C and Kim J S 2014 Understanding the role of ultra-thin polymeric interlayers in improving efficiency of polymer light emitting diodes *J. Appl. Phys.* **115** 12
[440] Shen Y and Giebink N C 2015 Monte Carlo simulations of nanoscale electrical inhomogeneity in organic light-emitting diodes and its impact on their efficiency and lifetime *Phys. Rev. Appl.* **4** 054017
[441] Giebink N C, D'Andrade B W, Weaver M S, Mackenzie P B, Brown J J, Thompson M E and Forrest S R 2008 Intrinsic luminance loss in phosphorescent small-molecule organic light emitting devices due to bimolecular annihilation reactions *J. Appl. Phys.* **103** 044509
[442] Coehoorn R, van Eersel H, Bobbert P and Janssen R 2015 Kinetic Monte Carlo study of the sensitivity of OLED efficiency and lifetime to materials parameters *Adv. Funct. Mater.* **25** 2024–37
[443] Geoghegan M and Krausch G 2003 Wetting at polymer surfaces and interfaces *Prog. Polym. Sci.* **28** 261–302
[444] Vaynzof Y, Kabra D, Zhao L H, Chua L L, Steiner U and Friend R H 2011 Surface-directed spinodal decomposition in poly[3-hexylthiophene] and C-61-butyric acid methyl ester blends *ACS Nano* **5** 329–36
[445] Tillack A F *et al* 2011 Surface characterization of polythiophene:fullerene blends on different electrodes using near edge x-ray absorption fine structure *ACS Appl. Mater. Interfaces* **3** 726–32
[446] Germack D S, Chan C K, Kline R J, Fischer D A, Gundlach D J, Toney M F, Richter L J and DeLongchamp D M 2010 Interfacial segregation in polymer/fullerene blend films for photovoltaic devices *Macromolecules* **43** 3828–36
[447] McNeill C R, Halls J J M, Wilson R, Whiting G L, Berkebile S, Ramsey M G, Friend R H and Greenham N C 2008 Efficient polythiophene/polyfluorene copolymer bulk heterojunction photovoltaic devices: device physics and annealing effects *Adv. Funct. Mater.* **18** 2309–21
[448] Watts B and McNeill C R 2010 Simultaneous surface and bulk imaging of polymer blends with x-ray spectromicroscopy *Macromol. Rapid Commun.* **31** 1706–12
[449] Rehmann N, Hertel D, Meerholz K, Becker H and Heun S 2007 Highly efficient solution-processed phosphorescent multilayer organic light-emitting diodes based on small-molecule hosts *Appl. Phys. Lett.* **91** 103507
[450] Scaccabarozzi A D and Stingelin N 2014 Semiconducting:insulating polymer blends for optoelectronic applications-a review of recent advances *J. Mater. Chem.* A **2** 10818–24
[451] Arias A C, Endicott F and Street R A 2006 Surface-induced self-encapsulation of polymer thin-film transistors *Adv. Mater.* **18** 2900–4
[452] Goffri S *et al* 2006 Multicomponent semiconducting polymer systems with low crystallization-induced percolation threshold *Nat. Mater.* **5** 950–6
[453] Henderson I C and Clarke N 2005 On modelling surface directed spinodal decomposition *Macromol. Theory Simul.* **14** 435–43
[454] Fukuda J, Yoneya M and Yokoyama H 2006 Numerical treatment of the dynamics of a conserved order parameter in the presence of walls *Phys. Rev.* E **73** 9
[455] Michels J J and Moons E 2013 Simulation of surface-directed phase separation in a solution-processed polymer/PCBM blend *Macromolecules* **46** 8693–701

[456] Wodo O and Ganapathysubramanian B 2012 Modeling morphology evolution during solvent-based fabrication of organic solar cells *Comput. Mater. Sci.* **55** 113–26
[457] Hellmann C, Treat N D, Scaccabarozzi A D, Hollis J R, Fleischli F D, Bannock J H, de Mello J, Michels J J, Kim J S and Stingelin N 2015 Solution processing of polymer semiconductor: insulator blends-tailored optical properties through liquid-liquid phase separation control *J. Polym. Sci.* B **53** 304–10
[458] Kouijzer S, Michels J J, van den Berg M, Gevaerts V S, Turbiez M, Wienk M M and Janssen R A J 2013 Predicting morphologies of solution processed polymer:fullerene blends *J. Am. Chem. Soc.* **135** 12057–67
[459] van Franeker J J, Westhoff D, Turbiez M, Wienk M M, Schmidt V and Janssen R A J 2015 Controlling the dominant length scale of liquid–liquid phase separation in spin-coated organic semiconductor films *Adv. Funct. Mater.* **25** 855–63
[460] Schmidt-Hansberg B *et al* 2011 Moving through the phase diagram: morphology formation in solution cast polymer-fullerene blend films for organic solar cells *ACS Nano* **5** 8579–90
[461] Stenzel O, Hassfeld H, Thiedmann R, Koster L J A, Oosterhout S D, van Bavel S S, Wienk M M, Loos J, Janssen R A J and Schmidt V 2011 Spatial modeling of the 3D morphology of hybrid polymer-ZnO solar cells, based on electron tomography DATA *Ann. Appl. Stat.* **5** 1920–47
[462] Stenzel O, Koster L J A, Thiedmann R, Oosterhout S D, Janssen R A J and Schmidt V 2012 A new approach to model-based simulation of disordered polymer blend solar cells *Adv. Funct. Mater.* **22** 1236–44
[463] Westhoff D, Van Franeker J J, Brereton T, Kroese D P, Janssen R A J and Schmidt V 2015 Stochastic modeling and predictive simulations for the microstructure of organic semiconductor films processed with different spin coating velocities *Modelling Simul. Mater. Sci. Eng.* **23** 21
[464] Baumeier B, Stenzel O, Poelking C, Andrienko D and Schmidt V 2012 Stochastic modeling of molecular charge transport networks *Phys. Rev.* B **86** 7
[465] Kordt P, Stenzel O, Baumeier B, Schmidt V and Andrienko D 2014 Parametrization of extended Gaussian disorder models from microscopic charge transport simulations *J. Chem. Theory Comput.* **10** 2508–13

Dr Chris Groves is a Senior Lecturer at the School of Engineering and Computing Sciences at Durham University, UK, where he is also a Director of the Durham Centre for Molecular and Nanoscale Electronics. He completed his PhD on III-V photodetectors at Sheffield University in 2004, before completing postdoctoral positions in the field of organic electronics at the Cavendish Laboratory and University of Washington. His research interests focus on the use of experiment and simulation to examine the relationship between charge transport and the performance of electronic devices. Recently, this has involved the development of Monte Carlo models and experimental techniques to reveal how morphology influences charge transport, and ultimately performance, in organic photovoltaic diodes.